$43, 80

Selected Papers from the Workshop

Late Cenozoic Evolution of the Southern Great Basin

Convened by

D. B. Slemmons

R. A. Schweickert

J. W. Bell

held at

University of Nevada - Reno

November 10 - 13, 1987

under the auspices of the

Center for Neotectonic Studies

Director D. B. Slemmons

Edited by

Michael A. Ellis

Nevada Bureau of Mines and Geology Open File 89-1

Table of Contents

Preface,
Michael Ellis

Overview of the Role of Strike-slip and Normal Faulting in the Neogene History of the Region Northeast of Death Valley, California-Nevada
Lauren Wright 1

Timing and relation to volcanism of Cenozoic extension in east-central Nevada,
Wanda Taylor and John Bartley 13

Isostatic uplift, crustal attenuation, and the evolution of an extensional detachment system in southwestern Nevada,
Robert B. Scott 19

Structural geology of the Indian Springs 1:100,000 quadrangle, southern Nevada, and the role of mantle-tapping in Great Basin volcanism,
Peter L. Guth 27

Mid-Miocene igneous rocks in the Lake Mead area of Nevada and Arizona: Production of intermediate igneous rocks in an extensional environment,
Eugene I. Smith, Daniel L. Feuerbach, Terry R. Naumann and James G. Mills 33

Possible modes of deformation along "accommodation zones" in rifted continental crust: an example from the southern Basin and Range province,
James E. Faulds, Chris K. Mawer, John W. Geissman 39

Doming of the lower crust beneath an extensional orogen?,
Laura Serpa 47

New perspectives on Quaternary faulting in the southern Walker Lane, Nevada and California,
Marith C. Reheis and Jay S. Noller 57

Late Holocene paleoseismicity of the northern Death Valley fault system, Fish Lake Valley, Nevada,
Thomas L. Sawyer 63

The use of the relative comparison approach at Yucca Mountain and similarities between Yucca Mountain and the 1932 Cedar Mountain earthquake area,
Craig M. dePolo, John W. Bell and Alan R. Ramelli 79

Application of a refined method for determining principal stress orientations in southern Nevada,
Virgil A. Frizzell and Mary Lou Zoback 83

Paleomagnetic research in the Basin and Range province, western United States: Historical perspective, applications, and limitations,
John Wm. Geissman, Mark R. Hudson, James T. Faulds, James T. Callian, Steve S. Harlan, Qing Huang and Yianping Li 87

Earthquake clustering near Mina, Nevada, July and August 1987,
Kenneth D. Smith, William R. Walter, Raul R. Castro, Keith F. Priestley and Abdol R. Anooshepoor 99

Source parameters of the 1987 Edgecumbe New Zealand earthquake,
Keith F. Priestley and Russel Robinson. 123

Rates and patterns of piedmont evolution in the southwest Basin and Range,
John Dohrenwend. 151

Late Quaternary paleoclimate studies -- geologic problems and questions,
Emily M. Taylor. 153

Preface

This volume represents the content of a workshop held at the University of Nevada - Reno, under the auspices of the Center for Neotectonic Studies, organized by Professors Slemmons, Schweickert, and Bell. The workshop consisted of a variety of specialised presentations, each aimed toward a clearer understanding of the southern Great Basin and addressing a number of disparate topics within the fields of geology and geophysics. Our aim was to bring together a number of experts whose state-of-the-art ideas and data represent the front line of Basin and Range research; without doubt, the workshop hit the bull's eye not only in this respect but also in bringing together an audience whose equally disparate elements may not otherwise have met and talked were it not for the workshop. It is a pleasure, therefore, to be able to collect these workshop papers and abstracts for this volume; the reader should regard them as a photographic still of the rapidly changing picture of our ideas about the development of the southern Great Basin.

The last decade has witnessed a rising surge of interest in all aspects of Basin and Range geology, motivated in part by new ideas about the mechanisms of crustal extension and the significance of low-angle normal faults and detachments. Our understanding of the processes of continental extension has benefitted from the application of a number of different disciplines in both geology and geophysics and, in particular, from the integration of these disciplines. The benefit of this interdisciplinary and cooperative approach is most dramatically seen in the growing field of neotectonics, in which the relative newcomers in the fields of structural geology, seismology, volcanology, etc., are able to add their insights to produce a more coherent view of the active Basin and Range.

The burgeoning of neotectonics as a field of study is due in part to the excitement generated by Basin and Range geology, but also to the dramatic development of various paleoseismological techniques in the last decade, and the realization that the seismic record is woefully inadequate in characterizing active tectonics and seismic hazard. The field of neotectonics is really no more than the application of every geological and geophysical tool to the understanding of active tectonics, and for this reason the term neotectonics is often criticized for being jargon. But the fact that the term was invented represents a real and tangible realization by geologists and geophysicists alike that true significant progress is not only possible by cooperative and interdisciplinary work, but is impossible without it.

This volume and the workshop from which it comes represents this type of interdisciplinary and cooperative work and, in this sense, represents the flavor of our current understanding, including the remaining controversies, of the southern Great Basin.

* * * * *

Acknowledgements My greatest thanks and debt are owed to Barbara Matz, whose untiring, unquestioning, and enthusiastic help made both the workshop and the preparation of this volume a far easier task than it might have otherwise been. The workshop would not have been possible without the guidance of the convenors, Professors Slemmons, Schweickert, and Bell. The following students helped in various ways in making the workshop run smoothly and successfully (in no particular order): Paul Buchanan, Doug Clark, John Caskey, Dave Green, Mary Lahren, Mary Wells, Janet Sawyer, Kati Killeen, Steve Nitchman, Diane Donovan, and Diane dePolo. If I've forgotten anyone I hope they'll forgive me - to those I owe a special thanks.

Michael A. Ellis
Center for Neotectonic Studies
June 6, 1989

Overview of the Role of Strike-slip and Normal Faulting in the Neogene History of the Region Northeast of Death Valley, California-Nevada

Lauren A. Wright, Department of Geosciences
Pennsylvania State University
University Park, PA 16802

The complexity of Neogene faulting in the Death Valley region (Fig. 1) has been widely recognized since Levi Noble presented his classic paper on this subject in 1941. Subsequent detailed mapping by many workers has produced a progressively clearer documentation of the fault pattern, but also has led to divergent views concerning the tectonic evolution of the region in Neogene time. This paper is intended as a brief commentary on a recently compiled fault map of the Death Valley region (Fig. 2) and on what can be seen in a compiled Bouguer gravity map (Figs. 3 and 4) that may add to an understanding of the fault pattern. The paper will focus upon the chronology of the inception of movement on major faults and the interplay between two fault types in the Neogene framework - northwest striking faults with a dominant right-lateral component of movement, and north-northwest to northeast-striking, essentially normal faults of steep to moderate dip.

Several lines of evidence strongly suggest that, (1) in a belt that includes Death Valley on the southwest and Pahrump Valley and the Amargosa Desert on the northeast, these two types of faults are the principal expressions of crustal failure in the shaping of the present basins and ranges, (2) that this region was divided into blocks bounded by major zones of strike-slip faults and normal faults 16 to 14 Ma ago, (3) that each block has evolved semi-independently with separate deformational and thermal histories, and (4) that low-angle normal faults, of which some have been identified as "detachment faults", are unconnected, later features originating within the individual blocks. This interpretation differs from others in which the failure is attributed mainly to low-angle detachment faults of regional extent (Wernicke, 1981; Wernicke and others, 1988; Hamilton, 1988).

Northeast of Death Valley, isolated occurrences of low-angle faults in the Black Mountains (Noble, 1941; Wright and Troxel, 1985) and in the northern Funeral Mountains-Bare Mountain area (Ransome and others, 1910; Carr and Monseri, 1988; Maldonado, in press) have been viewed by Hamilton (1988) as belonging to a single regional detachment surface. The former, however , have been interpreted by Noble and Wright (1954) and Drewes (1963) as confined to the Black Mountains; they have recently been viewed by Wright and Troxel (1987) as providing a linkage between the Sheephead fault zone on the southwest and Furnace Creek fault zone on the northeast. The latter, for reasons cited below, seem best interpreted as localized within the northern Funeral Mountains-Bare Mountain area. The origin of these faults in both areas, however, remains controversial.

The interplay between the strike-slip and normal faults was first emphasized by Burchfiel and Stewart (1966) who, in defining the type "pull-apart" basin, observed that the active, dominantly normal and north-striking faults that occupy central Death Valley provide a right-stepping connection between the zones of active northwest-striking right-lateral faults that occupy southern and northern Death Valley. Burchfiel and others (1983) later recognized a repetition of this pattern of faulting in the area of the Montgomery Mountains and the Nopah and Resting Spring Ranges east of Death Valley. In addition, Wright and Troxel (1971) observed that the central Death Valley plutonic-volcanic field and the Furnace Creek basin which borders it on the northeast occupy a similarly oriented right-stepping position between the en echelon terminations of the Furnace Creek and Sheephead right-lateral fault zones (Fig. 3) thereby qualifying as a rhombochasm. The various bodies of igneous rock that compose this field also have been broken by normal faults and intruded by dikes, most of each striking north-northeast. The right-stepping relation-ship between the strike-slip and normal faults also is expressed, but on a smaller scale, by joins between the Grandview fault and the Furnace Creek fault zone and between the Furnace Creek fault zone and the Keane Wonder fault zone.

If we have correctly interpreted the tectonic setting of the central Death Valley plutonic-volcanic field, the age of the oldest igneous rocks originating within it or of the oldest basinal deposits associated with the proposed rhombochasm should provide a minimum age for the beginning of movement on both the Furnace Creek and Sheephead fault zones which bound the field. The oldest age thus far obtained from either of these sources is the 13.7 $\pm$ .4 Ma (K/Ar biotite) obtained from a tuff bed low in the Artist Drive Formation of the Furnace Creek basin (Cemen and others, 1985). A 10.4 $\pm$ .3 Ma (K/Ar biotite, personal communication, R.E. Drake, 198) age determination from a dacitic rock unit at Sheephead Pass, which is both intrusive into the Sheephead fault zone and exists as flows adjacent to it, provides a minimum date for the initiation of movement on that fault zone. A considerably older date for the initiation of movement on the Sheephead fault zone is suggested by evidence that the chaotic defor-mation of pre-Cenozoic and Cenozoic rock units (producing the Amargosa chaos of Noble, 1941) is associated with movement on the Sheephead fault (Wright and Troxel, 1987) and began prior to the advent of volcanism in the Black Mountains (Wright and Troxel, 1985).

The time of inception of igneous activity in the Black Mountains and Greenwater Range, between the en echelon terminations of the Furnace Creek and Sheephead fault zones, remains undetermined as the ages of most of the plutons are unknown. A quartz monzonite pluton, about 2.5 km west of Jubilee Pass, dated at 11.4 $\pm$ .04 Ma (K/Ar biotite, R.E. Drake, personal communication, 198) is the oldest yet identified.

A feature expressed mainly by gravity anomalies on Figures 3 and 4 and designated in Figure 4 as the "Amargosa Desert rift

zone" extends from the vicinity of Crater Flat and Yucca Mountain southward to the southern end of the Amargosa Desert. Carr (1988), in independently observing the gravity low, has shown it as the southern part of a lengthier feature, named by him the "Kawich-Greenwater volcano-tectonic rift". From the Crater Flat-Yucca Mountain area north-northeastward, the northern part of the Kawich-Greenwater rift, as defined by Carr, is delineated by a belt of north-northeast striking normal faults and an alignment of mid-Miocene calderas, including those of the Timber Mountain-Oasis Valley and the Crater Flat-Prospector Pass complexes. Those of the latter are the most southerly calderas which Carr identifies with the rift zone, although he would extend the rift zone southwestward from the Amargosa Desert to include the central Death Valley plutonic-volcanic field (his Greenwater volcanic center).

Beneath the Amargosa Desert, the rift zone is recorded principally by the negative gravity anomaly of Figures 3 and 4 and by exposures of Miocene sedimentary rocks of the Ash Meadows basin at the southern end of the Amargosa Desert and the northern end of the Resting Spring Range. In the absence, beneath the rest of the Amargosa Desert, of strong magnetic anomalies (Kane and Bracken, 1983) that would indicate the presence of large bodies of volcanic rock, this part of the gravity anomaly is best attributed to a sedimentary fill of the rift zone. That the entire Amargosa Desert segment of the rift zone opened in mid-Miocene time is indicated by the observations that the Crater Flat-Prospector Pass caldera complex involves rock units as old as 15 Ma (Carr, 1989) and that an ash bed low in the sedimentary fill of the Ash Meadows basin has been radio-metrically dated (K/Ar biotite) at 13.2 $\pm$ .04 Ma (R.E. Drake, personal communication, 1980, cited in Cemen, 1983).

As an alternative to the inclusion of the central Death Valley volcanic field within the rift zone of the Amargosa Desert, I suggest a linkage with the Pahrump fault zone in the manner shown in Figure 4. Extending northwestward from Pahrump Valley to the southern end of the Amargosa Desert is a continuous alignment of faults and apparently fault-related gravity anomalies which I interpret as joining the Pahrump fault zone with the rift zone of the Amargosa Desert. The faults that compose the Pahrump fault zone and displace Quaternary alluvium of Pahrump Valley connect with faults that define Stewart Valley and the Stewart Valley pull-apart basin of Burchfiel and others (1983). The latter coincides with a negative gravity anomaly and is, in turn, succeeded northwestward by three other similarly shaped and oriented negative anomalies which can be assumed to also delineate pull-apart basins, including the partly exposed Ash Meadows basin at the southern end of the Amargosa Desert. In the northern part of the Amargosa Desert, the eastern margin of the rift-zone coincides with a north-northeast trending groundwater barrier (Winograd and Thordarson, 1975) and a negative, west-facing gravity gradient.

The time of the initiation of movement on the Pahrump fault zone is conjectural. Evidence that it moved contemporaneously

with the development of sedimentary basins along its trace is seen in the presence of pronounced negative gravity anomalies, elongate parallel with the fault zone beneath the Late Cenozoic cover of Pahrump Valley. Its parallelism with the Furnace Creek fault zone, its association with gravity anomalies as strong as those along the Furnace Creek fault zone and its apparent linkage with the rift zone beneath the Amargosa Desert suggest that it evolved contemporaneously with these features.

Thus if these interpretations of the geometry and chronology of major strike-slip and normal faults in the region east of Death Valley are correct, the faults have divided the region into several discrete blocks 16 to 14 Ma ago, each having subsequently undergone a separate deforma-tional and thermal history. If so, the detachment features of the Black Mountains and those of the area of the northern Funeral Mountains, Bullfrog Hills and Bare Mountain could not have developed as parts of a single surface and an overlying plate while separated by a major strike-slip (Furnace Creek) fault zone. Although the detachment surfaces and the overlying plates in the two areas are similar in major respects, they also display significant differences in deformational style, tectonic setting, and chronology. These are being detailed in a paper now in preparation.

Quaternary surface faulting has been long recognized as much less abundantly expressed in the region northeast of Death Valley than from Death Valley westward. The most prominent ground ruptures in the northeast region are those of the Pahrump fault zone in Pahrump Valley and another along the east side of Bare Mountain (Reheis, 1988). The latter clearly records renewed movement on the fault that separates the Paleozoic rocks of Bare Mountain from the thick volcanic section beneath Crater Flat (Carr, 1988). Evidence that the northwest-trending ground ruptures of Pahrump Valley also represent renewed movement on an earlier established (mid-Miocene?) fault zone exists in the elongate, northwest-trending gravity anomalies beneath Pahrump Valley and coinciding with the fault zone.

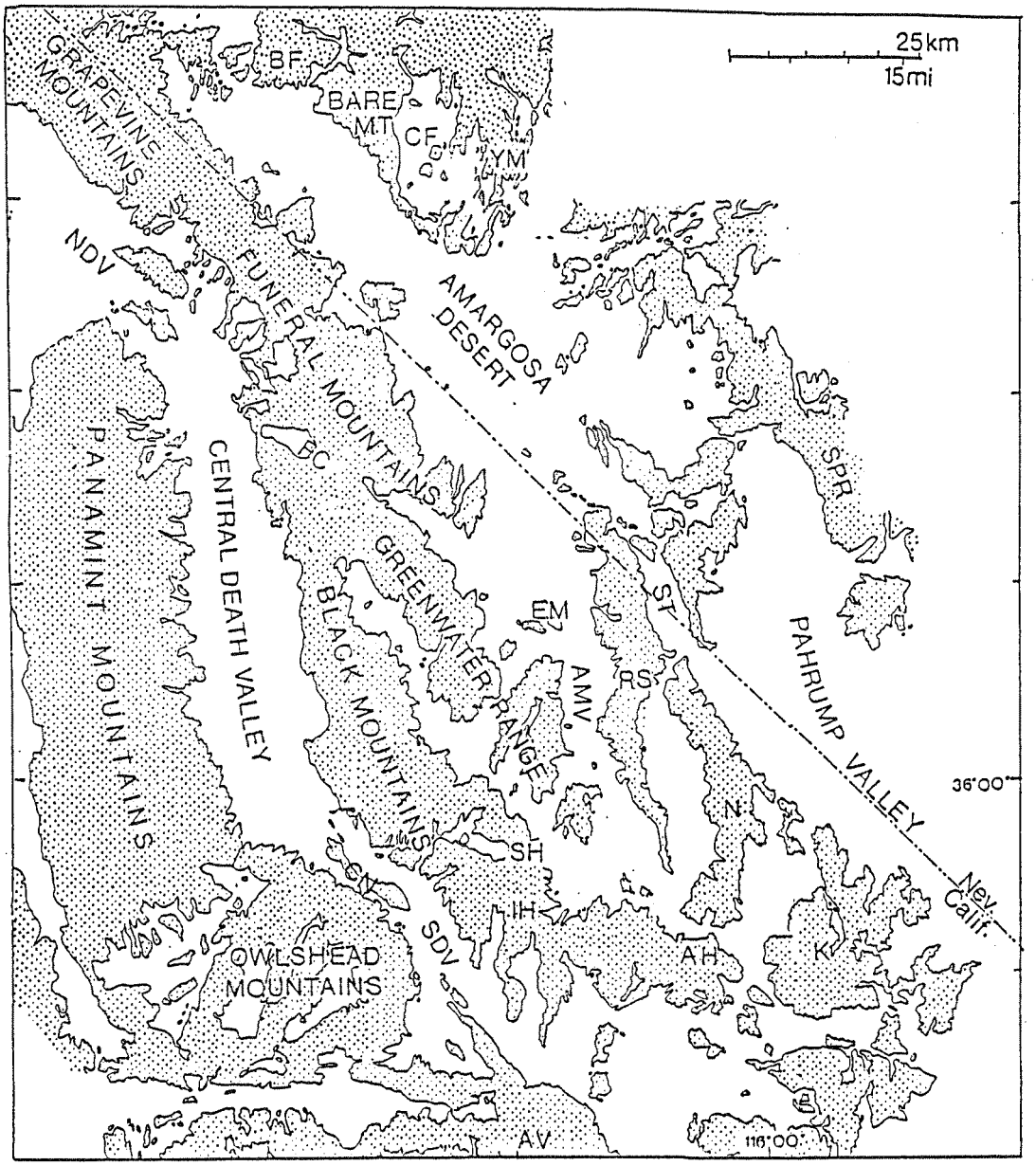

Figure 1. Map showing topographic features of Death Valley region. AH = Alexander Hills; AMV = Amargosa Valley; AV = Avawatz Mts.; BF = Bullfrog Hills; CF = Crater Flat; CN = Confidence Hills; EM = Eagle Mt.; FC = Furnace Creek Wash; IH = Ibex Hills; K = Kingston Range; N = Nopah Range; NDV = Northern Death Valley; RS = Resting Spring Range; SDV = Southern Death Valley; SH = Sheephead Pass; SPR = Spring Mts.; ST = Stewart Valley; YM = Yucca Mt.

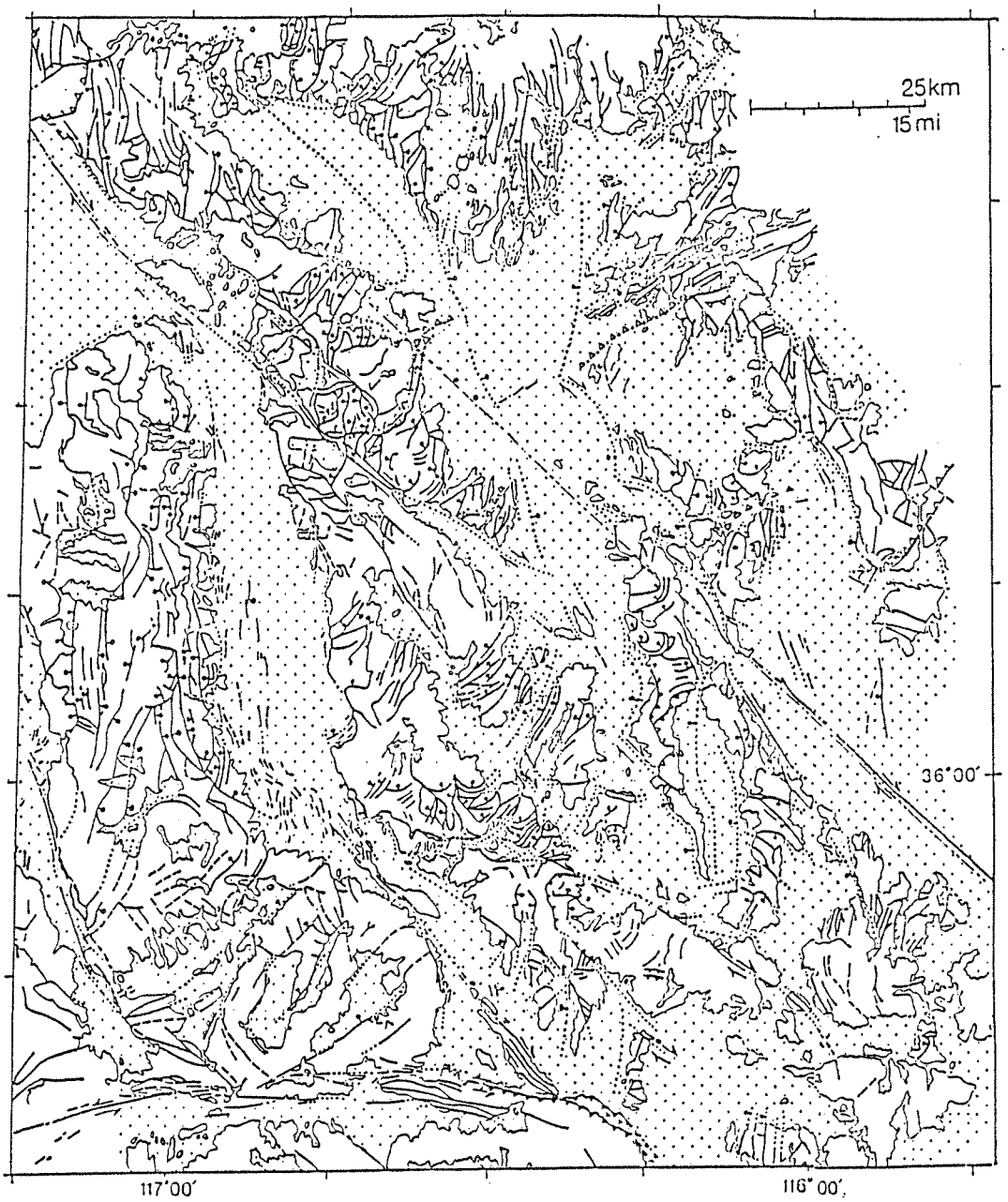

Figure 2. Fault map of Death Valley region. Compiled from sources too numerous to list here. Most of them are referenced on the Geologic Map of Nevada (Stewart and Carlson, 1978); Death Valley Sheet, Geologic Map of California (Streitz and Stinson, 1974); and Trona-Kingman quadrangle, Geologic Map of California (Wagner and Hsu, in preparation, 1989). Neogene strike-slip faults are indicated by arrows, Neogene normal faults by bar and ball on downthrown side, Neogene thrust and reverse faults by solid barbs, and Mesozoic thrust faults by open barbs.

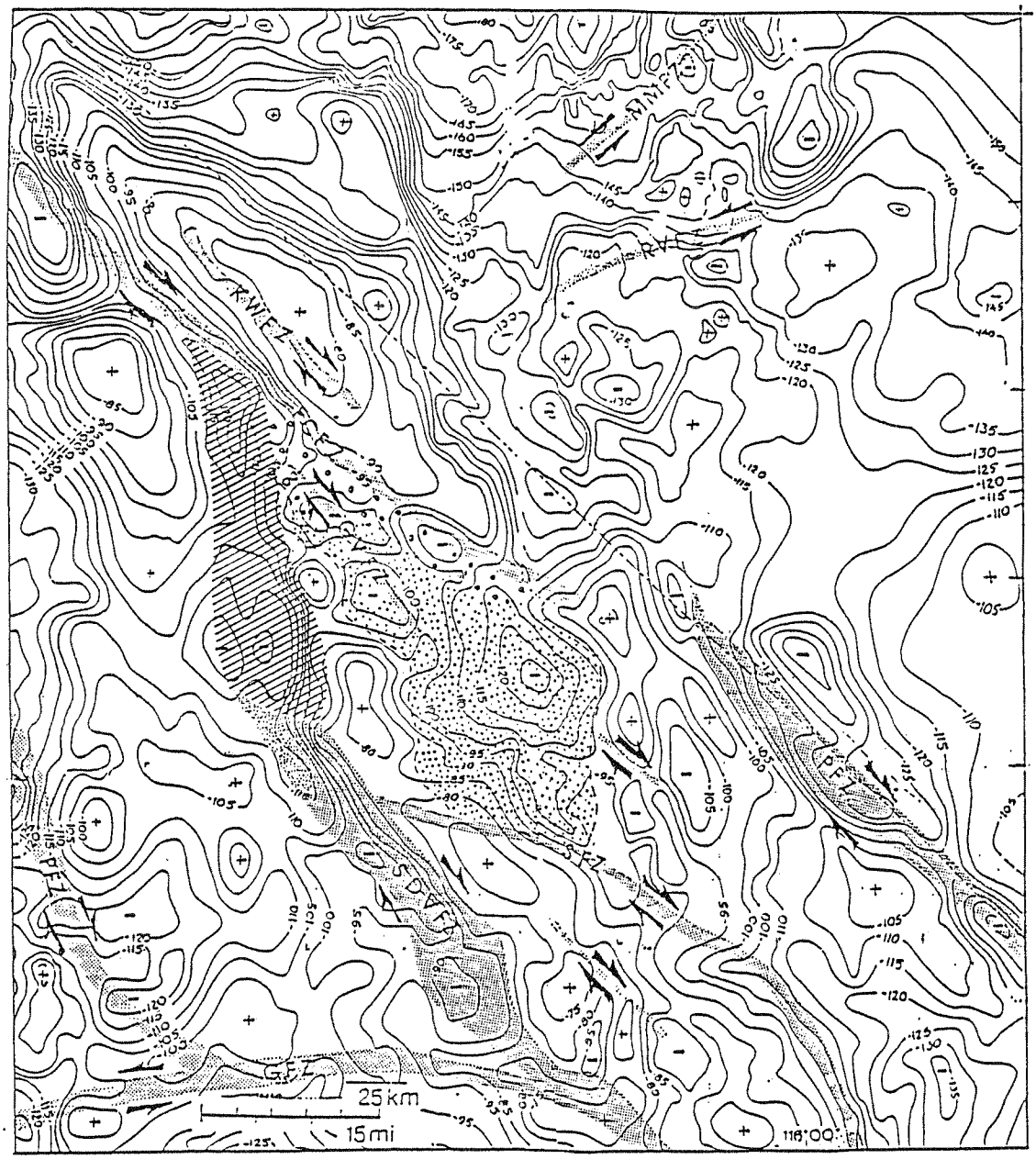

Figure 3. Bouguer gravity map of the Death Valley region; contour interval = 5 milligals. Compiled from Bracken and Kane, 1982; Chapman and others, 1973; Healey, 1973; Healey and others, 1980; Kane and others, 1979; and Nilson and Chapman, 1971. Map shows overprint of strike-slip fault zones (FCFZ = Furnace Creek; GVFZ = Grandview; GFZ = Garlock; KWFZ = Keane Wonder; MMFZ = Mine Mountain; PFZ = Panamint; PAFZ = Pahrump; RVFZ = Rock Valley; SFZ = Sheephead; and SDVFZ = Southern Death Valley), central Death Valley pull-apart basin (diagonal lines), general distribution of volcanic rocks of Central Death Valley plutonic-volcanic field (dots), and the Furnace Creek basin (open circles).

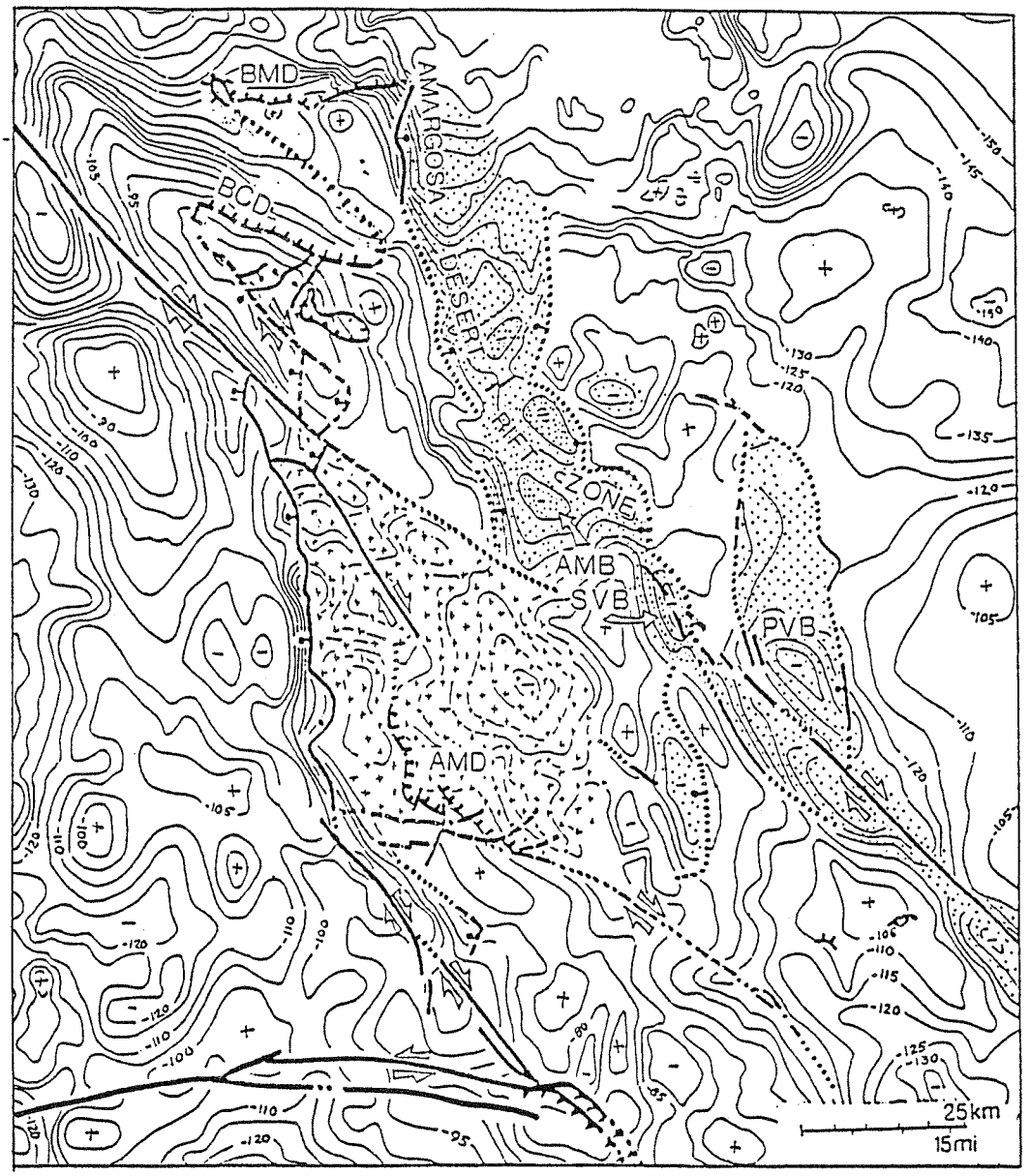

Figure 4. Bouguer gravity map of Figure 3 with an overprint of Neogene strike-slip faults (arrows), normal faults (bar and ball), thrust faults (solid barbs) and faults that have been commonly designated as "detachment faults" (hachures). Solid faults displace Quaternary rocks; dashed faults displace older rocks, dotted faults are hidden. Area of Central Death Valley plutonic-volcanic field and Furnace Creek basin is shown by pattern of crosses. ADRZ = Amargosa Desert rift zone; AMB = Ash Meadows basin; AMD = Amargosa detachment fault; BCD = Boundary Canyon detachment fault; BMD = Bullfrog Hills-Bare Mountain detachment fault; PVB = Pahrump Valley pull-apart basin; SVB = Stewart Valley pull-apart basin.

References Cited

Bracken, R. E. and Kane, H.F., Kingman Sheet, Bouguer gravity map of Nevada: Nevada Bureau of Mines and Geology Map 75.

Burchfiel, B.C. and Stewart, J.H., 1966, Pull apart origin of the central segment of Death Valley, California: Geological Society of America Bulletin, v. 77, p. 439-443.

Burchfiel, B.C., Hamill, G.S. IV and Wilhelms, D.E., 1983, Structural geology of the Montgomery Mountains and northern half of the Nopah and Resting Spring Ranges, Nevada and California: Geological Society of America Bulletin, v. 94, p. 1359.

Carr, M.D. and Munsen, S.A., 1988, A field trip guide to the geology of Bare Mountain: in Weide, D.L. and Gaber, M.L., eds., This Extended Land, Field Trip Guidebook, Geological Society of America, Cordilleran Section, Las Vegas, Nevada, p. 50-57.

Carr, W.J., 1984, Regional structural setting of Yucca Mountain, southwestern Nevada and Late Cenozoic rates of tectonic activity in part of the southwestern Great Basin, Nevada and California: U.S. Geological Survey Open-File Report 84-454, 109 p.

Carr, W.J. , in press, Styles of extension in the Nevada Test Site belt: an integration of the volcano-tectonic and detachment fault models: in Wernicke, B., ed., Basin and Range extensional tectonics near the Latitude of Las Vegas, Nevada: Geological Society of America Memoir.

Cemen, I., 1983, Stratigraphy, geochronology and structure of selected areas of the northern Death Valley region, eastern California - western Nevada and implications concerning Cenozoic tectonics of the region [Ph.D. thesis]: University Park, PA, Pennsylvania State Univ., 235 p.

Cemen, I., Wright, L.A., Drake, R.E. and Johnson, F.C., 1985, Cenozoic sedimentation and sequence of deformational events at the southeastern end of the Furnace Creek strike-slip fault zone, Death Valley region, California: in Biddle, K.T. and Christie-Blick, N., eds., Strike-slip Deformation, Basin Formation, and Sedimentation: Society of Economic Paleontologists and Mineralogists, Special Publication 37, p. 127-141.

Chapman, R.H., Healey, D.L., and Troxel, B.W., 1975, Death Valley sheet, Bouguer gravity map of California: California Division of Mines and Geology.

Drewes, H., 1963, Geology of the Funeral Peak quadrangle, California, on the eastern side of Death Valley: U.S. Geological Survey Professional Paper 413, p. 58-61.

Hamilton, W.B., 1988, Detachment faulting in the Death Valley region, California and Nevada: in Carr, M.D. and Yount, J.C., eds., Geologic and Hydrologic Investigations of a Potential Nuclear Waste Disposal Site at Yucca Mountain, southern Nevada: U.S. Geological Survey Bulletin 1790, p. 51-85.

Healey, D.L., 1973, Kingman Sheet, Bouguer gravity map of California: California Division of Mines and Geology.

Healey, D.L., Wahl, R.R. and Oliver, H.W., 1980, Death Valley Sheet, Bouguer gravity map of Nevada: Nevada Bureau of Mines and Geology Map 69.

Kane, M.F., Healey, D.L., Peterson, D.L., Kaufman, H.E. and Reidy, D., 1979, Las Vegas sheet, Bouguer gravity map of Nevada: Nevada Bureau of Mines and Geology Map 61.

Kane, M.F. and Bracken, R.E., 1983, Aeromagnetic map of Yucca Mountain and surrounding regions, southwestern Nevada: U.S. Geological Survey Open-File Report 83-616, 19 p.

Maldonado, F., in press, Structural geology of the upper plate of the Bullfrog Hills detachment system, southern Nevada: Geological Society of America Bulletin.

Nilsen, T.H. and Chapman, R.H., 1971, Trona sheet, Bouguer gravity map of California: California Division of Mines and Geology.

Noble, L.F., 1941, Structural features of the Virgin Spring area, Death Valley, California: Geological Society of America Bulletin, v. 52, p. 941-999.

Noble, L.F. and Wright, L.A. 1954, Geology of the central and southern Death Valley region, California: in Jahns, R.H., ed., Geology of southern California: California Division of Mines and Geology Bulletin 170, Chapter II, contribution 4, p. 143-160.

Ransome, F.L., Emmons, W.W. and Garry, G.H., 1910, Geology and ore deposits of the Bullfrog district, Nevada: U.S. Geological Survey Bulletin 407, 130 p.

Reheis, M.C., 1988, Preliminary study of Quaternary faulting on the east side of Bare Mountain, Nye County, Nevada: in Carr, M.D. and Yount, J.C. eds., Geologic and Hydrologic Investigations of a Potential Nuclear Waste Disposal Site at Yucca Mountain, southern Nevada: U.S. Geological Survey Bulletin 1790, p. 103-111.

Stewart, J.H. and Carlson, J.E., 1978, Geologic map of Nevada: U.S. Geological Survey and Nevada Bureau of Mines and Geology.

Streitz, R. and Stinson, M.C., 1974, Death Valley sheet, Geologic Map of California: California Division of Mines and Geology.

Wagner, D.L. and Hsu, E.Y., in preparation 1989, Trona-Kingman quadrangle, Geologic Map of California: California Division of Mines and Geology.

Wernicke, B., 1981, Low angle normal faults in the Basin and Range province: Nappe tectonics in an extending orogen: Nature, v. 291, p. 645-648.

Wernicke, B., Axen, G.J. and Snow, J.K., 1988, Basin and Range extensional tectonics at the latitude of Las Vegas Nevada: Geological Society of America Bulletin, v. 100, p. 1738-1757.

Wright L.A. and Troxel, B.W., 1971, Evidence for tectonic control of volcanism, Death Valley [abstract]: Geological Society of America, Abstracts with Programs, (Cordilleran Section), v. 3, no. 2, p. 221.

_____, 1987, Tectonic-chronologic model for wrench fault related crustal extension, Death Valley area, California [abstract]: Geological Society of America, Abstracts with Programs, p. 898.

_____, 1985, Geology of the northern half of the Confidence Hills 15' quadrangle, Death Valley region, California: The area of the Amargosa chaos: California Division of Mines and Geology Map Sheet 34.

Timing and relation to volcanism of Cenozoic extension in east-central Nevada

Wanda Taylor and John Bartley
Dept. of Geology and Geophysics, University of Utah
Salt Lake City, Utah 84112

Fundamental questions about Tertiary extensional processes in the Great Basin include the following three. Are tectonic extension and magmatism genetically linked? Was deformation episodic or did it occur gradually as a temporal continuum? Has the structural style of extension changed through time? Data from the North Pahroc Range (NPR) and Seaman Range (SR), Nevada, supply constraints on time-space relations of extension and volcanism, and thereby on the answers to these questions (Fig. 1).

These ranges record four separate episodes of normal faulting over a period of more than 31 Ma: (1) prevolcanic normal faults older than 31 Ma; (2) small, synvolcanic faults that were active between 30 and 27 Ma; (3) Middle Miocene faults, bracketed between 18.8 Ma and Quaternary, but which, based on stratigraphic evidence, probably were active around 15 Ma; and (4) latest Miocene(?) or Pliocene-Quaternary faults that control modern basin-range topography (Fig. 2).

Prevolcanic extension

In the Ely Springs Range (Fig. 1), prevolcanic normal faults cut Cambrian to Silurian rocks (Axen, 1986), and are overlapped by the oldest tuff in the area which yielded an $^{40}Ar/^{39}Ar$ plateau age of 31.3 Ma (Taylor and others, in prep.). Restored cross-sections show that these east-dipping normal faults correlate with east-dipping normal faults exposed in the the Highland Range (Fig. 1; Axen and others, 1988) that end at (sole into?) the Stampede decollement. The Stampede decollement is a detachment within Middle Cambrian shales that recent mapping shows is present throughout the area east of Dry Lake Valley (Axen and others, 1988).

Although no unequivocal prevolcanic normal faults are exposed west of Dry Lake Valley, field evidence strongly indicates their presence. Restoring syn- and postvolcanic faults in the study area, and returning Tertiary strata near the base of the section to horizontal, requires that a major down-on-the-east fault is buried under southern White River Valley (Taylor and Bartley, 1988) (Fig. 1). This fault explains a large discordance in dip of Paleozoic rocks under the sub-Tertiary unconformity. If the concealed fault cuts bedding at 90°, it would have extended the area about 3 km. This fault must be listric to allow the Paleozoic units in the NPR to rotate 65° relative to those in the SR.

Prevolcanic faults are common only to the east of this inferred fault. We interpret the concealed fault as the breakaway of a major east-dipping prevolcanic detachment system, called the Seaman breakaway (new name). The basal detachment of the system probably is the Stampede decollement.

The age of the Seaman breakaway and Stampede decollement are constrained to between Permian and 31 Ma. Based on structural similarities and compatible timing, Bartley and others (1988) propose that this prevolcanic extensional system is tectonically equivalent to and coeval with the Snake Range decollement and related structures. The Seaman breakaway may be structurally connected to the breakaway of the Snake Range system. Miller and others (1983) inferred that the Snake Range system was active from about 35 to 27 Ma, and we therefore suggest a similar age for prevolcanic extension in the study area (Fig. 1).

Synvolcanic extension

In the NPR, unconformities within the volcanic section define two ages of synvolcanic faults separated by less than 1 Ma (Fig. 1). Because of their temporal similarity, the faults probably record a single period of extension. The oldest synvolcanic faults cut units as young as a tuff that yielded $^{40}Ar/^{39}Ar$ dates of about 30.5 Ma. The oldest strata that overlap the youngest of these faults yielded ages of about 27 Ma. An unconformity between 27 and 30 Ma is regionally extensive (Bartley and others, 1988), but mapped synvolcanic normal faults only extend the area a small amount.

Mid-Miocene extension

The major fault active during the third extension phase of the area (post-18.8 Ma) is the Highland detachment (Fig. 1; Axen, 1986). A 15.3 Ma air-fall tuff is intercalated with syntectonic deposits related to the Highland detachment, demonstrating that the detachment was active at about 15 Ma (Taylor and others, in prep.).

This extensional system consists of the west-dipping Highland detachment and its upper-plate faults. Among the upper-plate faults are at least some of the postvolcanic normal faults in the study area. These postvolcanic faults cut units as young as the 18.8 Ma Hiko Tuff, and include three distinct groups of faults that together accommodate about 4 km of extension. In chronologic order, determined from cross-cutting relations, they are (1) east-dipping normal faults that are probably listric, (2) a west-dipping low-angle normal fault and its upper-plate faults and, (3) the west-dipping White River fault (Tschanz and Pampeyan, 1970) and related faults.

Of particular interest is the low-angle normal fault, which extended the area about 2 km, based in part on correlation of offset segments of the older, listric postvolcanic faults. The low-angle fault originally dipped about 50°W. Three arguements suggest that the fault formed at this low dip. First, the bedding-fault angle is low, which suggests that the strata and the fault had similar dips at the beginning of faulting. Restoring cross sections suggests these strata dipped gently at this time, and therefore so did the fault. Second, faults that cut the low-angle normal fault (Fig. 1). Their combined movement only served to steepen the low-angle normal fault (by about 3°). Third, the low-angle normal fault cuts the listric faults. Restoring the low-angle normal fault to a high angle reduces the dip of the listric faults, and probably rotates them through the horizontal to an apparent reverse gemetry. No structures are known that could explain such a previous orientation of the listric faults.

Pliocene-Quaternary extension

The Pahroc fault bounds the eastern side of the SR. Although no Quaternary scarp occurs along it, it probably was active early in the Quaternary because it cuts sediments of probable early Pleistocene age (William DiGuiseppi, personal communication). The Dry Lake Valley fault is marked by a Quaternary fault scarp 40 km long (Fig. 1; Tschanz and Pampeyan, 1970).

The Pahroc and Dry Lake Valley faults are both high-angle faults. Late Cenozoic faults are commonly presumed to represent a different fault style from the older detachment or core-complex style (e.g., Coney and Harms, 1983). However, these high-angle faults may correspond to upper-plate faults of detachments and therefore sole into a detachment at depth (Wright and Troxel, 1973). Such buried detachments are well known (e.g., Allmendinger and others, 1983).

One difference between the Quaternary faults and faults that sole into older detachments is that the Quaternary faults appear to be more widely spaced. This may indicate a greater depth to the detachment.

One motivation for drawing a distinction between older and younger types of faulting is that older faults have been associated with the mid-Tertiary "igminbrite flare-up," whereas the younger basin-and-range faults postdate it (e.g., Coney, 1978). The Dry Lake Valley area data show that the older faults need not correlate in time or space with volcanic activity. This relationship removes one reason for assuming two different fault styles.

SUMMARY

Our data and interpretations from the North Pahroc and Seaman Ranges allow us to draw several conclusions. (1) The temporally distinct extensional episodes documented in this area are pre-, syn- and post-volcanic. There is thus no consistent relationship between time of extension and volcanic eruptions. This argues against a simple, direct genetic relationship between magmatism and tectonic extension. (2) The oldest extension in the area is older than 31 Ma and prevolcanic. It is represented by the Seaman breakaway and the Stampede decollement. This extension is structurally similar to and may be coeval with the Snake Range extensional system located to the north. (3) Synvolcanic faulting in the area occurred between 30 and 27 Ma and resulted in a Late OLigocene regional unconformity. However, resulting extension was minor. (4) Some, and perhaps most, of the postvolcanic extension in the NPR may reflect upper-plate extension above the Highland detachment, which dips westward under the NPR. (5) The high-angle Quaternary faults in the area may sole into detachments at depth because similar fault geometries are seen in the upper plates of older detachments. (6) At least two major extensional systems were active in this area at different times, defining two overlapping regions of major crustal extension: the east-dipping prevolcanic (pre-31 Ma) system, and the west-dipping postvolcanic (post-18.8 Ma) and pre-Quaternary Highland detachment system. The younger shear system dips the opposite direction from the older one and therefore cuts it rather than reactivating it. More generally, it appears that each episode of extension represents the initiation and later deactivation of a distinct extensional shear system. The Quaternary fault activity in the region may reflect displacement along the youngest of these systems.

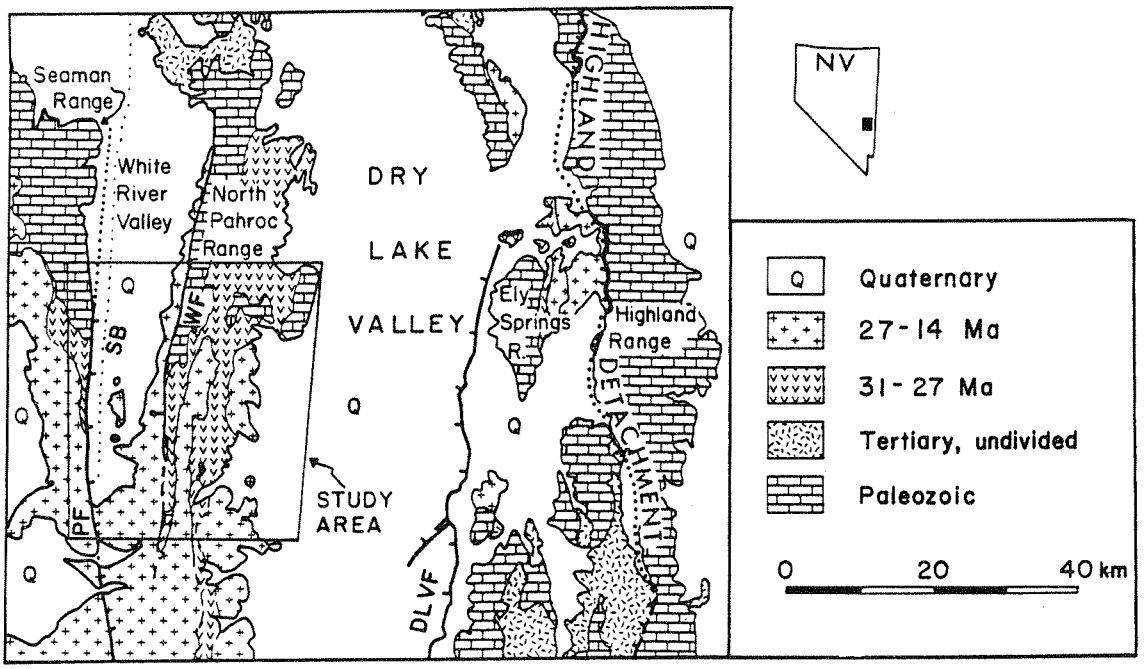

Figure 1. Location of study area and geographic places. DLVF - Dry Lake Valley fault, PF - Pahroc fault, WF - White River Fault, SB - Seaman breakaway.

Diagramatic Sketch of Relationships Between Tertiary Units and Faults

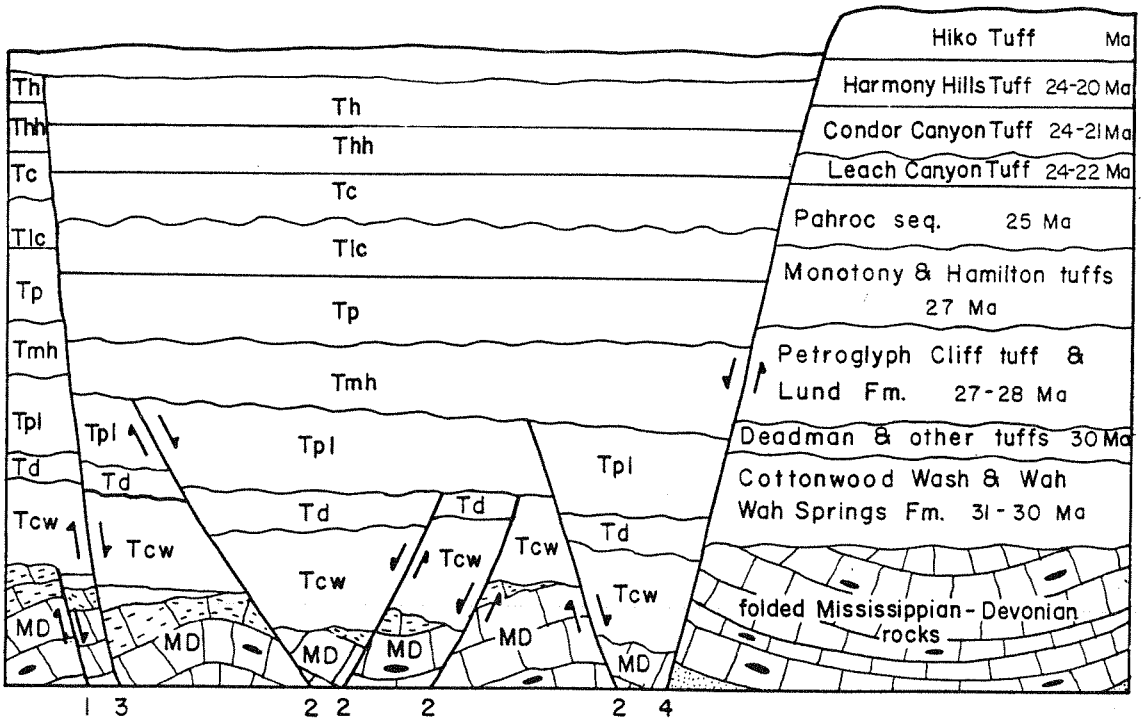

Figure 2. Diagramatic sketch of the relationships between stratigraphic units and faults. Representative faults are numbered according to their order of occurence. Dates for some of the tuffs from Best (1986).

REFERENCES

Allmendinger, R.W., Sharp, J.W., Von Tisch, D., Serpa, L., Brown, L., Kaufman, S., Oliver, J., and R.B. Smith, 1983, Cenozoic and Mesozoic structure of the eastern Basin and Range province, Utah, from COCORP seismic reflection data: Geology, v. 11, p. 532 - 536.

Axen, G.J., 1986, Superposed normal faults in the Ely Springs Range, Nevada: estimates of extension: Jour. of Struc. Geol., v. 8, p. 711-713.

Axen, G.J., Lewis, P.R., Burke, K.J., Sleeper, and Fletcher, J.M., 1988, in press, Tertiary extension in the Pioche area, Lincoln County, Nevada: in Weide, D.L., Geol. Soc. Am. Cordilleran Section Field Trip Guidebook.

Bartley, J.M., G.J. Axen, W.J. Taylor and J.E. Fryxell, 1988, in press, Cenozoic tectonics of a transect through eastern Nevada near 38°N latitude: in Weide, D.L., Geol. Soc. Am. Cordilleran Section Field Trip Guidebook.

Best, M.G., 1986, Tertiary geology of the area between Milford, Utah and Pioche, Nevada: Utah Geological Assoc. Pub. 15, Thrusting and Extensional Structures and Mineralization in the Beaver Dam Mountains, Southwestern Utah, p. 77-86.

Coney, P.J., 1978, Cordilleran metamorphic core complexes: an overview: Geol. Soc. Amer. Memoir 153, p. 7-31.

Coney, P.J., and Harms, T., 1983, Cordilleran metamorphic core complexes: Cenozoic extensional relics of Mesozoic compression: Geology, v. 12, p. 550-554.

Miller, E.L., Gans, P.B., and Garing, J., 1983, The Snake Range decollement: an exhumed mid-Tertiary ductile-brittle transition: Tectonics, v. 2, p. 239-263.

Taylor, W.J., and Bartley, J.M., 1988, in press, Stratigraphy and structure of the North Pahroc and eastern Seaman Ranges: in Weide, D.L., Geol. Soc. Am. Cordilleran Section Field Trip Guidebook.

Taylor, W.J., Bartley, J.M., Lux, D.R., and Axen, G.J., in preparation, Timing of Tertiary extension in the Railroad Valley-Pioche Transect, Nevada: Constraints from $^{40}Ar/^{39}Ar$ ages of volcanic rocks.

Tschanz, C.M., and Pampeyan, E.H., 1970, Geology and mineral deposits of Lincoln County, Nevada: Nevada Bur. of Mines and Geol. Bull. 73, p. 1-109.

Wright, L.A., and Troxel, B.W., 1973, Shallow-fault interpretation of Basin and Range structure, southwestern Great Basin: in K.A. De Jong and R. Scholton, eds., Gravity and Tectonics, John Wiley, New York, p. 397-407.

ISOSTATIC UPLIFT, CRUSTAL ATTENUATION, AND THE EVOLUTION OF AN EXTENSIONAL DETACHMENT SYSTEM IN SOUTHWESTERN NEVADA

by Robert B. Scott
U.S. Geological Survey, MS 913, Federal Center, Denver, CO 80225

Introduction

Geological and geophysical evidence supports the existence of extensional detachments between the Sheep Range and Death Valley (fig. 1). I propose that geographically separated pieces of detachments between Death Valley and the Sheep Range are parts of a regional detachment system that has evolved since the Miocene, and that the system consists of lenses of strata separated by an anastomosing network of low- and high-angle normal faults (fig. 2). This manuscript emphasizes the probability that isostatic uplift within the region of greatest crustal attenuation in this system, the Bullfrog Hills core complex, controlled the evolution of the detachment system between the breakaway zone at the Sheep Range and the core complex. Features in this system are described from east to west, which is the apparent direction of tectonic transport.

Interpretation of Detachment System

West of the Sheep Range breakaway (Guth, 1981; Wernicke and others, 1984), relatively few detachments are reported in the literature. Myers (1987) reported the detachment of the Oligocene Horse Springs Formation from the underlying Paleozoic strata a few kilometers north of Mercury. The Tertiary sedimentary rocks are tightly folded and locally overturned; they overlie a low-angle fault above relatively gently dipping, massive Paleozoic rocks. Based on other field evidence, principally at the northern end of Yucca Flat, Myers considered the Mercury detachment part of a regional feature, not a local phenomenon related only to bending of Paleozoic strata at the northwestern end of the Las Vegas shear zone.

South of Mercury and a few kilometers south of U.S. Highway 95, Burchfiel (1965) mapped three levels of low-angle faults in Cambrian and upper Precambrian clastic strata; this zone of faults separates middle Paleozoic carbonate rocks of an upper plate from Precambrian clastic rocks of a lower plate. The steep normal faults of the upper plate rocks are abundant and strike generally northeastward, whereas the normal faults of the lower plate rocks are less abundant and strike more nearly northward. These relationships suggest that a multitiered system of detachment faults may exist throughout the region as shown conceptually on figure 2. The system south of Mercury is at a lower structural and stratigraphic level than the relatively shallow feature north of Mercury.

Seismic reflection data in the Mid Valley region, about 30 km northwest of Mercury, have been interpreted by McArthur and Burkhard (1986) to indicate the presence of a series of northeast-

and southwest-dipping listric normal faults that sole into a flat-lying detachment marked by a conspicuous reflector at a depth of about 3 km. The listric faults cut through surficial basin-fill deposits, Miocene volcanic strata, and Paleozoic rocks. McArthur and Burkhard further speculated from nearby field evidence that this Mid Valley detachment may be part of a regional feature.

Roughly 15 km to the southwest of Mid Valley in the Calico Hills, low-angle faults form complex anastomosing patterns within Miocene volcanic strata and possibly within Paleozoic rocks. These faults are considered to be part of the detachment system (Simonds and Scott, 1987). Structural geometry indicates that blocks at two localities in the Calico Hills have moved northward on local scoop-shaped low-angle faults, not in directions predicted from the geometry of gentle doming of the area. These local "scoops", which are similar to those in the upper plate of the Bullfrog Hills core complex (Maldonado, 1985), have moved in directions that are independent of the overall detachment system movement direction. The youngest rock affected by low-angle faulting in the Calico Hills area is the 11-Ma Timber Mountain Tuff on the northern side of the dome, and the oldest unaffected rock is the 9-Ma Shoshone Mountain Rhyolite on the eastern side of the dome. Two low-angle faults that are exposed along the western flank of the Calico Hills dip westward toward Yucca Mountain. Fault striae, which are essentially dip slip, indicate a westward movement of the upper plate at this locality.

Although detachment surfaces are not exposed on Yucca Mountain itself, there is geometric structural evidence that the mountain is underlain by a detachment surface and that the degree of extension increases from north to south (Scott, 1986). Miocene ash-flow tuffs, which dip uniformly eastward, are repeated by west-dipping normal faults (Scott and Bonk, 1984). The strata dip 5-10o in the northern part but dip 20-50o in the southern part of the mountain. The amount of offset on and abundance of normal faults increase southward. Also, paleomagnetic evidence of a progressive, vertical-axis, clockwise 35o rotation of the tuffs may indicate an interaction between a relatively shallow detachment and underlying right-lateral oroclinal bending and shearing that were associated with the Walker Lane belt as suggested by Scott and Rosenbaum (1986). The 11-Ma Timber Mountain Tuff at Yucca Mountain is significantly less affected by extension than is the 13-Ma Paintbrush Tuff. Extension continued to affect the Yucca Mountain area at a greatly reduced rate after 11 Ma and into the Quaternary along a secondary "breakaway" fault system (Scott and Whitney, 1987).

The detachment fault that is postulated to exist under Yucca Mountain appears to extend westward under Crater Flat. At the northern end of Bare Mountain, Cornwall and Kleinhampl (1961) mapped a north-dipping low-angle fault that separates Tertiary strata from underlying Paleozoic strata. This fault may be the uplifted northwestern extension of the detachment under Crater Flat and Yucca Mountain. Three lines of evidence suggest Bare Mountain

began to rise between 11 and 13 Ma and uplift has continued to the present. 1) Monolithologic Paleozoic carbonate strata are intercalated as sedimentary breccias immediately above a 11-Ma basalt in Tertiary basin-fill deposits and are exposed only in adjacent Bare Mountain (Carr and Parrish, 1985). 2) The 13-Ma Paintbrush Tuff does not thin against Bare Mountain, as does the 11-Ma Timber Mountain Tuff (Paul P. Orkild, USGS, oral commun., 1985). 3) Studies of the steep normal faults along the eastern side of Bare Mountain suggest that movement occurred during the Holocene or late Pleistocene (Reheis, 1986).

Uplift of Bare Mountain along normal faults on its eastern flank has disrupted and tilted northward the southern part of the upper detachment surface between Tertiary and Paleozoic strata (figs. 1 and 2). At the northern end of the mountain, this detachment progressively thins the Paleozoic sequence, cuts Devonian strata on the east and Cambrian strata on the west, tectonically, and removes most of the Paleozoic rocks (Cornwall and Kleinhampl, 1961). Below the upper detachment surface, the northwestern part of Bare Mountain is cut by numerous low-angle faults that further attenuate Paleozoic strata (Monsen, 1982). North of the Paleozoic exposures, in the east-dipping upper-plate Miocene tuffs, rocks as young as the Timber Mountain Tuff are tilted eastward and west-dipping normal faults terminate at the detachment surface. Striae on the detachment fault plunge northwestward.

Maldonado (1985) demonstrated that the upper detachment surface in northwestern Bare Mountain can be traced across the Amargosa Narrows into the Bullfrog Hills south and west of Beatty and can be extended westward where it forms a nearly horizontal fault that bounds the Bullfrog Hills core complex. The geometry of these relationships had been previously mapped by Ransome and others (1910). At the core complex, steeply dipping Miocene volcanic strata abut a gently domed fault surface that overlies amphibolite-grade gneisses, schists, granites, and pegmatites. The rocks in the core complex may consist of the metamorphosed equivalent of upper Precambrian sedimentary rocks (Bennie Troxel, University of California at Davis, oral commun., 1987), but the rocks appear to have experienced multiple periods of deformation similar to that expected in older Proterozoic crust. Based on the amphibolite grade of metamorphism and the thickness of missing upper Precambrian and Paleozoic strata, the amount of attenuation and uplift can be estimated to be roughly 10-15 km. This conclusion is supported by other examples of similar core complexes in the Death Valley area (Wright and Troxel, 1984; Wright and others, 1974) and by regional geophysical relationships. Seismic refraction and gravity data west of Yucca Mountain show a shallowing of midcrustal rocks; rocks with velocities of 6.3 km/sec are estimated to be at a depth between 1.5 and 0.5 km, and rocks with densities of 2.74 g/cm3 are at a depth of about 2 km beneath the core complex (Ackermann and others, in press). A minor Bouguer gravity crest runs southeastward through the core complex to follow the western edge of Bare Mountain (Healey and others, 1980). The

youngest rocks involved in the tilting of upper plate rocks are 7-Ma tuffs (Maldonado, 1985). Lineations on the detachment surface and in the mylonitized core complex trend westward.

South of the Bullfrog Hills core complex, the detachment surface disappears under alluvial deposits of the Amargosa Desert. South and west of the Amargosa Desert, the thickness of the Paleozoic and upper Precambrian strata increase in the Funeral and in the Grapevine Mountains as a result of a decrease in the degree of crustal attenuation. In the east-central part of the Funeral Mountains, low-angle faults that were mapped by Swadley and Carr (1987) between the Tertiary and underlying Paleozoic strata can be interpreted as detachment faults. Also, at Daylight Pass cobbles within the Tertiary sequence are sheared above a contact with Paleozoic carbonate rocks. In the Funeral Mountains, detachment faults (for example, the Boundary Canyon fault that forms the northern part of the detachment shown on figure 1) occur within the Precambrian sequence (Hamilton, in press). Although this stack of detachments seems to be the mirror image of the stack on the eastern side of the Bullfrog Hills core complex, the age of detachment decreases toward the southwest. The oldest rocks unaffected by detachment in the Funeral Mountains area are 4-Ma basalts (Hamilton, in press). Southwest of the Furnace Creek fault zone in the Death Valley area, the age of detachment is still younger (Hamilton, in press). Farther south, Burchfiel and others (1987) reported 8-10 km of movement during the Quaternary along a detachment fault between the northwestern end of the Panamint Range and the Darwin rise.

Summary

Before attenuation in the Bullfrog Hills area, the detachment system probably existed as a series of detachment surfaces at different stratigraphic levels, similar to that seen east and west of the core complex. These detachment surfaces now appear to be interconnected in an anastomosing pattern where lenses of Paleozoic strata are stranded between upper and lower detachment surfaces; this is similar to the structure seen on a smaller scale in the Calico Hills (Simonds and Scott, 1987). During the concentration of attenuation in the Bullfrog Hills area, the Paleozoic and upper Precambrian strata were tectonically transported along low-angle faults until the Tertiary volcanic strata abutted midcrustal rocks and formed the core complex (fig. 2). Concurrent isostatic uplift probably caused doming of the detachment surfaces. Between about 13 and 11 Ma, Bare Mountain began to rise on the eastern shoulder of this uplift. Ultimately, the uplift created steep normal faults on the eastern flank of Bare Mountain and broke the upper detachment fault into two parts, one east of and one west of Bare Mountain (fig. 2). Bare Mountain continues to be uplifted on that steep normal fault system. Although the region east of Bare Mountain has been isolated since 11 Ma, it still experiences extension on a detachment (Scott and Whitney, 1987), but only at a much reduced rate. In contrast, more rapid extension occurs southwest of the Bullfrog Hills.

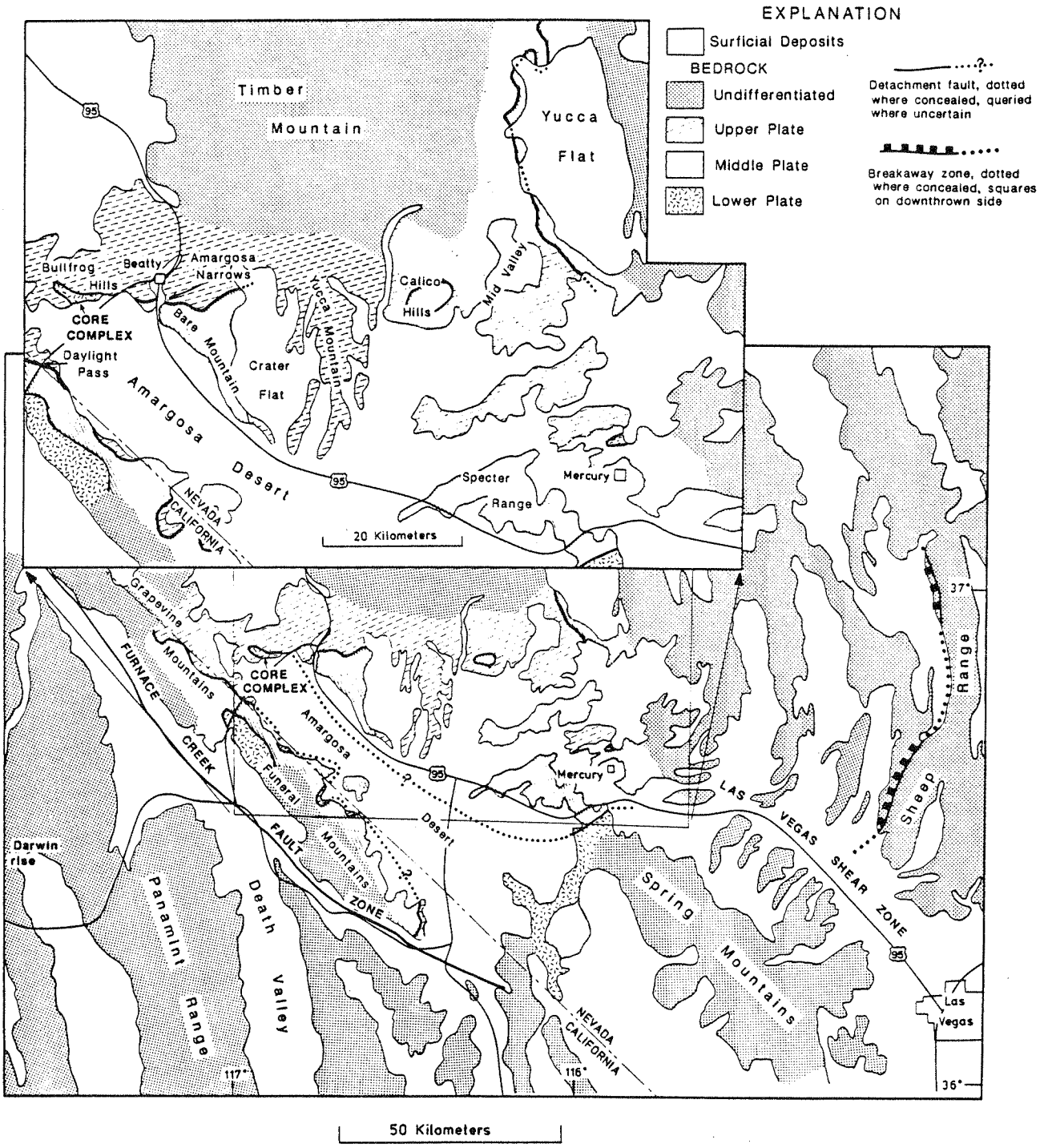

Figure 1. Generalized Cenozoic tectonic map of the Sheep Range-Death Valley area. At least two levels of major detachment fault planes exist; these detachment faults separate rocks into upper, middle, and lower plates. At the Bullfrog Hills core complex, the entire middle plate is locally missing.

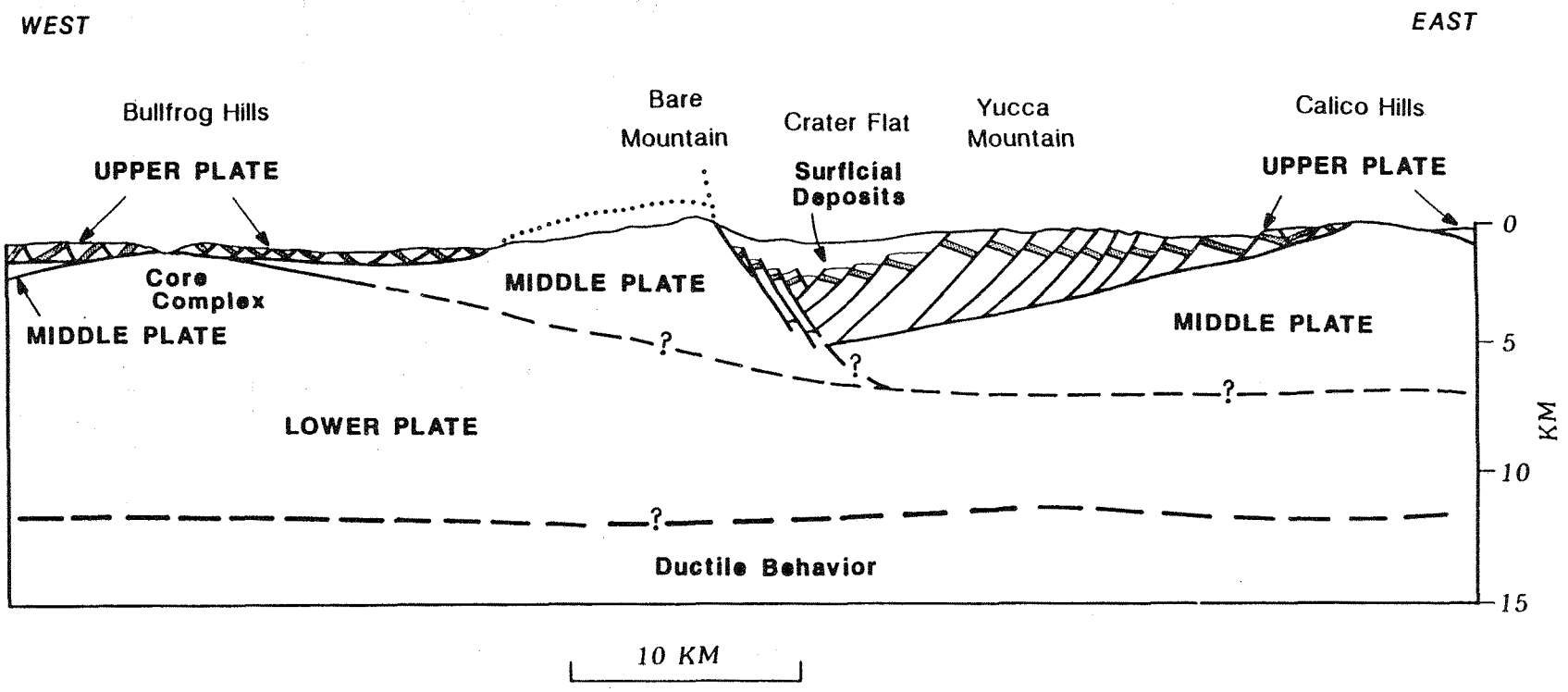

Figure 2. Generalized conceptual cross section from the Bullfrog Hills core complex to the Calico Hills. No vertical exaggeration. The depths and configuration of lower detachment faults are speculative. The dips of generalized strata are shown conceptually by shaded "unit" in the upper plate. Because the original positions of the plates relative to one another are difficult to determine, no relative movement directions are shown. The lowest detachment surface, between 10 and 15 km is the theoretical modern shear between relatively ductile and brittle crust. Steep normal faults, not shown here, probably translate extension on this lowest detachment upward to shallower detachment faults and to the surface.

References

Ackermann, H.D., Mooney, W.D., Snyder, D.B., and Sutton, V.D., in press, Preliminary interpretation of seismic refraction and gravity studies west of Yucca Mountain, Nevada and California, in Investigations of the geological and geophysical characterization of a potential nuclear waste disposal site at Yucca Mountain, southern Nevada: U.S. Geological Survey Bulletin 1790.

Burchfiel, B.C., 1965, Structural geology of the Specter Range quadrangle, Nevada, and its regional significance: Geological Society America Bulletin, v. 76, p. 175-192.

Burchfiel, B.C., Hodges, K.V., and Royden, L.H., 1987, Geology of Panamint Valley-Saline Valley pull-apart system, California: Palinspastic evidence for low-angle geometry of a Neogene range-bounding fault: Journal Geophysical Research, v. 92, p. 10,422-10,426.

Carr, W.J., and Parrish, L.D., 1985, Geology of drill hole USW VH-2, and structure of Crater Flat, southwestern Nevada: U.S. Geological Survey Open-File Report 85-475, p. 1-41.

Cornwall, H.R., and Kleinhampl, F.J., 1961, Geology of the Bare Mountain Quadrangle, Nevada: U.S. Geological Survey Geologic Quadrangle Map GQ 157, scale 1:62,500.

Guth, P.L., 1981, Tertiary extension north of the Las Vegas shear zone, Sheep and Desert Ranges, Clark County, Nevada: Geological Society America Bulletin, v. 92, p. 763-771.

Hamilton, W.B., in press, Detachment faulting in the Death Valley region, California and Nevada, in Investigations of the geological and geophysical characterization of a potential nuclear waste disposal site at Yucca Mountain, southern Nevada: U.S. Geological Survey Bulletin 1790.

Healey, D.L., Wahl, R.R., and Oliver, H.W., 1980, Bouguer gravity map of Nevada, Death Valley sheet: Nevada Bureau of Mines and Geology Map 69, scale 1:250,000.

Maldonado, Florian, 1985, Late Tertiary detachment faults in the Bullfrog Hills, southwestern Nevada [abs.]: Geological Society America Abstracts with Programs, v. 17, p. 651.

McArthur, R.D., and Burkhard, N.R., 1986, Geological and geophysical investigations of Mid Valley: Lawrence Livermore National Laboratory Report UCID-20740, p. 1-92.

Monsen, S.A., 1982, Structural evolution and metamorphic petrology of the Precambrian-Cambrain strata, northwest Bare Mountain, Nevada: Davis, University of California, M.S. thesis, 66 p.

Myers, W.B., 1987, Detachment of Tertiary strata from their Paleozoic floor near Mercury, Nevada [abs.]: Geological Society America Abstracts with Programs, v. 19, p. 783.

Ransome, F.L., Emmons, W.H., and Garry, G.H., 1910, Geology and ore deposits of the Bullfrog district, Nevada: U.S. Geological Survey Bulletin 407, 130 p.

Reheis, M.C., 1986, Preliminary study of Quaternary faulting on the east side of Bare Mountain, Nye County, Nevada: U.S. Geological Survey Open-File Report 86-576, p. 1-13.

Scott, R.B., 1986, Extensional tectonics at Yucca Mountain, Southern Nevada [abs.]: Geological Society America Abstracts with Programs, v. 18, p. 411.

Scott, R.B., and Bonk, Jerry, 1984, Preliminary geologic map of Yucca Mountain, Nye County, Nevada, with geologic sections: U.S. Geological Survey Open-File Report 84-494, scale 1:12,000.

Scott, R.B., and Rosenbaum, J.G., 1986, Evidence of rotation about a vertical axis during extension at Yucca Mountain, southern Nevada [abs]: Eos, Transactions American Geophysical Union, v. 67, p. 358.

Scott, R.B., and Whitney, J.W. 1987, The upper crustal detachment system at Yucca Mountain, SW Nevada [abs.]: Geological Society America Abstracts with Programs, v. 19, p. 332-333.

Simonds, F.W., and Scott, R.B., 1987, Detachment faulting and hydrothermal alteration in the Calico Hills, SW Nevada [abs.]: Eos, Transactions American Geophysical Union, v. 68, p. 1475.

Swadley, W C, and Carr, W.J., 1987, Geologic map of the Quaternary and Tertiary deposits of the Big Dune quadrangle, Nye County, Nevada, and Inyo County, California: U.S. Geological Survey Miscellaneous Investigations Series Map I-1767, scale 1:48,000.

Wernicke, Brian, Guth, P.L., and Axen, G.J., 1984, Tertiary extensional tectonics in the Sevier thrust belt of southern Nevada (Field Trip 19), in Linz, J.P., ed., Western Geological Excursions, v. 4: Reno, Nevada, Mackay School of Mines, p. 473-510.

Wright, L.A., Otton, J.K., and Troxel, B.W., 1974, Turtleback surfaces of Death Valley viewed as phenomena of extensional tectonics: Geology, v. 2, p. 53-54.

Wright, L.A., and Troxel, B.W., 1984, Geology of the northern half of the Confidence Hills 15-minute quadrangle, Death Valley region, eastern California--The area of the Amargosa Chaos: California Division of Mines and Geology Map Sheet 34, 31 p., and map, scale 1:24,000.

STRUCTURAL GEOLOGY OF THE INDIAN SPRINGS 1:100,000 QUADRANGLE, SOUTHERN NEVADA, AND THE ROLE OF MANTLE-TAPPING IN GREAT BASIN VOLCANISM

Peter L. Guth
PETMAR Trilobite Breeding Ranch
105-A Chaucer Road
Mt. Laurel, NJ 08054

The geology of the Indian Springs 1:100,000 quadrangle, northwest of Las Vegas and immediately east of the Nevada Test Site, remains poorly known. Recent mapping (Guth, in prep.) has revealed the major geologic features, with both practical and theoretical implications. Detailed knowledge of the regional geology of southern Nevada is critical to the decision on siting a nuclear waste repository, and that same knowledge will provide fundamental data to support models of continental extension.

The Indian Springs quadrangle contains portions of seven mountain ranges north of Las Vegas Valley. From west to east, these are: the Spotted Range, Pintwater Range, Desert Range, East Desert Range, Black Hills, Sheep Range, and Las Vegas Range. Smaller but significant bedrock outcrops occur south of Las Vegas Valley on Indian Ridge and in unnamed hills south of the town of Indian Springs, and in a small portion of the northwestern Spring Mountains. Except for three U.S.G.S. 1:24,000 quadrangle maps covering part of the Nevada Test Site and the small area in the northwest Spring Mountains, the only previous mapping in the area was the reconnaissance work of Longwell (Longwell and others, 1965).

The Indian Springs quadrangle is characterized by late Precambrian and Paleozoic miogeosynclinal strata, large-scale Mesozoic thrust faults, and Tertiary extensional tectonics. Normal and strike-slip faults, clastic and lacustrine strata, regional volcanism, and widespread landslides characterize the Tertiary history. Outstanding exposures of the structures at the breakaway zone of a detachment fault occur along the west side of the Sheep Range.

Miogeosynclinal rocks exposed in the quadrangle range in age from Late Precambrian to Late Mississippian; Pennsylvanian and Permian units occur south of Las Vegas Valley and below the Gass Peak thrust. Late Precambrian (?) and Early Cambrian clastic strata consist largely of sandstone, quartzite, and siltstone, exposed in the Desert Range and Las Vegas Range. Middle Cambrian to mid Devonian rocks are mostly dolomite with some limestone and a few clastic units. The higher Devonian units and the Mississippian rocks are mostly limestone with a few shale and quartzite interbeds.

MESOZOIC THRUST FAULTS

Paleozoic rocks in this area may belong to three thrust plates: Dry Lake thrust (Las Vegas and Pintwater Ranges), Gass Peak thrust (Sheep, East

Desert, Desert, and eastern Spotted Ranges), and Spotted Range thrust (western Spotted Range). The Gass Peak thrust does not appear to have been reactivated during the Tertiary along its current outcrop trace, but may have been reactivated to the north where it disappears under alluvium. The thrust plate must have been at least 9000 m thick and probably had at least 40 km of horizontal displacement. Two additional thrusts have been mapped to the west, in the Pintwater Range (Longwell and others, 1965) and the Spotted Range (Barnes and others, 1982; Longwell and others, 1965). The faults had a thrust history because units adjacent to the fault developed cleavage, which regionally did not develop during Tertiary extension. New mapping reveals that both thrusts have been reactivated during Tertiary extensional tectonism. I interpret the Pintwater thrust as a deeper ramp of the Gass Peak thrust system, and the Spotted Range thrust as a higher, regional thrust riding on a decollement in the Mississippian shales. The nature of the thrusts reported in the Nevada Test Site (Barnes and Poole, 1968) requires reinvestigation; probably they are at least in part Tertiary extensional features. Royse (1983) suggested that the Las Vegas Valley shear zone formed a lateral ramp in the thrust belt; if so, the ramp was reactivated during during Tertiary extension.

The youngest preserved Paleozoic unit north of the Las Vegas Valley shear zone in northwest Clark County is the Mississippian Indian Springs Formation, preserved in both the Sheep and Spotted Ranges, suggesting that all younger units were removed prior to major extension. Because of this shale's incompetence and potential to act as a decollement horizon, the removal of Pennsylvanian, Permian, and Mesozoic units (or, alternatively, higher thrusts including the Spotted Range plate) may have been by tectonic processes rather than erosion.

TERTIARY EXTENSION

All Tertiary structures exhibit brittle, surficial deformation, including landslides and limited folding. Tertiary structures include synchronous strike-slip faults, low- and high-angle normal faults, and landslides. The Las Vegas Valley shear zone forms the southern boundary of a large extensional terrane (Anderson, 1973; Guth, 1981; Wernicke and others, 1984).

Associated with these structures are sedimentary deposits in small tectonic basins. Two generations of Tertiary basins occur in northwestern Clark County: a Horse Spring Formation equivalent that formed during Miocene extension, and a poorly understood older group of rocks in the Pintwater Range and Fallout Hills deposited by a major river system. Tertiary basins occur above the hanging walls of the extensional faults, were rotated about a horizontal north-south axis, and have fault-bounded east-west trending terminations. In the western part of the quadrangle the basins include volcanic flows, while in the eastern part they include only air-fall tuffs. Tertiary basinal sediments were deformed beneath landslide masses composed of Paleozoic carbonate rocks that slid into the basins.

Breakaway zones for major west-dipping extensional normal faults of the Sheep Range detachment system occur on the west sides of the Sheep, Pintwater, and Spotted Ranges. The extensional fault in the Sheep Range avoids the Gass Peak thrust ramp exposed just to the east in the Las Vegas Range, but may reactivate the thrust at depth. The Pintwater and Spotted Range extensional faults reactivate Mesozoic thrusts. Traces of these breakaway faults are irregular and cut obliquely through range blocks. I interpret the north-south high-angle faults as soling into one or more major west-dipping detachments in the subsurface. The breakaway zone in the Spotted Range may be the most significant of the three. It bounds a region of extreme upper crustal extension, since to the west only scattered remnants of the Paleozoic sequence poke through thick Tertiary volcanic rocks. These detachment faults extend toward the west under the Nevada Test Site.

RELATION OF EXTENSION TO VOLCANISM

The relationship between Cenozoic extension in the Great Basin and the widespread, coeval volcanism remains enigmatic. Many authors have pointed out the close relationships (e.g. Axen and others, 1987; Gans and others, 1987), but other authors have pointed out that areas of extreme surficial extension do not correspond directly with any volcanic or plutonic activity (e.g. Wernicke and others, 1984, 1985). The Sheep Range detachment represents a prime example of extreme extension with coeval volcanism located in the Nevada Test Site about 100 km from the extensional breakaway zone.

Bosworth (1987) developed a detachment model for the East African rifts, and noted that the major volcanism occurred off the rift axis. In his cross section the volcanoes occur above the point where the detachments reach the mantle, but suggested that strike-slip "accommodation zones" may have provided the conduit for magma to reach the surface. Faults penetrating through the crust to the mantle have been clearly imaged on seismic reflection studies both by BIRPS (Klemperer and Matthews, 1987), and a COCORP line in eastern Nevada (feature SCF on Line 5, shown but not discussed in Klemperer and others, 1986, figs.2 and 3).

The master detachment for the Sheep Range system dips westerly from its breakaway zone in the Sheep Range, normal to the north-south trend of volcanic centers in the Nevada Test Site. Extension in the Indian Springs quadrangle was roughly coeval with the Test Site volcanism. Over a distance of 100 km with a crustal thickness about 30-35 km, this requires a dip of 20° if the detachment intersects the mantle below the volcanic centers of the Test Site. The Test Site's location at the junction of two strike-slip accommodation zones (Las Vegas Valley and Pahranagat shear zones) might aid the ascent of magma, or magma may rise along a linear trace above the detachment-mantle intersection.

This interpretation can be extended to other volcanic centers in the Great Basin. The currently active Death Valley extensional fault system (Jones, 1987) also dips to the west and its master detachment might reach

the mantle in the vicinity of Owen's Valley where volcanic activity (Long Valley Caldera, Mono Craters, Bishop Tuff) may be controlled by the detachment. A breakaway zone at the Colorado Plateau for a west dipping normal fault system (Smith and others, 1987) could reach the mantle to create the Lake Mead volcanic field; this geometry would require a 30° dipping fault, equal to the dip observed on the fault penetrating the crust on COCORP line 5. This analysis suggests three major detachment systems between the Colorado Plateau and the Sierra Nevada at the latitude of Las Vegas. As other detachment systems are traced in detail through the Great Basin, other volcanic centers may well be found to lie above the intersections of the faults with the mantle.

The details of magma generation and ascent must be complicated, modified by local geology. Mantle tapping by the detachment produces pressure release to generate magmas, which rise to the surface with minimal contamination. This model is similar to subduction zone magma generation, modified by the local state of stress. In extension, the least principle stress will be horizontal and magmas will ascend normal to it (hydrofracture failure and the familiar orientation of dikes). In the Great Basin the least principal stress will be roughly east-west, and the magmas should be aligned in north-south trends. In compression at a subduction zone, the least principal stress will not be oriented to produce a favorable path normal to the plate boundary for magmas to follow. Subduction zone magmas will slowly work their way to the surface and undergo greater contamination.

The mantle-tapping model can be tested as detachment systems are traced and dated throughout the Great Basin. Breakaway zones and extreme upper crustal extension consistently occurring 75-200 km away from coeval volcanism in the upper plate of the detachment systems will support the model.

REFERENCES CITED

Anderson, R.E., 1973, Large-magnitude late Tertiary strike-slip faulting north of Lake Mead, Nevada: U.S. Geological Survey Professional Paper 794, 18 p.

Axen, G.J., Bartley, J.M., and Taylor, W.J., 1987, Time-space relationships of Tertiary extension and magmatism in the eastern Great Basin: Geological Society of America Abstracts with Programs, vol.19, no.6, p.355.

Barnes, H., and Poole, F.G., 1968, Regional thrust-fault system in Nevada Test Site and vicinity: Geological Society of America Memoir 110, p.233-238.

Barnes, H., Ekren, E.B., Rodgers, C.L., and Hedlund, D.C., 1982, Geologic and tectonic maps of the Mercury quadrangle, Nye and Clark Counties, Nevada: U.S. Geological Survey Map I-1197.

Bosworth,W., 1987, Off-axis volcanism in the Gregory rift, east Africa: implications for models of continental rifting: Geology, vol.15, p.397-400.

Gans, P.B., Mahood, G., and Schermer, E., 1987, Synextensional magmatism in the Basin and Range Province: A case study from the eastern Great Basin: Geological Society of America Abstracts with Programs, vol.19, no.7, p.671.

Guth, P.L., 1981, Tertiary extension north of the Las Vegas Valley shear zone, Sheep and Desert Ranges, Clark County, Nevada: Geological Society of America Bulletin, vol.92, p.763-771.

Jones, C.H., 1987, Is extension in Death Valley accommodated by thinning of the mantle lithosphere beneath the Sierra Nevada, California: Tectonics, vol.6, no.4, p.449-473.

Klemperer, S.L., and Matthews, D.H., 1987, Iapetus suture located beneath the North Sea by BIRPS deep seismic reflection profiling: Geology, vol.15, p.195-198.

Klemperer, S.L., Hauge, T.L., Hauser, E.C., Oliver, J.E., and Potter, C.J., 1986, the Moho in the northern Basin and Range province, Nevada, along the COCORP 40°N seismic-reflection transect: Geological Society of America Bulletin, vol.97,p.603-618.

Longwell, C.R., Pampeyan, E.H., Bowyer, B., and Roberts, R.J., 1965, Geology and mineral deposits of Clark County, Nevada: Nevada Bureau of Mines Bulletin 62, 218 p.

Royse, F., 1983, Comment on 'Magnitude of crustal extension in the southern Great Basin': Geology, vol.11, p.495-496.

Smith, E.I., Anderson, R.E., Bohannon, R.G., and Axen, G.J., 1987, Miocene extension, volcanism, and sedimentation in the eastern Basin and Range province, southern Nevada: in G.H. Davis and E.M. VandenDolder, eds., Geologic Diversity of Arizona and its Margins: Excursions to Choice Areas, Arizona Bureau of Geology and Mineral Technology Special Paper 5, p.383-397.

Wernicke, B., Guth, P.L., and Axen, G.J., 1984, Tertiary extensional tectonics in the Sevier belt of southern Nevada: in J. Lintz, Jr., ed., Western Geological Excursions, Geological Society of America and Department of Geological Sciences, Mackay School of Mines, vol. 4, p.473-510.

Wernicke, B., Walker, J.D., and Beaufait, M.S., 1985, Structural discordance between Neogene detachments and frontal Sevier thrusts, central Mormon Mountains, southern Nevada: Tectonics, vol.4, p.213-246.

Mid-Miocene Igneous Rocks in the Lake Mead Area of Nevada and Arizona: Production of Intermediate Igneous Rocks in an Extensional Environment

Eugene I. Smith, Daniel L. Feuerbach, Terry R. Naumann

Department of Geoscience, University of Nevada, Las Vegas, Nevada 89154

James G. Mills

Department of Geology, Michigan State University, East Lansing, Michigan 48824

Summary of a paper in Press: Geological Society of America Special Paper; "Cordilleran Magmatism" edited by J.L. Anderson

INTRODUCTION

Mid-Tertiary volcanic rocks of the Lake Mead field (Figure 1) are calc-alkalic to alkali-calcic and vary continuously in composition from basalt to rhyolite. Volcanic rocks formed during Basin-and-Range extension and are spatially and genetically associated with diorite to granite of the Wilson Ridge pluton. Locally, igneous rocks were subjected to potassium metasomatism.

Field relations and petrography provide evidence of disequilibrium mineral assemblages and liquid-liquid mixing of basalt and granite magmas to form the intermediate rocks types of the Lake Mead volcanic field. Evidence of mixing includes incompatible phase assemblages of euhedral olivine, embayed quartz and sodic plagioclase within andesite flows. Plagioclase occurs in rounded and partially resorbed clusters of equant crystals and commonly displays oscillatory zoning and outer glass charged zones (fretted texture). Quartz phenocrysts are commonly surrounded by rims of prismatic augite and glass. Fine-grained spheroidal to ellipsoidal inclusions of basalt are common in dacite flows and dikes. Thus, various mixing ratios of olivine basalt and granite end members may be responsible for the textural variations observed in volcanic rocks of the Lake Mead field.

CHEMICAL EVOLUTION

The evolution of the igneous rocks of the Lake Mead field was evaluated by petrogenetic models involving both crystal fractionation and magma mixing. Magma evolution was complex and probably involved episodic and/or coeval fractional crystallization, magma mixing, crustal assimilation and partial melting. Models based on trace elements confirm that concurrent and/or episodic mixing and fractionation are the dominant differentiation processes. Open system models provide estimates of the relative importance of the two processes and suggest that mixing was more important in the

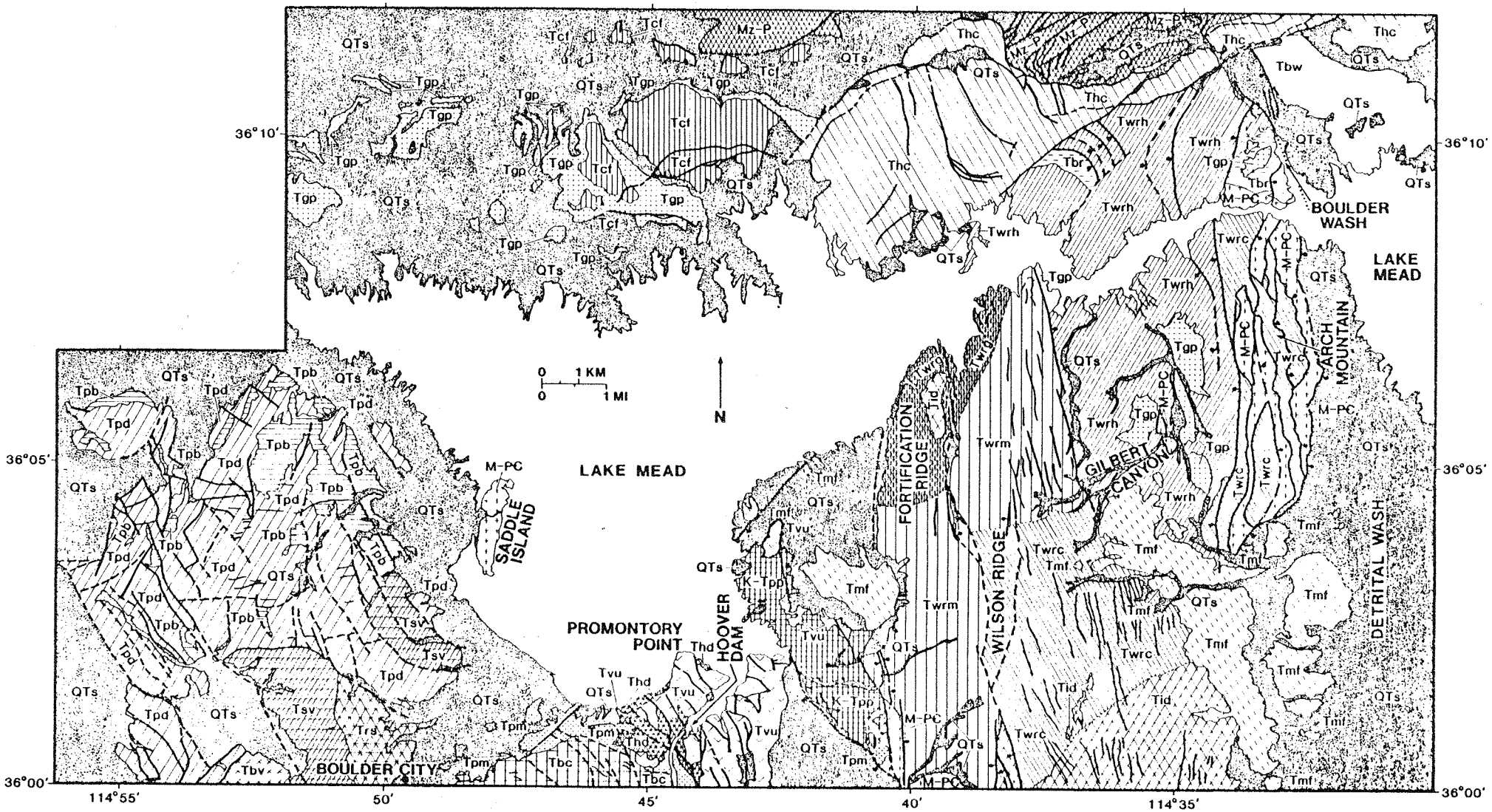

Figure 1. Geological Map of the Lake Mead Volcanic Field.

Quaternary

Tertiary

Mesozoic

Paleozoic

Precambrian

Tpd Tpb

Powerline Road volcanic rocks
Tpd - dacite
Tpb - basalt and andesite

Tbv - Bootleg Wash volcanic rocks

Tbv

Trs Tsv

River Mountains Stratovolcano
Trs - quartz monzonite stock
Tsv - andesite and dacite

QTs - Tertiary and younger sediments

Tmf - Fortification Hill Basalt

Tcf - Callville Mesa volcanic rocks

Thc - Hamblin-Cleopatra volcanic rocks

Tgp - Unassigned volcanic rocks

Tvu - Upper Hoover Dam volcanic rocks includes:
Dry Camp Conglomerate
Kingman Wash Road Andesite
Sugarloaf Dacite
Arch Rock Dacite
Switchyard Andesite
Spillway Conglomerate

Thd Tbw Tbr

Thd - Tuff of Hoover Dam and Dam Conglomerate
Tbw - Boulder Wash volcanic rocks
Tbr - Breccia

Tpm - Patsy Mine volcanic rocks

K-Tpp - Paint Pots intrusive rocks

Mz-P - Pennsylvanian through Mesozoic rocks

M-PC - Precambrian through Mississippian rocks

Faults - dotted where concealed - dashed where inferred bar and ball on downthrown side

Contact - dashed where inferred

Dike

Tbc

Tbc - Boulder City Pluton

Twrh Twrm Twrc Twrg Tid

Wilson Ridge Pluton
Twrh - hypabyssal phase
Twrm - medium-grained phase
Twrc - coarse-grained phase
Twrg - red feldspar granite phase
Tid - diorite phase

Figure 1. Geological Map of the Lake Mead Volcanic Field-Explanation.

derivation of the andesites and diorites than in the formation of dacite, quartz monzonite or granite.

PRODUCTION OF INTERMEDIATE COMPOSITION IGNEOUS ROCKS IN AN EXTENSIONAL ENVIRONMENT

Lipman et al. (1972) and Christiansen and Lipman (1972) suggested that the change from calc-alkaline intermediate volcanism to a bimodal rhyolite-basalt suite marked the charge from regional compression to extension. Even though bimodal suites form during periods of extension in many parts of the Basin-and-Range province (for example, Suneson and Lucchitta, 1983), recent work suggests that volcanism before and during the main pulses of extension is mainly calc-alkalic or alkali-calcic with basaltic-andesite, andesite and dacite predominating (Eaton, 1982, Anderson, 1973, Elston and Bornhorst, 1979, Smith, 1982, Otton, 1982). The tectonic transition between regional compression and extension may pass without affecting the nature of magmatic activity. Our observations suggest that the combined effect of mixing of basalt and granite end members and crystal fractionation results in magma compositions with many of the characteristics of a calc-alkaline or alkali-calcic suite formed during plate convergence. In the Lake Mead area, basalt and high silica granite (rhyolite) are inferred to be parental magmas, so, if mixing was prevented, a bimodal suite may have resulted. The occurrence of a bimodal suite, therefore may be more a function of the tectonic "state" of the crust rather than some primary petrogenetic process. If fractures dip steeply and penetrate to deep levels of the crust, magma may rise to the surface along these zones of weakness without mixing and volcanism will be characterized by bimodal suites. Alternately, if extension results in shallow faults (e.g., detachment structures), magma may rise until encountering a low-angle fault zone where it may accumulate. In this structural scenario, the opportunity for magma mixing is high, and intermediate rock series will predominate.

In the Lake Mead field, intermediate alkali-calcic volcanism (and plutonism) occurred just prior to detachment faulting (Weber and Smith, 1987). Basaltic volcanism, recorded by the Fortification Hill basalt (4-8 Ma) and by younger alkali basalt dikes and flows (Campbell et al., 1950; Anderson, 1973; Feuerbach and Smith, 1987) is dominant only during the waning stages of extension. Basaltic volcanism was controlled by high-angle normal faults that may penetrate deep within the crust (Feuerbach and Smith, 1987; Smith et al., 1987). The transition from calc-alkaline to bimodal volcanism may have occurred at the onset of basin-and-range extension as predicted by Lipman and Christiansen (1972), but this transition was obscured by the magma mixing process which resulted in magmas having a similar chemical affinity to those formed earlier during subduction related magmatism.

REFERENCES CITED

Anderson, R.E., 1973, Large-magnitude late Tertiary strike-slip faulting north of Lake Mead, Nevada: U.S. Geological Survey Professional Paper 794, 18 p.

Campbell, Ian and Schenk, E.T., 1950, Camptonite dikes near Boulder Dam, Arizona: American Mineralogist, v. 35, nos. 9-10, p. 671-692.

Christiansen, R.L. and Lipman, P.W., 1972, Cenozoic volcanism and plate-tectonic evolution of the western United States, II, Late Cenozoic: Philos. Transactions Royal Society of London Series A, v. 271. p. 249-284.

Eaton, G.P., 1982, The Basin and Range Province: origin and tectonic significance: Annual Review of Earth and Planetary Sciences, v. 10, p. 409-440.

Elston, W.E. and Bornhorst, T.J., 1979, The Rio Grande rift in context of regional post-40 m.y. volcanic and tectonic events: in Rio Grande Rift: Tectonics and Magmatism, ed. R.E. Riecker, pp. 418-438. Washington, D.C.: American Geophysical Union.

Feuerbach, D.L., and Smith, E.I., 1987, Late-Miocene Fortification Hill basalt, Lake Mead area, Nevada and Arizona: source areas and conduit geometry: Geological Society of America Abstracts with Programs, v. 19, no. 6, p. 376-377.

Lipman, P.W., Prostka, H.J., and Christiansen, R.L., 1972, Cenozoic volcanism and plate-tectonic evolution of the western United States, I, Early and middle Cenozoic: Philos. Transactions Royal Society of London Series A, v. 271. p. 217-248

Otton, J.K., 1982, Tertiary extensional tectonics and associated volcanism in west-central Arizona: in Frost, E.G., and Martin, D.L., eds., Mesozoic-Cenozoic tectonic evolution of the Colorado River region, California, Arizona and Nevada: San Diego, California, Cordilleran Publishers, p. 143-157.

Smith, E.I., 1982, Geology and geochemistry of the volcanic rocks in the River Mountains, Clark County, Nevada and comparisons with volcanic rocks in nearby areas, in Frost, E.G., and Martin, D.L., eds., Mesozoic-Cenozoic tectonic evolution of the Colorado River region, California, Arizona and Nevada: San Diego, California, Cordilleran Publishers, p. 41-54.

Smith, E.I., Eschner, E., Feuerbach, D.L., Naumann, T.R., and Sewall, A., 1987, Mid-Tertiary extension in the eastern Basin and Range Province, Nevada and Arizona: The Las Vegas Valley-Detrital Wash transect: Geological Society of America, Abstracts with Programs, v. 19, no. 7, p. 848-849.

Suneson, N.H. and Lucchitta, Ivo, 1983, Origin of bimodal volcanism, southern Basin and Range province, west-central Arizona: Geological Society of America Bulletin, v. 94, p. 1005-1019.

Weber, M.E., and Smith, E.I. 1987, Structural and geochemical constraints on the reassembly mid-Tertiary volcanoes in the Lake Mead area of southern Nevada: Geology, v. 15, p. 553-556.

POSSIBLE MODES OF DEFORMATION ALONG "ACCOMMODATION ZONES" IN RIFTED CONTINENTAL CRUST: AN EXAMPLE FROM THE SOUTHERN BASIN AND RANGE PROVINCE

Faulds, James E., Mawer, Chris. K., and Geissman, John. W., Department of Geology, University of New Mexico, Albuquerque, NM 87131

Rifted continental crust is characterized by structural asymmetry. Structural zones that coordinate reversals in the sense of rift asymmetry have been referred to as "accommodation zones" (Bosworth et al., 1986) or "transfer zones" (Gibbs, 1984). Accommodation zones facilitate reversals in the dominant tilt direction of fault blocks and possibly inversions in the dip of regional detachment systems. Despite recent significant contributions addressing accommodation zones in rifted continental crust (Chapin et al., 1978; Chamberlin, 1983; Dokka, 1983, 1986; Bally and Oldow, 1984; Etheridge et al., 1985; Lister et al., 1986a; Bosworth et al., 1986; Bosworth, 1987; Rosendahl, 1987), the nature of these zones remains controversial (Chapin et al., 1978; Bosworth, 1986; Lister et al., 1986b; Coffield, 1987; Faulds et al., 1987, 1988a, 1988b).

The key element of accommodation zones is that their deformational style is dictated by the amount and direction of movement of upper- and lower-plate rocks of the detachment terrane (Faulds et al., 1987). Thus, various models of extension can potentially be evaluated by defining the modes of deformation along a zone, especially if both lower- and upper-plate rocks crop out along the zone. Studies of accommodation zones can at least place some constraints on the overall kinematic evolution of rifted continental crust.

For example, major strike-slip displacement in the lower-plate rocks of accommodation zones, if contemporaneous with extension, would indicate that the zones facilitate reversal in the regional dip direction of major detachment faults and that lower-plate rocks are at least partly drawn out from upper-plate rocks in accordance with the models of Lucchitta and Suneson (1981) and Wernicke (1981, 1985). Confinement of strike-slip displacement to the lower-plate would suggest that the upper-plate of detachment terranes distends "passively", or more-or-less in situ, above an "actively" extending lower-plate. Strike-slip offset would be restricted in this case to areas in which lower-plate rocks of one domain are juxtaposed with upper- and/or lower-plate rocks of an adjacent domain (Fig. 1a). If strike-slip displacement also occurs between the upper-plate rocks of adjacent domains, documentation of its slip sense will determine whether upper-plate rocks are generally transported away from their tilt direction. If the accommodation zone facilitated movement in opposing directions of both upper- and lower-plate rocks, the sense of strike-slip displacement in the lower-plate would be opposite that in the upper-plate, and lateral offset may cease where lower- and upper-plate rocks of adjacent domains are juxtaposed (Fig. 1b).

In contrast, several possible scenarios (Fig. 1c) would result in little, if any, strike-slip displacement along accommodation zones, including (1) lateral transport in similar directions on either side of the zone of only the lower-plate; (2) diametrical movement between upper- and lower-plate but in similar directions on either side of the zone; and (3)

little movement in upper- and lower-plates, perhaps as a brittle upper-plate deforms more-or-less in situ above a lower-plate dominated by pure shear (e.g., Miller et al., 1983). In these cases, the accommodation zone would not facilitate inversion in the dip of regional detachment systems, but may simply accommodate interaction between laterally propagating conjugate normal faults in the upper-plate.

A major east-west-trending, middle Miocene accommodation zone cuts the central Black Mountains, northwestern Arizona, and southern Eldorado Mountains, southern Nevada. This sublinear, 5-km-wide zone separates more than 5,000 km^2 of east-tilted fault blocks on the north from 25,000 km^2 of dominantly west-tilted fault blocks on the south (Fig. 2). Fault-block tilting on either side of the zone commonly exceeds 60°. Tilting progressively decreases toward the axis of the zone (Fig. 3), where transversely oriented, oblique-slip normal faults accommodate scissors-like (or torsional) offset between gently ($20-35^{\circ}$) tilted, individual fault blocks of opposing polarity. Concomitant with the decrease in tilting, fault spacing decreases and average fault dip increases. East- and west-dipping faults are equally common in the axial part of the zone, whereas east- and west-dipping faults dominate the west- and east-tilted domains, respectively. Many of the major normal faults in the steeply tilted parts of the west- and east-tilted domains terminate in drag folds within the axial part of the accommodation zone. These features indicate that this accommodation zone in the upper-plate rocks corresponds to an area of interference between conjugate normal faults. Fault blocks within the zone were probably periodically tilted in opposite directions during the same episode of extension.

The lack of significant strike-slip faulting in the upper-plate rocks of the accommodation zone in the Black and Eldorado Mountains indicates little relative movement between the opposing tilt-block domains. Oblique-slip transverse faults in the accommodation zone facilitate torsional offset, associated with differential tilting, rather than transport of upper-plate rocks away from the tilt direction. Similar structures may account for interpretations of accommodation zones in the upper-plate rocks of passive continental margins as strike-slip faults, which supposedly accommodated diametrical lateral transport of opposing tilt-block domains (e.g., Lister et al., 1986a).

If the style of deformation observed in the upper-plate rocks of the Black and Eldorado Mountains is typical of accommodation zones in rifted continental crust, then the upper-plate rocks of detachment terranes probably deform more-or-less in situ, as hypothesized by Lucchitta and Suneson (1981). Unfortunately, very few accommodation zones have been studied in detail. Where comprehensive investigations of accommodation zones have been carried out, however, only minor strike-slip displacement has been recognized (e.g., Chapin et al., 1978; Chamberlin, 1983; Coffield, 1987). The sublinear trace of transversely-oriented accommodation zones in relatively autochthonous upper-plate rocks may, however, represent a surface manifestation of strike-slip faulting in actively extending, allochthonous lower-plate rocks, which lie beneath oppositely-dipping detachment faults.

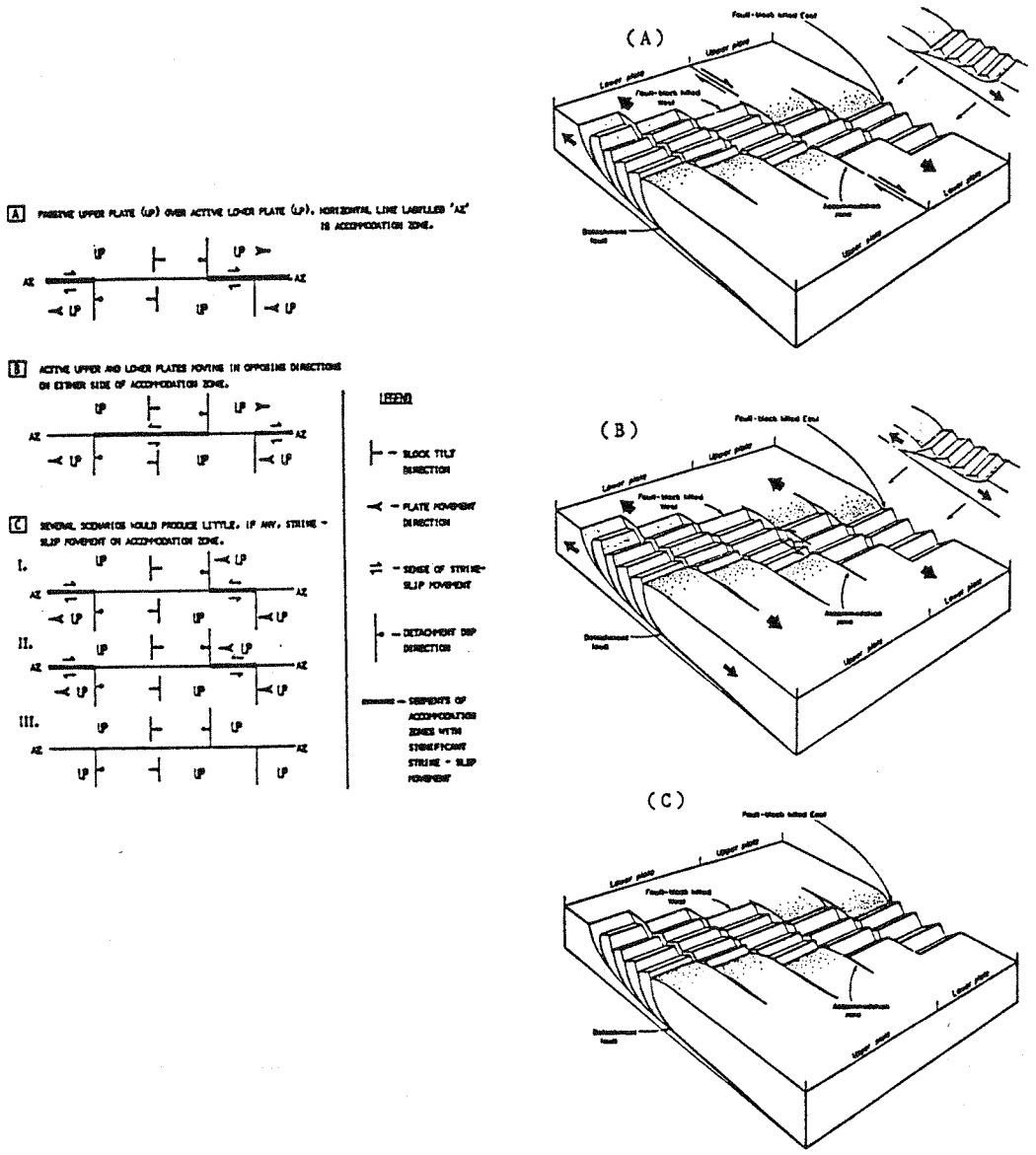

Figure 1. Possible modes of deformation along accommodation zones in rifted continental crust.

In (A) and (B), the accommodation zone facilitates inversion in the dip of detachment systems (inset at top right of diagram is a cross section of east-tilted domain). In (C), the accommodation zone does not facilitate reversal in the dip of detachment faults, but simply accommodates interaction between conjugate normal faults in the upper-plate. See text for further information.

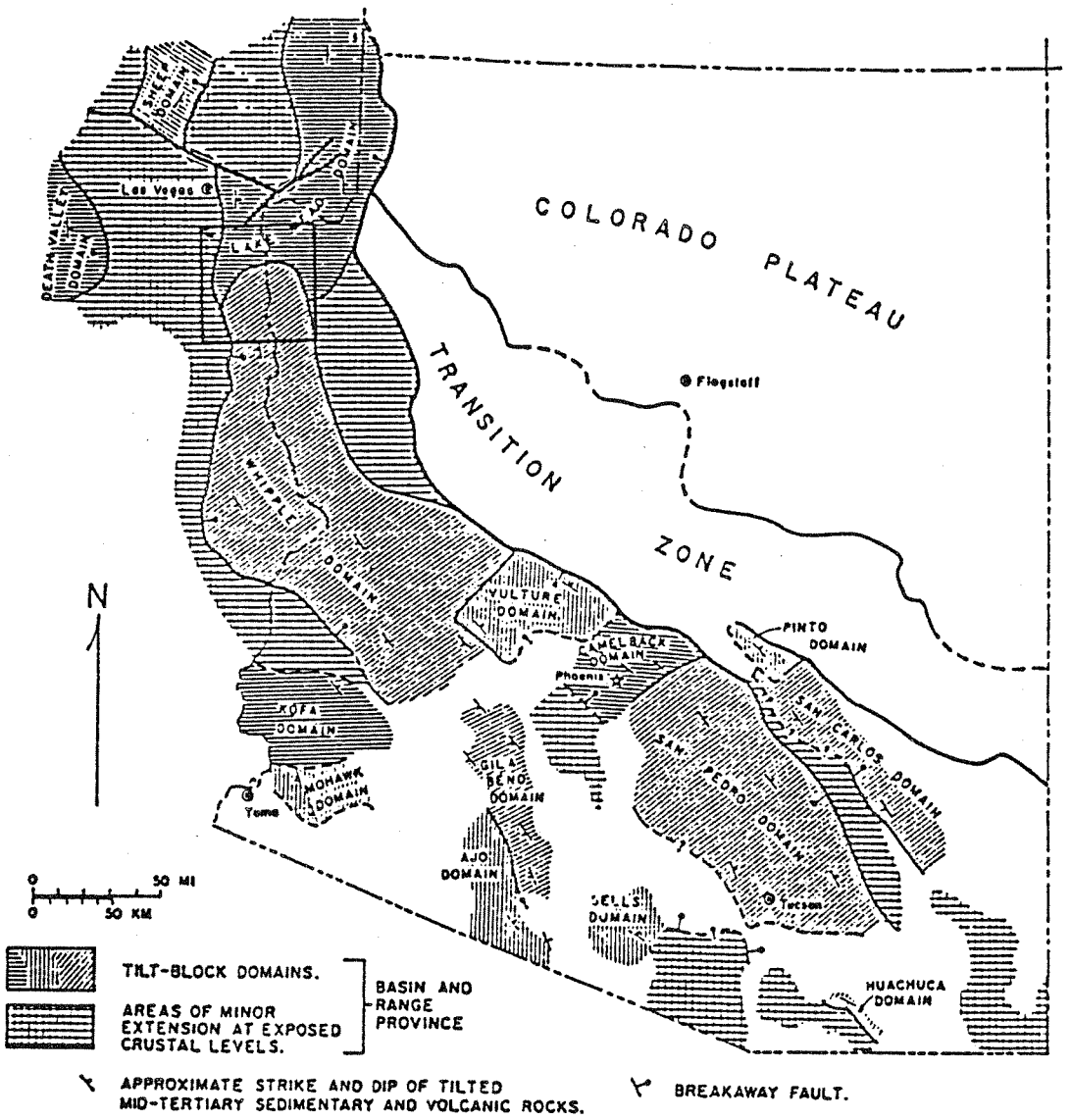

Figure 2. Tilt-block domains.

Map of tilt-block domains in the Basin and Range province of Arizona and adjacent areas (from Spencer and Reynolds, 1986). The accommodation zone in the Black and Eldorado Mountains lies within the blocked out area (upper left).

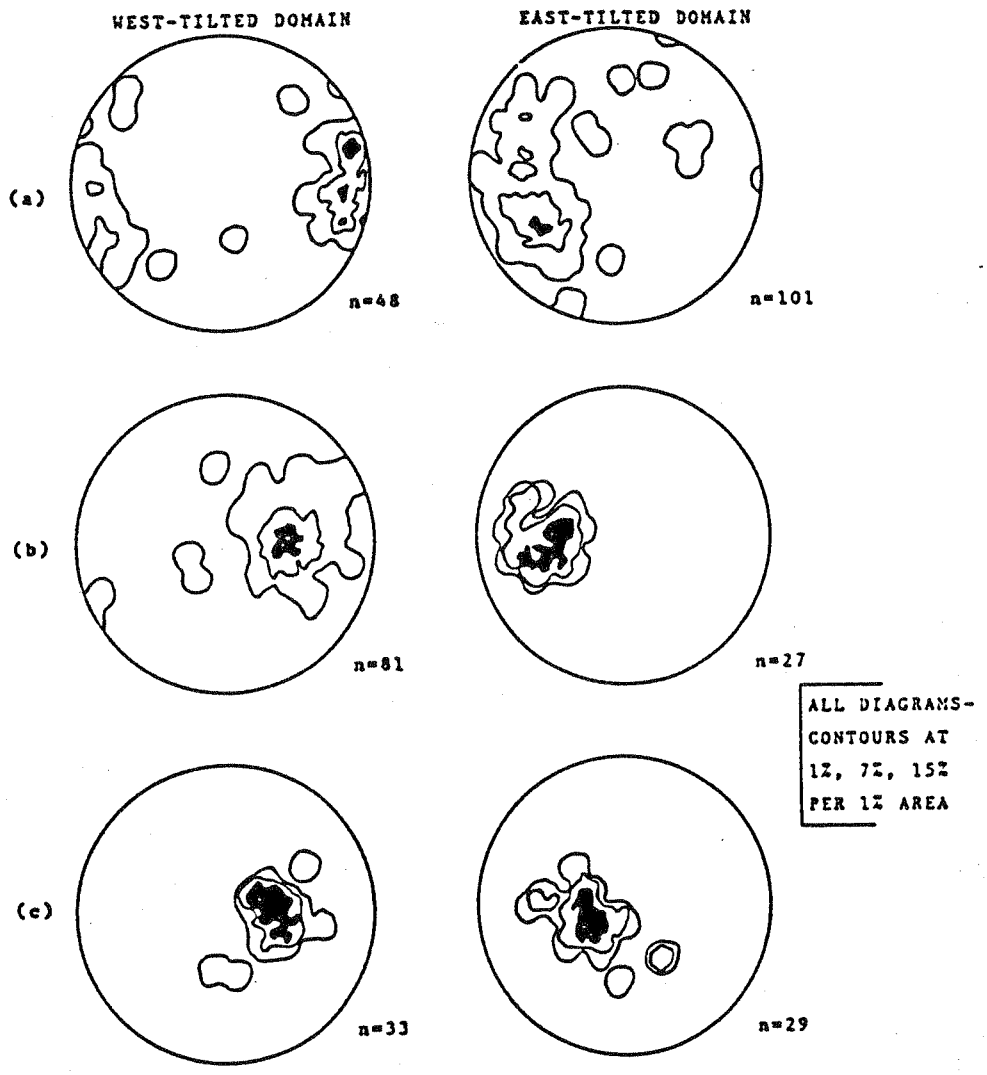

Figure 3. Equal-area stereo plots of poles to bedding and layering in Tertiary strata of central Black Mountains.

(a) More than 2.0 km from axis of accommodation zone. (b) 0.5 to 2.0 km from axis. (c) Less than 0.5 km from axis. Note that tilting progressively decreases toward the axial part of the accommodation zone in both east- and west-tilted domains. This decrease in tilt is accompanied by an increase in fault dip and decrease in fault spacing.

REFERENCES CITED

Bally, A. W., and Oldow, J. S., 1984, Late tectonics, structural styles, and the evolution of sedimentary basins: American Association of Petroleum Geologists Short Course Notes, 238 p.

Bosworth, W., 1986, Comment on "Detachment faulting and the evolution of passive continental margins": Geology, v. 14, p. 890-891.

_____ 1987, Off-axis volcanism in the Gregory rift, east Africa: Implications for models of continental rifting: Geology, v. 15, p. 397-400.

Bosworth, W., Lambiase, J., and Keisler, R., 1986, A new look at Gregory's rift: The structural style of continental rifting: EOS (American Geophysical Union Transactions), v. 67, p. 577-583.

Chamberlin, R. M., 1983, Cenozoic domino-style crustal extension in the Lemitar Mountains, New Mexico: A summary: New Mexico Geological Society Guidebook, 34th Field Conference, Socorro Region II, p. 111-118.

Chapin, C. E., Chamberlin, R. M., Osburn, G. R., White, D. L., and Sanford, A. R., 1978, Exploration framework of the Socorro geothermal area, in Field guide to selected cauldrons and mining districts of the Datil-Mogollon volcanic field: New Mexico Geological Society Special Publication No. 7, p. 114-129.

Coffield, D. Q., 1987, Surface expression and internal structure of an accommodation zone, Gulf of Suez, Egypt: (Abstract) American Association of Petroleum Geologists Bulletin, v. 71, no. 5, p. 540.

Dokka, R. K., 1983, Displacements on late Cenozoic strike-slip faults of the central Mojave Desert, California: Geology, v. 11, p. 305-308.

Dokka, R. K., and Baksi, A. K., 1986, Structure and sedimentation along the lateral boundaries of a detachment fault terrane, central Mojave extensional complex, California: Geological Society of America Abstracts with Programs, v. 18, p. 102.

Etheridge, M. A., Branson, J. C., and Stuart-Smith, P. G., 1985, Extensional basin-forming structures in Bass Strait and their importance for hydrocarbon exploration: Australian Petroleum Exploration Association Journal, v. 25, p. 344-361.

Faulds, J. E., Mawer, C. K., and Geissman, J. W., 1987, Possible modes of deformation along "accommodation zones" in rifted continental crust: Geological Society of America Abstracts with Programs, v. 19, p. 659-660.

Faulds, J. E., Hillemeyer, F. L., and Smith, E. I., 1988a, Geometry and kinematics of a Miocene "accommodation zone" in the central Black and southern Eldorado Mountains, Arizona and Nevada, in Weide, D. L., and Faber, M. L., eds., This extended land, geological journeys in the southern Basin and Range, Geological Society of America, Cordilleran Section, Field Trip Guidebook, p. 293-310.

Faulds, J. E., Mawer, C. K., and Geissman, J. W., 1988b, Geometry and kinematics of a major accommodation zone in the highly extended upper-plate rocks of the northern Colorado River trough, northwestern Arizona and southern Nevada: Geological Society of America Abstracts with Programs, v. 20, p. 159.

Gibbs, A. D., 1984, Structural evolution of extensional basin margins: Geological Society of London Journal, v. 141, p. 609-620.

Lister, G. S., Etheridge, M. A., and Symonds, P. A., 1986a, Detachment faulting and the evolution of passive continental margins: Geology, v.

14, p. 246-250.
Lister, G. S., Etheridge, M. A., and Symonds, P. A., 1986b, Reply to Discussion of "Detachment faulting and the evolution of passive continental margins": Geology, v. 14, p. 891-892.
Lucchitta, I., and Suneson, N., 1981, Comment on "Tertiary tectonic denudation of a Mesozoic-early Tertiary (?) gneiss complex, Rawhide Mountains, western Arizona": Geology, v. 9, p. 50-52.
Miller, E. L., Gans, P. B., and Garing, J., 1983, The Snake Range decollement-an exhumed mid-Tertiary ductile-brittle transition: Tectonics, v. 2, p. 239-263.
Rosendahl, B. R., 1987, Architecture of continental rifts with special reference to East Africa: Annual Reviews of Earth and Planetary Science Letters, v. 15, p. 445-503.
Spencer, J. E., and Reynolds, S. J., 1986, Some aspects of the middle Tertiary tectonics of Arizona and southeastern California: Arizona Geological Society Digest, v. 16, p. 102-107.
Wernicke, B., 1981, Low-angle faults in the Basin and Range province--Nappe tectonics in an extending orogen: Nature, v. 291, p. 645-648.
_____ 1985, Uniform-sense normal simple shear of the continental lithosphere: Canadian Journal of Earth Sciences, v. 22, p. 108-125.

DOMING OF THE LOWER CRUST BENEATH AN EXTENSIONAL OROGEN?

Laura Serpa, Dept. of Geology and Geophysics, University of New Orleans, New Orleans, LA 70148

ABSTRACT

COCORP deep seismic reflection data from the Mojave and Death Valley regions provide a cross-section across an extensional orogen. Those data suggest that the lower crust domes beneath the area of rapid extension while the Moho remains relatively flat. In this report, potential causes of the doming and the significance of that doming on crustal models of extensional terranes are discussed.

INTRODUCTION

During the past 15 Ma., the area (Fig. 1) of the Basin and Range province between the Garlock fault zone, the Nopah Range, the Furnace Creek fault zone, and the Sierra Nevada batholith has been the site of active extension, characterized by rapid basin subsidence, tilting of mountain blocks, both normal and strike-slip faulting, and volcanic activity (e.g. Burchfiel and Stewart. 1966; Stewart, 1983; Wright, 1976; Wright and Troxel, 1973). In contrast, the Mojave region and the area to the east of the Nopah Range, (Fig. 1) have experienced significantly less deformation during that time (e.g. Burchfiel et al., 1982; Burchfiel and Davis, 1975; Davis and Burchfiel, 1973; Dokka, 1986). The COCORP Death Valley survey provides continuous subsurface coverage of the area from the eastern side of the Nopah Range into the area of active extension, while the Mojave COCORP survey crosses the Mojave desert region and extends across the Garlock fault zone into the area of active extension (de Voogd et al., 1986; Serpa et al., 1988; Cheadle et al., 1986a; b). Thus those seismic reflection data provide insight on the changes occurring in the lower crust of an extensional orogen.

Those two survey areas are separated by a distance of 50 km where there is no available seismic coverage. However, comparison of reflections from either side of the data gap indicate that there are two possible reflecting horizons which are continuous between the two survey areas. The nature of those horizons is the topic of this paper.

Throughout the following discussion a velocity of 6 km/s is assumed for the conversion of travel times to depths. That velocity is an approximation which is consistent with the results of previous refraction surveys in the area (e.g. Roller and Healy, 1963; Johnson, 1965; Prodehl, 1979). True depths may vary significantly from those estimated due to both lateral velocity variations in the subsurface. Based on the available velocity information derived from the seismic reflection data and the range of reported refraction velocities, those variations are inferred to produce no more than a 10 percent uncertainty in the estimated depths to the reflecting horizons. However, reflections from out of the plane of the seismic sections have also been identified and

their depths may vary significantly from those estimated. The reflections discussed in this paper can all be viewed on either intersecting seismic lines or throughout an area where the lines bend and, thus, their subsurface geometry is well constrained three-dimensionally in the subsurface.

IDENTIFICATION OF POSSIBLE CONTINUOUS REFLECTIONS

There are two reflecting zones which appear to be sufficiently continuous throughout the Death Valley survey region (Fig. 2) to be possible candidates for correlation with the Mojave survey area. The first is located at midcrustal depths (5.0 s +/- 1.5 s or approximately 15 km depth) and the other at or near the base of the crust (10.0 s +/- 1.0 s or approximately 30 km depth). The latter is designated the reflection Moho, following the nomenclature of Klemperer et al (1986) and the former is referred to here as the Death Valley detachment zone.

Similarly, there are two reflecting horizons which appear to be continuous throughout most of the Mojave survey area (Cheadle et al., 1986 a; b). The first dips to the southwest from a depth of approximately 9 km (3 s) near the Garlock fault zone to approximately 20 km (7 s) near the San Andreas fault zone. The second is located at a depth of approximately 27 km (9.0 s +/- 1.0 s). The deeper of the two horizons has been interpreted by Cheadle to be the reflection Moho and the shallower dipping horizon is designated here to be the upper Mojave reflecting zone. There is a third seismic event in the Mojave data which is not continuous beneath the Garlock fault zone and into the area of active extension. That event is designated the lower Mojave reflecting zone. All of the horizons are shown on Figure 2 with their assumed correlations across the data gap shown on Figure 3.

The reflection Moho

The reflection Moho in both areas appears to have offsets of up to 3 km, locally, and in areas where the signal penetration appears to be poor, beneath the central Death Valley basin and in the vicinity of the Garlock fault zone, these reflections are not observed (Cheadle et al., 1986 a; b; Serpa et al., 1988). However, refraction data (e.g. Roller and Healy, 1963; Johnson, 1965; Prodehl, 1979) indicate that the base of the crust lies at approximately the same depth (31 km +/- 5 km) in both the Mojave and Death Valley regions. Other geophysical data, such as gravity and magnetic data, do not indicate any major changes in crustal thickness between the two areas. In addition, the seismic reflection characteristics of the reflection Moho appear to be strikingly similar in both survey areas. Reflections from that horizon are strong and can be easily identified on both stacked

---

Figure 1. Location map of the COCORP Death Valley and Mojave Desert surveys. L1 through L6 are seismic profiles in the Mojave and L8 through L12 are the Death Valley profiles. The small triangles indicate the locations of seismic sections shown in Figure 3.

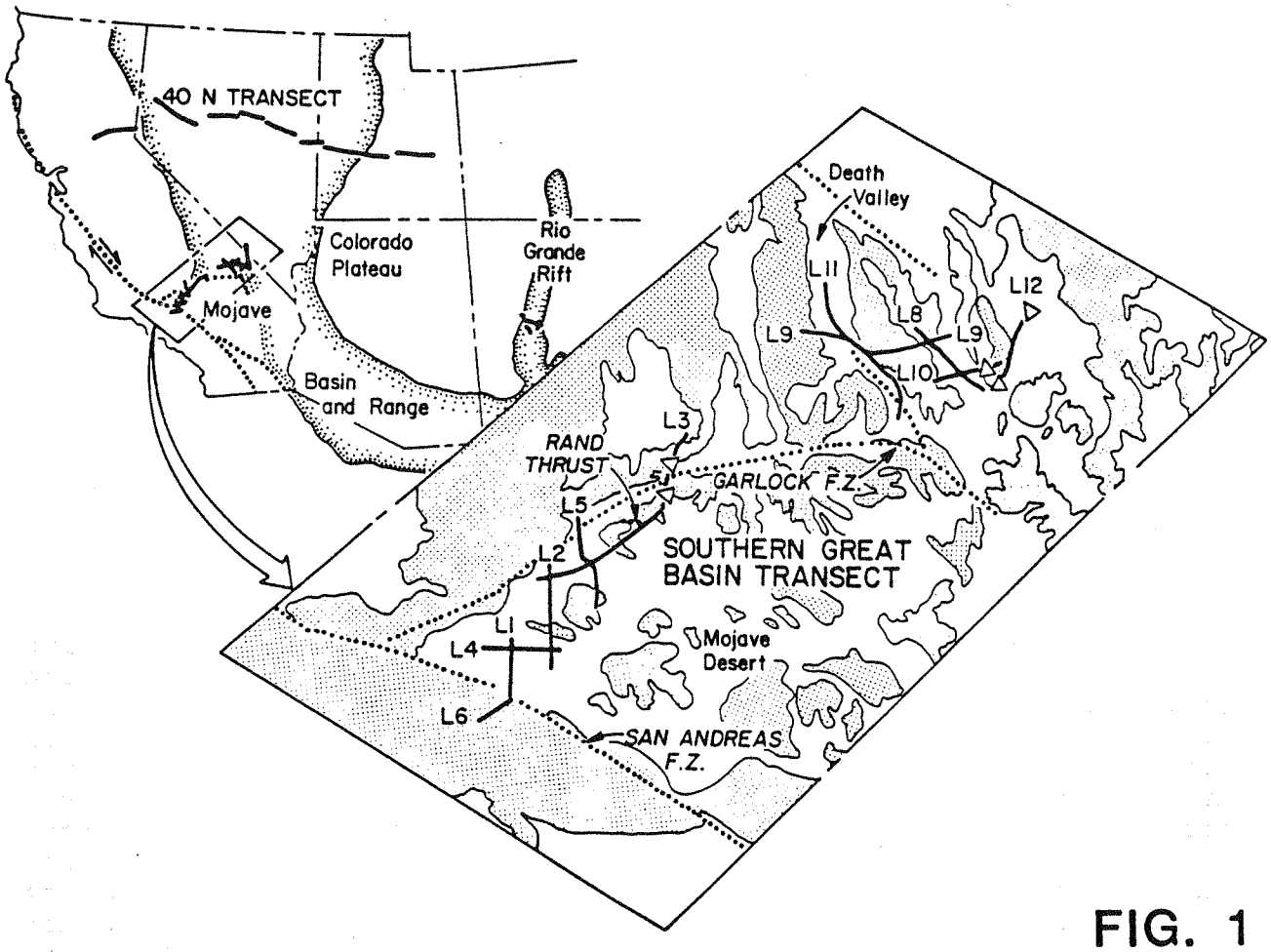
40 N TRANSECT
Colorado
Plateau
Rio
Grande
Rift
Mojave
Basin
and Range
Death
Valley
L11
L12
L8
L9
L9
L10
L3
RAND
THRUST
GARLOCK F.Z.
L5
L2
SOUTHERN GREAT
BASIN TRANSECT
L1
L4
Mojave
Desert
L6
SAN ANDREAS
F.Z.

FIG. 1

seismic sections and demultiplexed field files. The reflections are multicyclic, but contained within a relatively narrow (0.5 s) band in which no single cycle is prominent, but in which several discontinuous cycles stand out. Thus, the reflection Moho in both areas is assumed here to represent a relatively flat, continuous boundary throughout both the relatively stable Mojave area and the actively extending area north of the Garlock fault zone.

The presence of a relatively flat horizon near the base of the crust throughout the two adjacent regions is difficult to reconcile with the apparent differing amounts of crustal thinning which would be expected from extension during the past 15 Ma. There are three possible explanations considered here: 1) the area of active extension may have had a thicker crust than the adjoining regions prior to 15 Ma.; 2) thinning of the upper crust in the extensional region may be accommodated by flow of material in the lower crust of the surrounding regions into the area of active extension; 3) thinning of the upper crust in the extensional region may be accommodated by flow of material from the mantle into the crust. The first possibility that the crust was thicker beneath the area of active extension prior to 15 Ma. cannot be evaluated from the available data. However, the reflection Moho is located at a depth of approximately 30 km throughout the Basin and Range province (e.g. Klemperer et al., 1986). With the varying rates and times of extension throughout that region it would be unlikely that the crustal thickness would now be relatively constant. Thus the remaining two possible explanations appear more reasonable and are discussed in more detail in the following sections.

Midcrustal reflecting horizons

As mentioned previously, there are two possible reflecting zones in the midcrust of the Mojave data which may correlate across the data gap with a relatively continuous midcrustal reflecting zone in the Death Valley data. The correlation of either Mojave zone with the Death Valley reflecting zone would indicate that the lower crust of the active extensional region has the geometry of a flat topped dome because both Mojave reflectors dip to the southwest (Cheadle et al., 1986a; b) and the Death Valley reflecting zone dips to the northeast on the east side of the Nopah Range. However, the correlation of the Death Valley zone with the upper Mojave reflecting zone would suggest that the upper crust is thinnest near the Garlock fault zone and would support the inference that the flat reflection Moho was due to lateral flow of material from adjacent lower crustal regions into the area of active extension. The alternative correlation, that the lower Mojave reflecting zone continues into the Death Valley

---

Figure 2. Schematic representation of the major reflecting zones in the two survey areas. NR refers to the Nopah Range and the designations A through E are the reflecting zones as follows: A = the Death Valley reflection Moho, B = the Death Valley midcrustal reflecting zone, C = the Mojave reflection Moho, D = the Mojave lower reflecting zone, E = the Mojave upper reflecting zone.

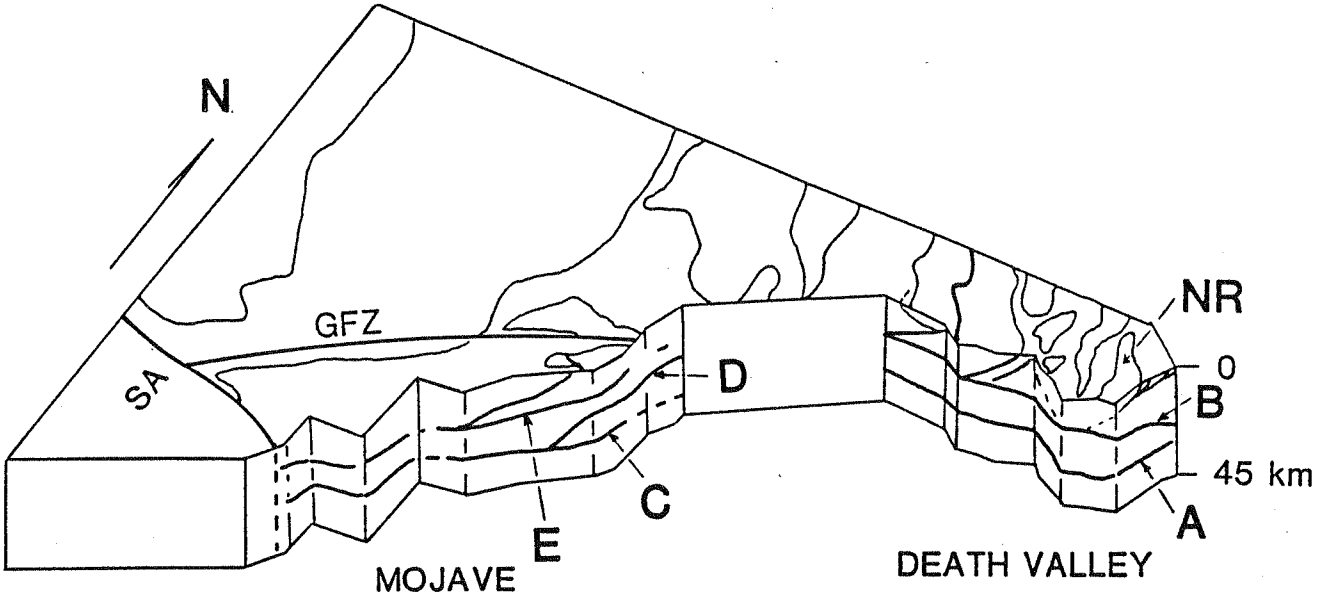

FIGURE 2

reflecting zone would indicate maximum upper crustal thinning beneath the area of active extension and support the inference that the flat Moho is the result of flow of material from the mantle into the lower crust of the extensional region.

As shown in Figure 3, it is the latter correlation, that is the lower Mojave reflecting zone with the Death Valley midcrustal zone, which is preferred here. That choice is based primarily on the fact that the upper reflecting horizon may not continue beneath the Garlock fault zone and may, in fact, be an out of the plane reflection from the Garlock fault surface (Serpa, 1987). However, the seismic characteristics of the two zones are similar to the south of the Garlock fault zone, in that the zones are comparably strong, locally contain high amplitude reflections, and have a similar width (1 s). On the north side of the Garlock fault zone, there are a few isolated events which may be continuations of the upper Mojave reflecting zone (Cheadle et al., 1986a; b) but that relationship is uncertain because the events cannot be traced below the surface position of the Garlock fault zone.

POSSIBLE SOURCE OF THE LOWER CRUSTAL DOME

Based on a variety of surface measurements, the amount of extension of the upper crust of the Basin and Range Province has been estimated to be between 10 and 140 percent (summarized by Wernicke et al., 1982). Two of these estimates, 50 and 65 percent, respectively, are derived (Wright, 1976; Wernicke et al., 1982) from observations in the vicinity of Death Valley. Those estimates are based on the assumption that the extensional deformation in the region is 2-dimensional. However, the patterns of block faulting discussed by Serpa et al. (1988) suggest that the extensional deformation in Death Valley is 3-dimensional. Thus the amount of crustal extension in Death Valley may be greater than those indicated by the previous estimates.

Assuming the crust in Death Valley has extended 2-dimensionally by 65 percent during the past 15 Ma., the midcrustal reflecting horizon would have been at a depth of 25 km prior to the extension. That depth coincides closely with the depth of the present-day reflection Moho (30 km depth) throughout the surrounding region and, if the recent extension in Death Valley has thinned the upper crust by 10 km, or more, relative to the surrounding region, then that horizon may have been located near the base of the crust prior to the extension. That depth suggests that the midcrustal reflecting zone may include remnants of an older, pre-extensional Moho, or attenuated deep crustal rocks or both.

Because the midcrustal zone passes, without apparent offset, beneath the upper crustal faults in Death Valley (Serpa et al., 1988), it also may be a zone of mylonites which formed, during the

---

Figure 3. Examples of seismic sections showing the features discussed in the text. For the locations of these sections refer to Figure 1. DET = the correlation of the midcrustal reflecting zone and MOHO = the reflection Moho.

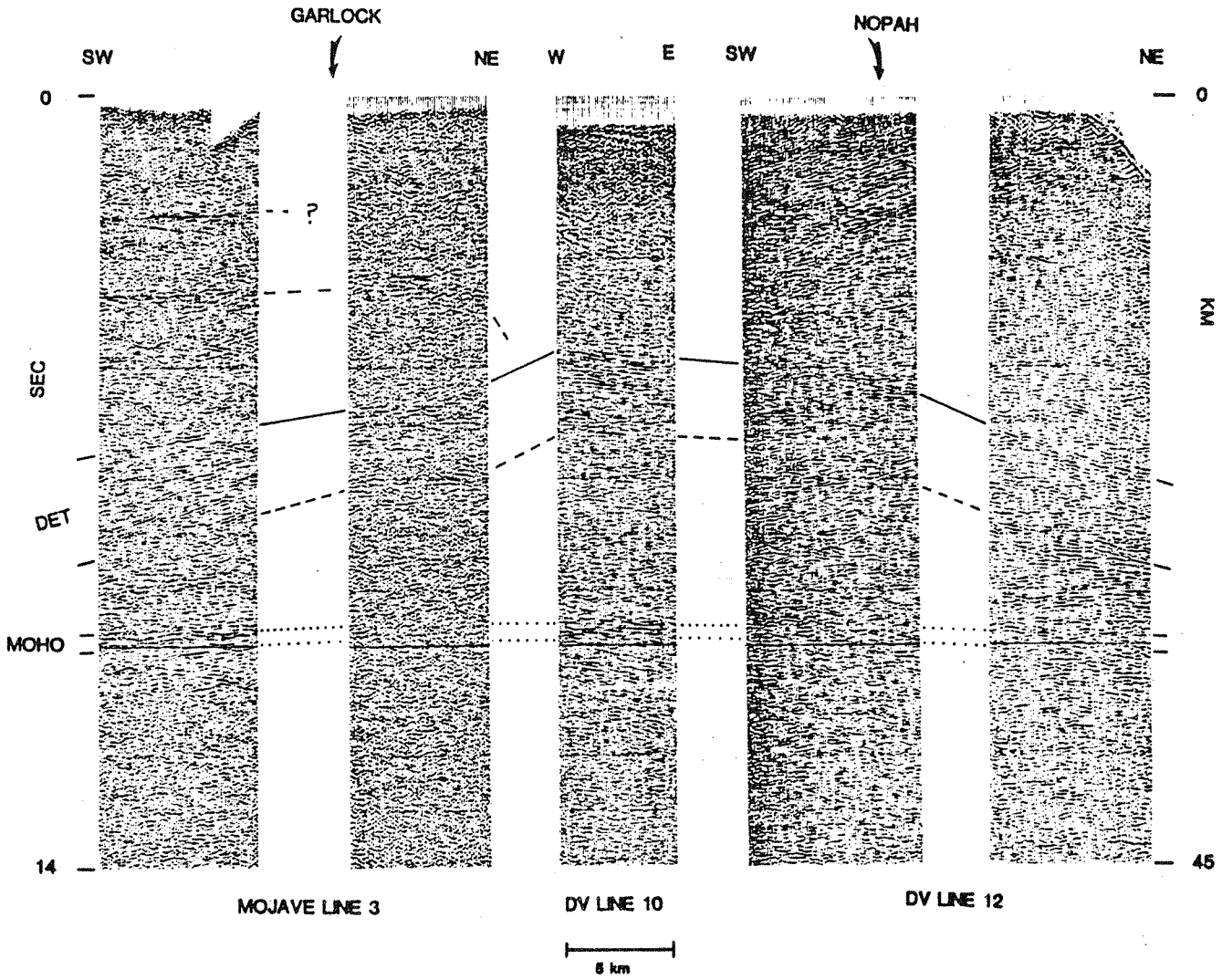
GARLOCK
NOPAH
SW
NE
W
E
SW
NE
0
14
SEC
DET
MOHO
?
0
45
KM
MOJAVE LINE 3
DV LINE 10
DV LINE 12
5 km

FIGURE 3

early stages of the crustal extension, as a result of the differential movement between the upper crustal fault blocks and the underlying rocks. The reflectors above the midcrustal zone are predominantly dipping while those below are subhorizontal. That change in reflector orientation suggests that the mid-crustal zone may be a rheologic boundary, possibly a zone of transition between brittle upper crustal rocks and more ductile lower crustal rocks. Finally, the presence of a possible magma body (de Voogd et al., 1986) along part of the midcrustal zone indicates that in some areas that zone may be an intrusive boundary. Although the origin of the midcrustal zone is uncertain, the possible interpretations mentioned above suggest that it is a complex feature which has evolved both during and prior to the recent extension.

The seismic data from the two survey regions strongly suggest that the reflection Moho is younger than the midcrustal zone because the midcrustal zones are truncated in the southwest and northeast by the reflection Moho. The estimated (Wright, 1976; Wernicke et al., 1982) amount of upper crustal extension further suggests that some of the rocks between the two reflecting zones formed at depths of 40 km or more prior to the extension in Death Valley. Mesozoic compression (e.g. Burchfiel and Davis, 1975) may have produced a 40 to 50 km thick crust prior to the extension, however, the volcanic rocks exposed at the surface (Wright and Troxel, 1973), the inferred presence of a magma body at midcrustal depths (de Voogd et al., 1986), and the apparent youth of the reflection Moho suggest that a significant amount of material may have been added to the crust from the mantle during the extension.

Although rifting generally has not been considered to be a significant continent building process, the seismic observations do not exclude the possibility that most or all of the lower crust of Death Valley is intrusive. Based on their theoretical calculations, Furlong and Fountain (1984) have suggested that the lower crust of extensional regions should be intrusive. Fuis et al (1982) have suggested that the lower crust of the Imperial Valley region, an area of active extension similar to Death Valley, is composed entirely of mafic igneous intrusions. In that area the upper boundary of the inferred intrusive lower crust is at a depth of 12 to 13 km beneath the area of maximum extension and appears to dip toward the base of the crust outside that area in a manner similar to that of the midcrustal zone discussed in this paper. Thus, both theoretical considerations and geophysical data from areas of active crustal extension suggest that the volume of crustal material may increase significantly as a result of igneous activity during extension (Serpa and de Voogd, 1986).

REFERENCES

Burchfiel, B.C., and Davis, G.A., 1975, Nature and controls of Cordilleran orogenesis, extensions of an earlier synthesis, Am. J. Science, v. 275-a, 363-396

Burchfiel, B.C., and Stewart, J.H., 1966, "Pull-apart" origin of the central segment of Death Valley, California, Geol. Soc. Am. Bull., v. 77, 439-440.

Burchfiel, B.C., Walker, D., Davis, G.A., 1982, Kingston Range and related detachment faults - a major "breakaway" zone in the southern Great Basin, Geol. Soc. Am., Abstracts with Programs, p. 536.

Cheadle, M.J., Czuchra, B.L., Byrne, T., Ando, C.J., Oliver, J.E., Brown, L.D., Kaufman, S., Malin, P.., and Phinney, R.A., 1986a, The deep crustal structure of the Mojave desert, California, from COCORP seismic reflection data, Tectonics, v. 5, 293-320.

Cheadle, M.J., Czuchra, B.L., Ando, C.J., Byrne, T., Oliver, J.E., and Kaufman, S., 1986b, Geometries of deep crustal faults: evidence from the COCORP Mojave survey, in Reflection Seismology: The Continental Crust, Geodynamics series volume 14, M. Barazangi and L. Brown (editors), AGU, 305-312.

Davis, G.A., and Burchfiel, B.C., 1973, Garlock fault: an intercontinental transform structure, southern California, Geol. Soc. Am. Bull., v. 84, 1407-1422.

Dokka, R.K., 1986, Patterns and modes of early Miocene crustal extension, central Mojave Desert, California, Geol. Soc. Am. Special Paper 208, 75-95.

Fuis, G.S., Mooney, W.D., Healy, J.H., McMechan, G.A., and Lutter, W.J., 1982, Crustal structure of the Imperial Valley region, U.S. Geol. Surv. Prof. Paper 1254, 25-49.

Furlong, K.P., and Fountain, D.M., 1986, Lithospheric evolution with underplating: thermal-physical considerations, J. Geophys. Res., v. 91, 8285-8294.

Johnson, L.R., 1965, Crustal structure between Lake Mead, Nevada, and Mono Lake, California, J. Geophys. Res., v. 70, 2863-2872.

Klemperer, S.L., Hauge, T.A., Hauser, E.C., Oliver, J.E., and Potter, C.J., 1986, The Moho in the northern Basin and Range province, Nevada, along COCORP 40 N seismic reflection transect, Geol. Soc. Am. Bull., v. 97, 603-618.

Prodehl, C., 1979, Crustal structure of the western United States, U.S. Geol. Surv. Prof. Paper 1034, 74 p.

Roller, J.C., and Healy, J.H., 1963, Seismic refraction measurements of crustal structure between Santa Monica Bay and Lake Mead, J. Geophys. Res., v. 68, 5837-5849.

Serpa, L., 1987, The three-dimensional geometry of the Garlock fault zone - a reinterpretation of the COCORP Mojave desert data, Geol. Soc. Am., Abstracts with programs, p. 838.

Serpa, L., and de Voogd, B., 1987, Deep seismic reflection evidence for the role of extension in the evolution of continental crust, Geophys. J. R. astr. Soc., v. 89, 55-60.

Stewart, J.H., 1983, Extensional tectonics in the Death Valley area, California: transport of the Panamint Range structural block 80 km northwestward, Geology, v. 11, 153-157.

de Voogd, B., Serpa, L., Brown, L., Hauser, E., Kaufman, S., Oliver, J., Troxel, B., Willemin, J., and Wright, L., 1986, The Death Valley bright spot: a midcrustal magma body in the southern Great Basin, California?, Geology, v. 14, 64-67.

Wernicke, B., Spencer, J.E., Burchfiel, B.C., and Guth, P.L., 1982, Magnitude of crustal extension in the southern Great Basin, Geology, v. 10, 499-502.

Wright, L.A., 1976, Late Cenozoic fault patterns and stress fields in the Great Basin and westward displacement of the Sierra Nevada block, Geology, v. 4, 489-494.

Wright, L.A., and Troxel, B.W., 1973, Shallow-fault interpretation of Basin and Range structure, southwestern Great Basin, in Gravity and Tectonics, K.A. Dejong and R. Scholten (editors), John Wiley and Sons, 397-407.

NEW PERSPECTIVES ON QUATERNARY FAULTING IN THE SOUTHERN WALKER LANE, NEVADA AND CALIFORNIA

by Marith C. Reheis and Jay S. Noller
U.S. Geological Survey, MS-913, Federal Center, Box 25046, Denver, CO 80225

Introduction

A preliminary survey of aerial photographs of the southern Walker Lane began in late 1986. The purpose of this survey is to determine the nature and scope of future studies required to (1) ascertain whether the apparent concentration of Quaternary faults in and near the Nevada Test Site is real or is simply a result of the greater effort invested in mapping Quaternary deposits in that area, and (2) determine whether faults in the southern Walker Lane are active and could produce significant earthquakes. The survey is focused on the area extending south from Lone Mountain to Pahrump Valley and east from the Furnace Creek fault zone to an irregular line passing through the Cactus Range and Pahute Mesa.

Lineaments and scarps were identified on stereopairs of black-and-white aerial photographs at scales of 1:80,000 or 1:60,000. The lineaments and scarps were plotted on 1:24,000- and 1:62,500-scale topographic maps using a PG-2 plotter, and were color-coded according to distinctness and occurrence in Quaternary or Tertiary deposits (age assignments based on appearance in aerial photographs and on existing geologic maps). Additional lineaments identified on the topographic maps were also plotted. Areas of particular interest were selected for more detailed study using larger-scale aerial photographs. Most of the lineaments and scarps identified in the survey, although referred to as faults in this paper, have not been checked in the field.

Description of Newly Found Faults

The area studied thus far extends south from Lone Mountain to Sarcobatus Flat and west from Pahute Mesa to Fish Lake Valley (fig. 1), an area that roughly corresponds to the Goldfield section of the Walker Lane tectonic belt, as defined by Stewart (1987). This section has been characterized by a conspicuous lack of both dip-slip basin-range faults and northwest-trending strike-slip faults in comparison to other sections of the Walker Lane belt (Carr, 1984; Stewart, 1987).

Our studies have revealed many clusters of previously unmapped Quaternary faults within the Goldfield section of the Walker Lane belt. Most of these faults trend northeast, but some faults near the Furnace Creek fault zone and on or north of Pahute Mesa trend north-northwest to north-northeast (fig. 1). The newly found faults include range-front faults and faults in Quaternary fan and basin-fill deposits.

Northeast-trending range-front faults identified in this study lie along the north and (or) west sides of Paymaster and Clayton Ridges, the Montezuma Range, Gold and Magruder Mountains, and the Grapevine Mountains, and along the southeast side of the General Thomas Hills and the Palmetto Mountains (fig. 1). Interpretation of aerial photographs and limited field data suggest that most of these faults place bedrock against Quaternary fans, and that they are

normal and dip steeply (70-90°) northwest. Left-lateral oblique slip, suggested by crenulations and slickensides within bedrock shear zones, has been seen only on the northeast end of the Clayton Ridge fault and the southwest end of the Stonewall Mountain fault. In addition, a horizontal mine adit at Stonewall Mountain penetrates about 65 m of unconsolidated Quaternary fan alluvium. Near the end of the shaft, Tertiary rhyolitic tuff appears to have been thrust over the alluvium at an angle greater than 70°, indicating high-angle reverse movement on part of the range-front fault. Late Pleistocene to Holocene alluvial fans abut several range fronts, such as parts of Paymaster and Clayton Ridges and Stonewall Mountain; they appear to bury older fans, suggesting fault movements in late Quaternary time (as described elsewhere by Bull, 1964). Layers of sheared alluvium and (or) colluvium were observed to overlie sheared bedrock along the Clayton Ridge and Grapevine Mountains faults. Variations in the particle size, extent of shearing, and cementation of these layers suggest that the layers become younger and less disturbed by faulting away from the bedrock; thus, they appear to record a succession of fault movements rather than one episode of faulting.

Northeast-trending faults found in this study in alluvial fans and basin-fill deposits commonly occur in clusters. Areas with fault clusters include Clayton Valley, the valleys east and west of the Montezuma Range, and the valleys north of the Goldfield Hills and Stonewall Mountain (fig. 1). Most of these faults are short and cut surfaces of only one age. Notable exceptions are (1) the scarps in Clayton Valley, which are relatively long and appear to offset surfaces of several ages, and (2) the faults east of the Montezuma Range that define the Palmetto graben. These faults appear to offset one fan and two graben-fill deposits which are middle to late Pleistocene in age; offsets are succesively smaller with decreasing age of the deposit.

Of the north- to north-northeast-trending faults near the Furnace Creek fault zone, only those at the northern end of Fish Lake Valley have been observed in the field. Prominent faults shatter the surface of the middle(?) Pleistocene Indian Creek fan on the northwest side of the valley. Some of these faults offset deposits down to the east, others offset deposits down to the west, but thus far none show clear evidence of strike-slip motion. Faults on the northeast side of the valley (some of which were mapped by Robinson and others, 1976) displace sediments ranging from late Pliocene to Holocene in age down to the west. These faults are here called the Emigrant Peak fault zone (Reheis, 1988). One of the faults in this zone appears to be offset in a left-lateral sense by a north-northwest-trending tear fault with Holocene displacement.

Most of the north-northwest- to north-northeast-trending lineaments and scarps on the west side of Pahute Mesa have not been observed in the field. Two sets of faults in the Oasis Valley have been observed to offset early to middle Pleistocene fan deposits. The eastern fault in Oasis Valley displaces old dissected fan gravel (QTa of Hoover and others, 1981) about 4 m down to the east, and may also displace younger deposits (Q2b or Q2c of Hoover and others, 1981). The western faults bound a narrow graben in middle Pleistocene fan deposits (Q2b or Q2c); this graben may be inset within an ill-defined larger graben that displaces older deposits.

Discussion and Preliminary Interpretation

The geomorphic and stratigraphic evidence discussed above suggests that many of the newly found faults in the Goldfield section of the Walker Lane belt have been recently active and have experienced recurrent movement in Quaternary time. Thus, these faults could generate earthquakes in the future. Some earthquakes as large as magnitude 5.0 recorded between 1931 and 1974 (W.J. Carr, written commun., 1987) were located near two areas of Quaternary displacement: the Emigrant Peak fault zone in northeast Fish Lake Valley and the faults on the northwest side of the Grapevine Mountains.

The many northeast-trending faults east of the Furnace Creek fault zone (fig. 1) are difficult to interpret. One possibility is that they are conjugate shears to the Furnace Creek fault zone, along which the least principal stress would be west-northwest and the greatest principal stress north-northeast (Wright, 1976; Zoback and Zoback, 1980; Carr, 1984). In such a stress field, however, northeast-trending faults should have a component of left-lateral motion in addition to normal dip-slip motion. Although much more field work needs to be done, at present there is little evidence to support left-lateral motion on the northeast-trending faults in the Goldfield section, with the exceptions mentioned above at Clayton Ridge and Stonewall Mountain. An alternative possibility is that the northeast-trending faults are a simple expression of dip-slip motion perpendicular to a northwest direction of least principal stress. If this is so, then east of the Furnace Creek fault zone the direction of least principal stress may be different from that along the Furnace Creek fault zone.

The north- to north-northeast-trending scarps and lineaments adjacent to the Furnace Creek fault zone appear to be normal dip-slip faults; their strikes are consistent with the interpretation that they are pull-apart faults related to strike-slip movement on the Furnace Creek fault zone. Faults with this orientation are common in Fish Lake Valley and in the foothills of the adjacent Silver Peak Range, especially at the northern end of the valley, where the Furnace Creek fault zone appears to die out. The north-trending faults in northern Fish Lake Valley may function as pull-apart faults in a giant right step between the northern end of the right-lateral Furnace Creek fault zone and the southern ends of the right-lateral Bettles Well and Soda Springs Valley faults to the north. This right step occurs in the area where Stewart (1985) described right-lateral offset along the Excelsior and Coaldale fault zones. The existence of the Silver Peak caldera (fig. 1) and associated volcanic rocks adjacent to northern Fish Lake Valley may indicate significant extension in this area (Carr, 1984).

North-trending faults in the area of Pahute Mesa (fig. 1) are most likely a continuation of the north-trending faults characteristic of the Basin and Range province to the north and east of the Walker Lane. Earthquakes and movements on north- to north-northeast-trending faults triggered by underground nuclear explosions on Pahute Mesa had both dip-slip and right-lateral components (Hamilton and others, 1972). Thus, the north-trending faults in western Pahute Mesa in part may be strike-slip conjugate shears; field work, however, is needed to determine whether these faults have a component of lateral slip.

The generally northeast-trending faults east of the Furnace Creek fault zone and west of Pahute Mesa have a preferred down-to-the-northwest displacement. Of the range-front faults, only those bounding the southeast sides of the General Thomas Hills and the Palmetto Mountains (fig. 1) have displaced deposits down to the southeast. Faults along the General Thomas Hills appear inactive. Faults in intermontane basins in the study area either displace sediments down to the northwest or else bound grabens that have about equal displacements on both sides. The relatively uniform down-to-the-northwest sense of displacement could be interpreted to suggest that the faults in the Goldfield section of the Walker Lane belt are rooted in a detachment at depth.

References Cited

Bull, W.B., 1964, Geomorphology of segmented alluvial fans in western Fresno County, California: U.S. Geological Survey Professional Paper 352-E, p. 89-129.

Carr, W.J., 1984, Regional structural setting of Yucca Mountain, southwestern Nevada, and late Cenozoic rates of tectonic activity in part of the southwestern Great Basin, Nevada and California: U.S. Geological Survey Open-File Report 84-854, 109 p.

Hamilton, R.M., Smith, B.E., Fischer, F.G., and Papanek, P.J., 1972, Earthquakes caused by underground nuclear explosions on Pahute Mesa, Nevada Test Site: Bulletin of the Seismological Society of America, v. 62, p. 1319-1341.

Hoover, D.L., Swadley, W C, and Gordon, A.J., 1981, Correlation characteristics of surficial deposits with a description of surficial stratigraphy in the Nevada Test Site region: U.S. Geological Survey Open-File Report 81-512, 27 p.

Nakata, J.K., Wentworth, C.M., and Machette, M.N., 1982, Quaternary fault map of the Basin and Range and Rio Grande Rift provinces, western United States: U.S. Geological Survey Open-File Report 82-579, scale 1:2,500,000.

Reheis, M.C., 1988, Quaternary activity on the Emigrant Peak fault zone, Fish Lake Valley, west-central Nevada: Geological Society of America, Abstracts with Programs, v. 20 (Cordilleran Section).

Robinson, P.T., Stewart, J.H., Moiola, R.J., and Albers, J.P., 1976, Geologic map of the Rhyolite Ridge quadrangle, Esmeralda County, Nevada: U.S. Geological Survey Geologic Quadrangle Map GQ-1325, scale 1:62,500.

Stewart, J.H., 1985, East-trending dextral faults in the western Great Basin: An explanation for anomalous trends of pre-Cenozoic strata and Cenozoic faults: Tectonics, v. 4, p. 547-564.

Stewart, J.H., 1987, Tectonics of the Walker Lane belt, western Great Basin--Mesozoic and Cenozoic deformation in a zone of shear, in Ernst, W.G., ed., Metamorphism and Crustal Evolution of the Western United States: Rubey Volume VII, Prentice-Hall Inc., New Jersey, p. 683-713.

Wright, L., 1976, Late Cenozoic fault patterns and stress fields in the Great Basin and westward displacment of the Sierra Nevada block: Geology, v. 4, p. 489-494.

Zoback, M.L., and Zoback, M.D., 1980, State of stress in the conterminous United States: Journal of Geophysical Research, v. 85, no. B11, p. 6113-6156.

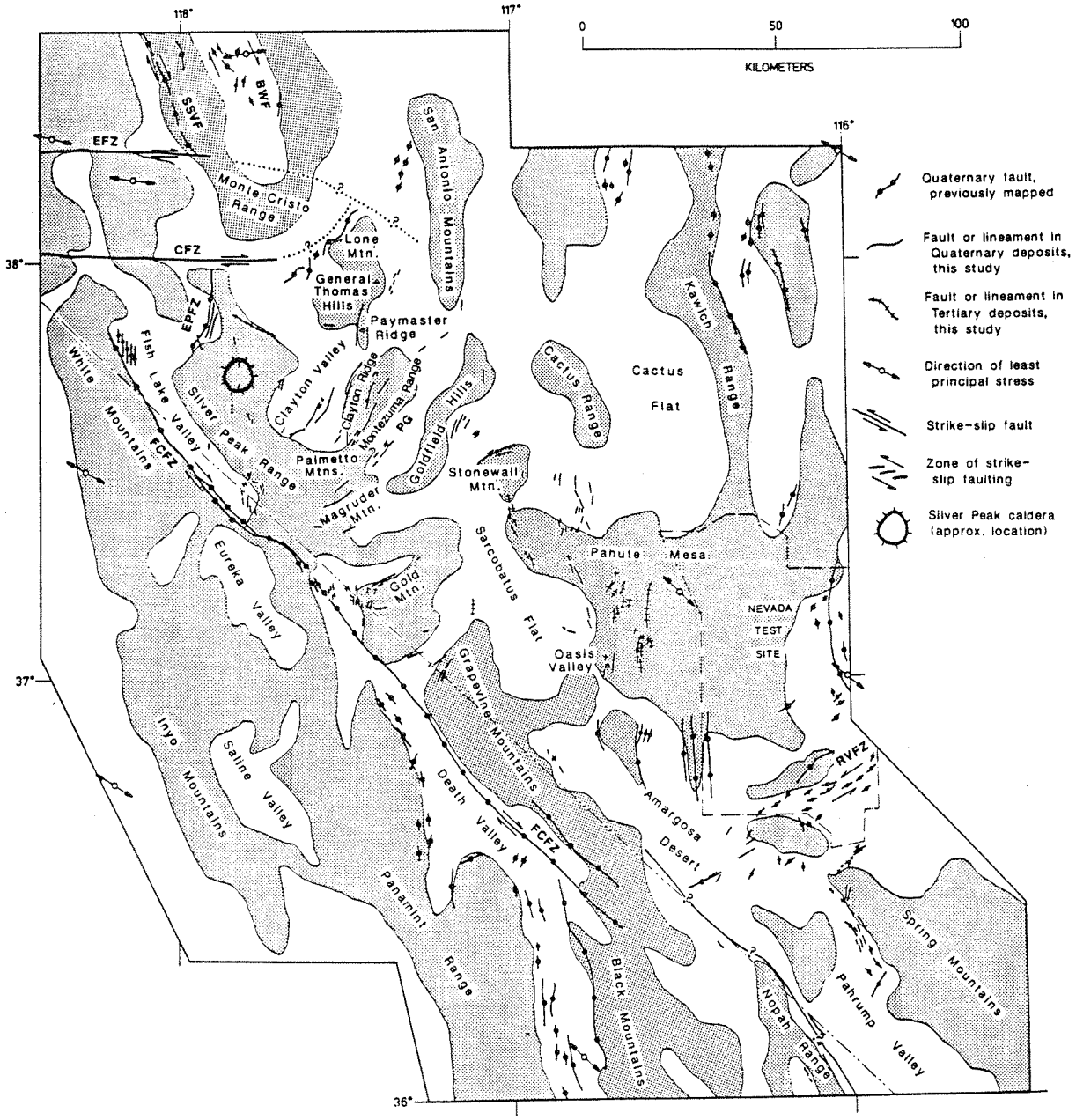

Figure 1. Physiography and Quaternary faults and lineaments of the southern Walker Lane. Previously mapped faults are taken mainly from Nakata and others (1982). Positions of Excelsior and Coaldale fault zones (EFZ and CFZ, respectively) from Stewart (1985). Faults west of Fish Lake Valley and Death Valley not shown. Data for least principal stress directions from Zoback and Zoback (1980). BWF, Bettles Well fault; SSVF, Soda Springs Valley fault; FCFZ, Furnace Creek fault zone; EPFZ, Emigrant Peak fault zone; PG, Palmetto graben; RVFZ, Rock Valley fault zone.

LATE HOLOCENE PALEOSEISMICITY OF THE NORTHERN DEATH VALLEY FAULT SYSTEM, FISH LAKE VALLEY, NEVADA

September 6, 1988

by

Thomas L. Sawyer

Center for Neotectonic Studies,

University of Nevada Reno

LATE HOLOCENE PALEOSEISMICITY

OF THE NORTHERN DEATH VALLEY FAULT SYSTEM,

FISH LAKE VALLEY, NEVADA

Sawyer, Thomas L., Center for Neotectonic Studies, LME #400, University of Nevada Reno, NV 89557-0047

ABSTRACT

A late-Holocene sequence of paleoseismicity consisting of at least three discrete, surface-faulting events is identified along the northern Fish Lake Valley fault zone (FLVFZ), a component of the Death Valley fault system (DVFS). The first event in the sequence, Event A, displaces a Mono tephra (3400-4100 yr B.P.). Wood from a deposit displaced by the second event, Event B, has an age of 1670 $\pm$ 40 ^{14}C yr B.P. This event displaces geomorphic surfaces that are estimated to have been established since about 1200 yr B.P. These two events were followed by the most recent event, Event C, which resulted in only relatively minor displacements.

Time-predictable models are developed from the time-displacement data and suggest the following chronology for the three-event sequence: 1950 yr B.P. for Event A; 1100 yr B.P. for Event B; and 200 yr B.P. for Event C. Interseismic intervals derived form the model range form 850 to 900 years. These rates of activity suggest that during the late-Holocene the FLVFZ, of the DVFS, was among the most active faults in the Basin and Range.

INTRODUCTION

The DVFS (Fig. 1) has defined a prominent role in the evolution of the southern Basin and Range, possibly since the Middle Jurassic (McKee, 1968). The cumulative right-lateral displacement across the system is as large as 80 km (Stewart, 1967), with about 48 km of right-slip (Mckee, 1968) across the northern half. Although the DVFS was among the first faults in California recognized as exhibiting Pleistocene activity (Ball, 1907), little is known about the Quaternary tectonic history and seismic potential of this regional, fault system.

The Fish Lake Valley fault zone (FLVFZ) in Fish Lake Valley, California and Nevada, is a component of the DVFS (Figs. 1 & 2). The fault zone separates the White Mountains on the west from Fish Lake Valley on the east. More than 2 km of relief lie between the crest of the range and the floor of the alluvial filled valley. Virtually the entire length of the FLVFZ exhibits abundant geomorphic evidence of late-Quaternary tectonic activity, including several indicators of strike-slip displacement.

In this study, a sequence of paleoseismicity consisting of at least three discrete surface-faulting events has been identified

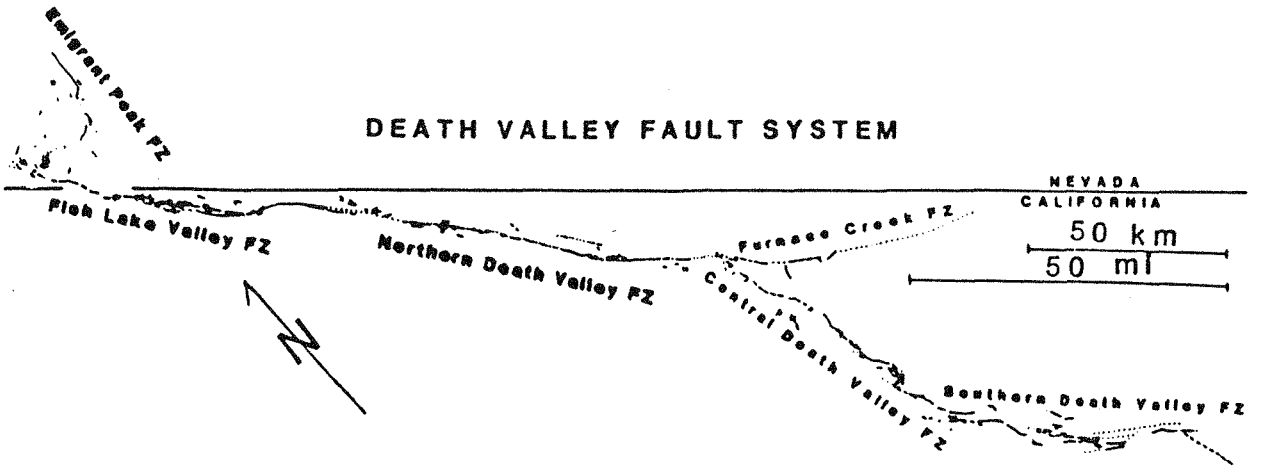

Figure 1. Quaternary fault trace of the Death Valley fault system, Nevada and California.

in two hand-dug exploratory trenches across the FLVFZ. Radiocarbon dated alluvial deposits provide age constraints for a series of overlying geomorphic surfaces. Both deposits and surfaces are displaced along the fault zone, and contribute time and displacement data for the three event sequence. Time-predictable models are development from the data and provide a tentative chronology of the paleoseismicity.

DEATH VALLEY FAULT SYSTEM

The DVFS is a dextral-slip, wrench fault system comprised of six intimately related and interconnected fault zones (Fig. 1). The primary trend of faults within the fault system is about N40°W, sub-parallel to the central San Andreas fault. From where the DVFS intersects and apparently terminates the Garlock fault in southern Death Valley (Brady, etal., 1981) to where it apparently terminates in northern Fish Lake Valley, is a distance of nearly 350 km. Making the DVFS one of the longest wrench faults in California.

There are few documented indicators of Quaternary right-lateral displacement along the DVFS. Curry (1938) concluded from geomorphic evidence in Death Valley that a significant component of Quaternary displacement along the DVFS is strike-slip in nature. Cinder Hill, in south-central Death Valley, is a cinder cone that straddles a trace of the southern Death Valley fault zone (Troxel, etal., 1986). The cone, K-Ar dated at about 700 K.a. by R. L. Drake (pers. comm. in Wright and Troxel, 1984), is offset approximately 200 m in a right-lateral sense along the fault trace (Troxel, etal., 1986). The data suggests a lateral slip-rate of 0.3 mm/yr. Mckee (1968) proposed about 0.9 km of right-slip along the southern FLVFZ, based on mismatched deposits of a drainage system. The deposits are as young as early Pleistocene (Reheis, pers. comm., 1987), based on the preliminary age of 1.5 M.a. for a tephra layer contained within. This data suggests a lateral slip-rate of

0.6 mm/yr for the southern FLVFZ.

FISH LAKE VALLEY FAULT ZONE

The FLVFZ bounds the east side of the White Mountains and the northern Last Chance Range (Fig. 2). The southern half of the fault zone trends N40°W and is comprised of two main traces. The western trace forms the eastern rangefront of the Last Chance Range. The eastern trace lies near the axis of southernmost Fish Lake Valley and extends to the north across the piedmont slope flanking of the eastern White Mountains. Local areas of apparent transpression at small left-steps are evident along this trace. Where the two join the fault-pattern is relatively complex. It consists of numerous arcuate splays of the western trace that are truncated by the through-going eastern trace. North of the junction in west-central Fish Lake Valley, a single trace forms the eastern rangefront of the White Mountains. Here the fault zone trends about N15°W. The significant relief of compound fault scarps (80 to 100 m) near Dyer, Nevada suggest that this section of the FLVFZ has a substantial component of vertical displacement. Which is consistent with the nearly north-south orientation of the maximum horizontal compressive stress direction (Zoback, etal. 1987).

The FLVFZ in northwestern Fish Lake Valley (Fig. 2) is comprised of two groups of faults with different orientations and apparent styles of faulting. The western group consists of NNW trending faults with right-oblique displacement. The group forms the eastern rangefront of the White Mountains. To the north this group of faults abruptly changes in orientation to ENE and may join in the subsurface with the Emigrant Peak fault zone in

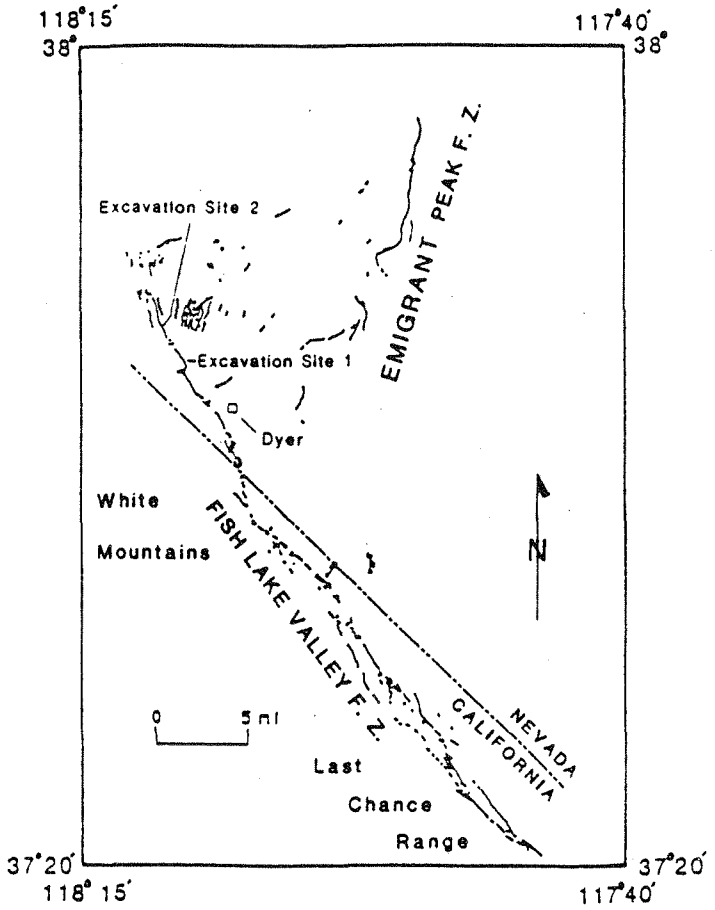

Figure 2. Quaternary surface trace of the Fish Lake Valley and Emigrant Peak fault zones in Fish Lake Valley, Nevada-California.

northeastern Fish Lake Valley. The eastern group consists of numerous NNE tending faults with normal to left-oblique (?) displacement. This group forms a graben-complex on the fan piedmont that is several kilometers wide. The geometric and apparent kinematic relations of the two groups of faults is suggestive of a conjugate set. Northern Fish Lake Valley appears to be a region of extension related to wrench fault tectonics along the DVFS.

GEOMORPHIC SETTING OF NORTHWESTERN FISH LAKE VALLEY

The area of study in northwestern Fish Lake Valley

includes portions of the Indian Creek, Marble Creek, and Liedy Creek alluvial fans (Figs. 3 & 6). The Indian Creek fan is among the largest in the valley and is comprised primarily of granitic alluvium of possible glacial outwash origin (Elliott-Fisk, 1987). In contrast, the upper reaches of the Marble Creek drainage have apparently not been glaciated. The Marble Creek fan is considerably smaller than the Indian Creek fan and is comprised of granitic alluvium with greater amounts of carbonate lithologies. The Liedy Creek drainage was repeatedly glaciated during the Pleistocene (Elliott-Fisk, 1987). The Liedy Creek fan, which is intermediate in size, is comprised of nearly equal proportions of granitic and metasedimentry alluvium.

DESCRIPTION AND AGE CONSTRAINT OF SURFACE MAP UNITS

A chronosequence consisting of seven Quaternary surface map units is identified in the study area (Figs. 3 & 6). A chronosequence is a series of soils that have all soil-forming factors, except time, in common (Jenning, 1941). Surface map units are soil-stratigraphic units formed in alluvium during a period of time. The surfaces are identified and correlated on the basis of several diagnostic criteria that vary systematically with surface age. These criteria include: micro-topography; soil, stone pavement, and desert varnish development; relative position; degree of rounding; boulder weathering; and air photo patterns (e.g., surface tones and texture, and degree and nature of dissection).

The surfaces are numerically designated 1 through 7, from youngest to oldest. Surface 1 is the modern surface of active drainage channels. Surfaces 2 through 4 and probably surface 5 are Holocene in age. In general, these surfaces primarily occur in the medial and distal fan positions, inset into surfaces 6 & 7, which are late- to mid-Pleistocene in age. Age estimates for the various surface units are shown in Table 1. Both radiocarbon dates and tentative tephrachronology are used to establish surface age estimates. All dated materials are from alluvial deposits below or within which the surfaces have formed, and therefore, the dates provide maximum age estimates for surface map units.

PALEOSEISMICITY OF THE FISH LAKE VALLEY FAULT ZONE

Dated, displaced alluvial deposits and soil-supported correlations of geomorphic surfaces (Sawyer, unpub. data, 1988) provide time constraints for a sequence of paleoseismicity identified along the FLVFZ. Stratigraphic and structural relations relative to the main trace of the northern FLVFZ are examined in two hand-dug exploratory trenches. The trenches are separated by about 4.5 km (Fig. 2), and were excavated into the youngest faulted surface (Figs. 3 & 6) at sites of syntectonic deposition. The stratigraphy and structure of both trenches are documented in graphical logs (Figs. 4 & 7). All displacements of stratigraphic units are assumed to be the result of coseismic-slip.

EXCAVATION SITE 1

Excavation Site 1 is located near the apex of a small alluvial fan on the Marble Creek fan (Fig. 3), where the main trace of the FLVFZ displaces surface 3. The

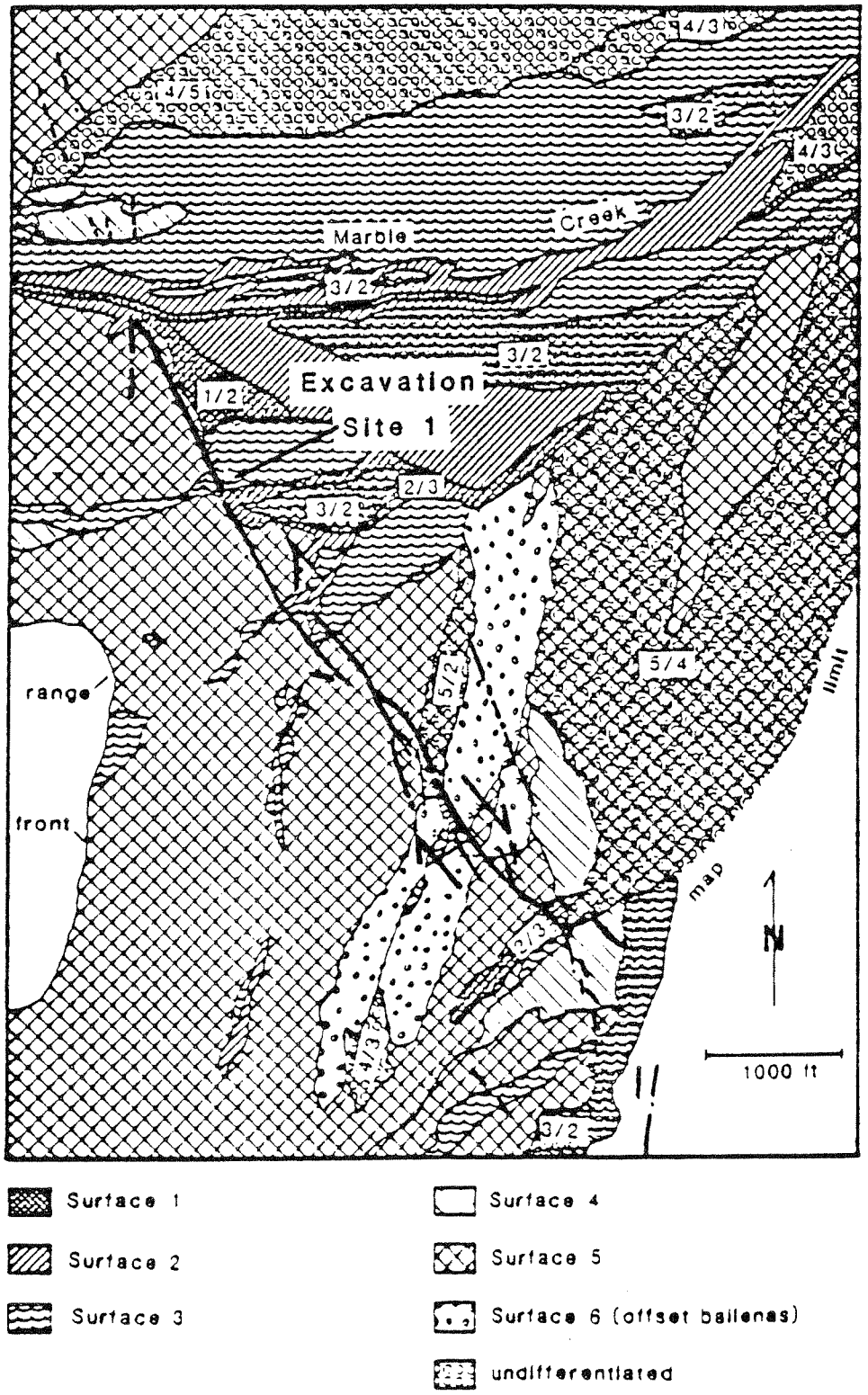

Figure 3. Distribution of surface map units on a portion of the Marble Creek and Liedy Creek alluvial fans in the vicinity of Excavation Site 1.

TABLE 1. Age estimates of surface map units.

Surface	^{14}C yr B.P.	Tephra-Chronology
1	modern	
2	$\leq$140 $\pm$ 40	-
Holocene		
3	$\leq$1160 $\pm$ 50	-
4	<2170 $\pm$ 45	-
5	>2290 $\pm$ 50	-
6		<0.74-1.0 M.a.
Pleistocene		
7		>0.74-1.0 M.a.

fault zone at this site is comprised of a single, linear trace that trends N35°W. Along the trace progressively larger displacements are exhibited in older surfaces, suggesting recurrent faulting.

The style of faulting along this trace is inferred from a pair of ballenas, offset in a dextral sense (Fig. 3). Ballenas are well-rounded ridgeline remnants of fan alluvium (Peterson, 1981). The northern ballena, located approximately 1 km southeast of Excavation Site 1, forms a small shutter ridge. Longitudinal profiles of the ballena summits were surveyed using a theodolite in conjunction with a EDM. The survey data suggests approximately 50 m of right-slip and 1 to 1.5 m of normal-slip (valley side relatively up) of the summits across the fault trace. Lateral-to-vertical displacement-ratios of 50:1 to 30:1 are calculated from this data. The displacement-ratio decreases to the northwest along the trace and at Excavation Site 1 is estimated to be a ratio of 10:1. This ratio is based on larger vertical offsets of surfaces at the site, relative to the same surfaces near the ballenas. The 10:1 displacement-ratio is considered to be representative of the late-Holocene style of faulting at the site.

Summary of Displacement Data and Paleoseismic Significance

Figure 4 is a graphical log of the north trench-wall at Excavation Site 1. Stratigraphic units I and II and the lower contact of unit III display cumulative vertical displacements from 33 to 35 cm, east side down (valley side down), across the main fracture (near meter 6). The upper contact of unit III, units IV through VI, and unit IX have cumulative displacements from 17 to 21 cm. Unit X is fractured and appears to be displaced from 2 to 4 cm between the main fracture and a secondary fracture near meter 9.

The paleoseismic significance of the displacement data is interpreted as follows. Units I through III were offset about 15 cm vertically during Event A - the first event identified in the trench. Unit II is a reworked tephra layer that chemically matches most closely with several ash beds erupted about 3400 to 4100 yr B.P. from Mono Craters (written comm., Sarna-Wojcicki, 1987), located approximately 70 km due west of northern Fish Lake Valley. Therefore, Event A occurred since deposition of the tephra or tentatively since 3400-4100 yr B.P. Following Event A, unit III was erosionally truncated and subsequently buried by units IV through IX. Units IV through VI and unit IX were unfaulted prior to Event B - the second event - and sustained from 16 to 18 cm of coseismic-slip during the event. A radiocarbon date of 1670 $\pm$ 40 yr B.P. (A-4768) was obtained from a

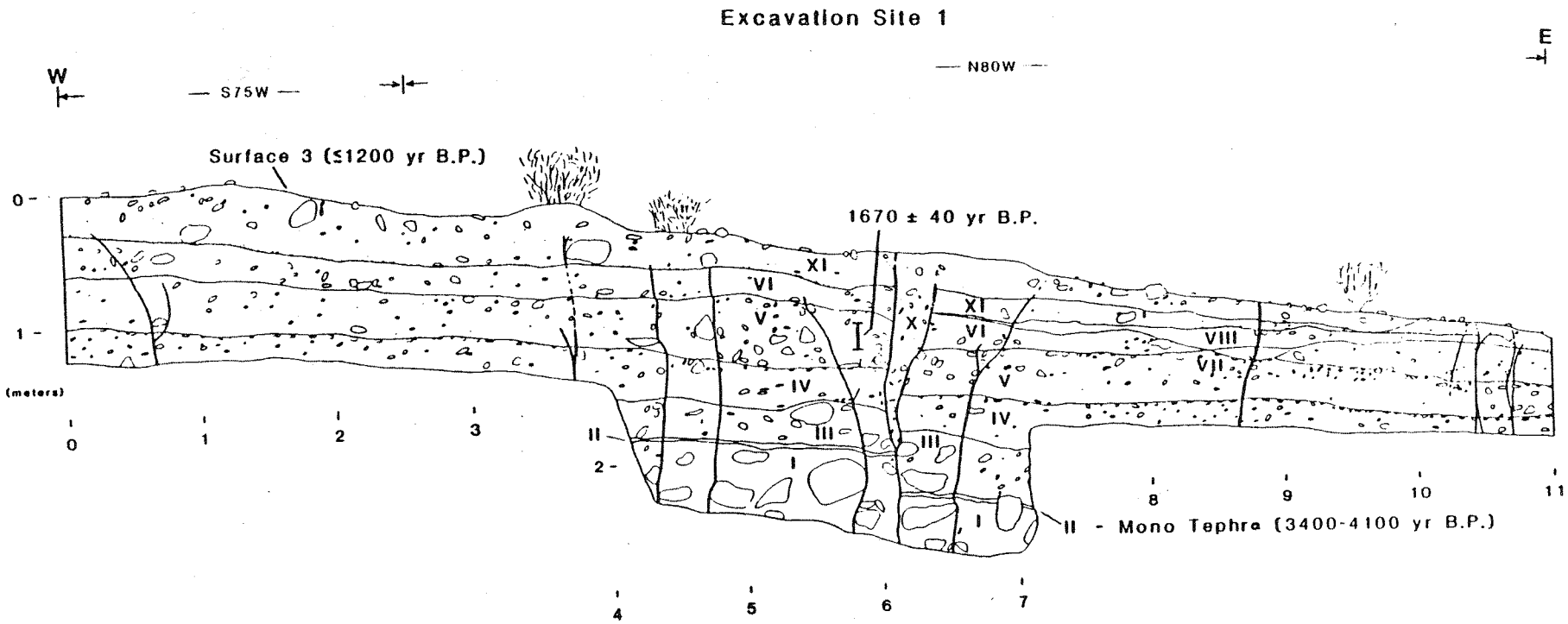

Figure 4. Graphical log of the north trench-wall at Excavation Site 1 on the Marble Creek alluvial fan. Vertical bar in unit V is the relative stratigraphic position of a log radiocarbon dated at 1670 ± 40 yr B.P. and located 20 m west of meter 0.

log contained within unit V. Hence, Event B occurred since 1670 ± 40 yr B.P. Surface 3 is estimated to have been established since about 1200 yr B.P. and has formed in Unit IX, which was faulted during Event B. Therefore, Event B is inferred to have occurred since 1200 yr B.P. Unit X is an infilling of a fissure that formed during Event B and a colluvial-tongue formed by fault scarp degradation succeeding the event. This unit has subsequently been fractured and displaced about 3 cm during Event C - the third and most recent event.

The following is a Summary of time constraints for the sequence of paleoseismicity at Excavation Site 1, based on field relations. Event A occurred since deposition of unit II (Fig. 4) or tentatively since 3400 to 4100 yr B.P. Events B and C occurred since deposition of unit V (Fig. 4), that is since 1670 ± 40 yr B.P. Also, both Events B & C occurred since surface 3 was established or since about 1200 yr B.P.

Time-Predictable Model

An equivalent time-predictable model to that of Shimazaki and Nakata (1980) is developed in Figure 5. The model is based on time and displacement data from Excavation Site 1. The model assumes a constant accumulation rate of tectonic stress and that stress release occurs at some relatively constant threshold. Given a slip-rate, and the time and amount of coseismic-slip of an event, the model predicts the time of the next event. This model may provide reasonable time estimates for major faults or fault segments that have relatively uniform behavior (Schwartz, etal., 1986). The DVFS is in a interplate region (Carr, 1984), where uniform behavior of faults (e.g., Calaveras and San Andras faults) is known to occur.

In Figure 5 the time of Event B was set at 1100 yr B.P. This is nearly the maximum time possible considering that the event displaced surface 3, which was established since about 1200 yr B.P. Therefore, a minimum vertical slip-rate of 0.18 mm/yr is calculated and

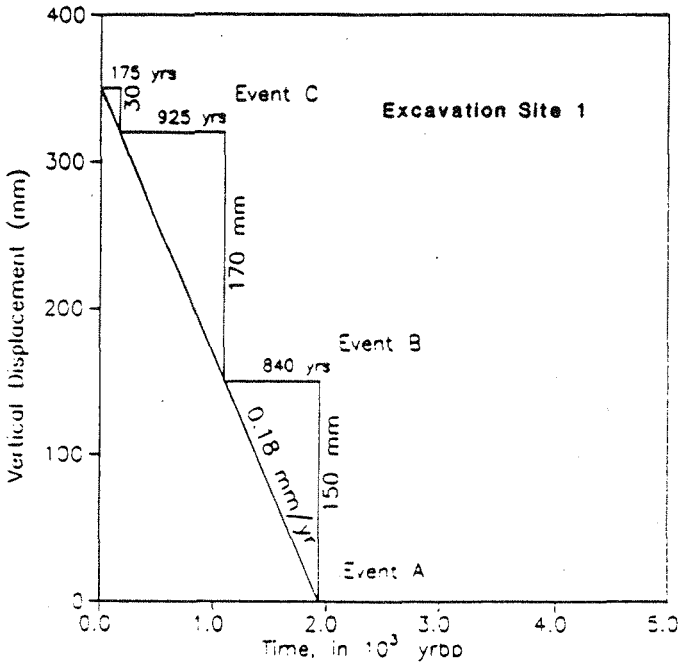

Figure 5. Time-predictable model developed for the timing and displacement constraints from Excavation Site 1. The timing of Event B is set at 1100 years b.p. (see explanation in text).

a lateral slip-rate of 1.8 mm/yr is inferred from the 10:1 displacement-ratio at this site. A tentative chronology for the three event sequence, estimated from the time-predictable model in Figure 5, is: 1950 yr B.P. for Event A; 1100 yr B.P. (timing set) for Event B; and about 180 yr B.P. for Event C.

EXCAVATION SITE 2

Excavation Site 2 is located 4.5 km to the northwest of Site 1 (Fig. 2), where the main trace of the FLVFZ displaces surface 3 approximately 0.8 m, vertically. The fault pattern at this site is relatively complex. As previously discussed, there are two groups of faults in northwestern Fish Lake Valley; one group trends NNW and the other NNE. Right-oblique displacement is evident for an abandoned drainage channel across the main trace of the NNW trending group of faults (Fig. 6). A theodolite/EDM survey of the offset channel indicates about 150 m of right-slip and about 50 m of normal-slip, east side down (valley side down). The survey data suggests a displacement-ratio of 3:1 (lateral:vertical) for this trace. At Excavation Site 2 a trench was excavated across the southern extension of the same trace (Fig. 6). The 3:1 displacement-ratio is considered to be representative of the late-Holocene style of faulting at this site.

Summary of Displacement Data and Paleoseismic Significance

Figure 7 is a graphical log of the south trench-wall at Excavation Site 2. Stratigraphic unit I and the lower contact of unit II display cumulative vertical displacements of about 66 cm, valley side down, across the main fracture in the trench located near meter 1.5. The upper contact of unit II and units III through V have cumulative displacements from 33 to 36 cm. The lower contact of unit VIII is displaced about 6 cm and unit X is apparently unfaulted.

The paleoseismic significance of the displacement data is interpreted as follows. Units I and II were displaced about 27 cm during Event A - the first event at this site. Subsequently, unit II was erosionally truncated and buried by units III through V. Units III through V were unfaulted prior to Event B - the second event - and sustained about 28 cm of coseismic-slip during the event. Unit VI represents an infilling of a fissure that formed during Event B. Unit VII is a colluvial-tongue the records the degradation of the Event B fault scarp, which accounts for the eastward taper of unit V, west of the main fracture. Subsequently, unit VIII was deposited and displaced about 6 cm during Event C - the third and most recent event at this site. Unit IX is a "keystone" block that was down-dropped during this event. Unit X was deposited after the sequence of three surface-faulting events and is unfaulted. Therefore, Event A occurred prior to Events B and C, which occurred since surface 3 was established or since about 1200 yr B.P.

Time-Predictable Model

In Figure 8 a time-predictable model is developed based on the time and displacement data from Excavation Site 2. As with the time-predictable model development for the first site (Fig. 5), the time of the second event was set at 1100 yr B.P. The reason is, that at both sites the second event displaces surface 3, which is estimated to have been established since about 1200 yr B.P. An estimated vertical slip-rate of 0.32 mm/yr is calculated from the data and a lateral slip-rate of 0.96 mm/yr is inferred from the 3:1 displacement-ratio at this site. A chronology for the sequence, estimated from the time-predictable model in Figure 8, is: 1970 yr B.P. for Event A; 1100 yr B.P. (time set) for Event B; and about 210 yr B.P.for Event C.

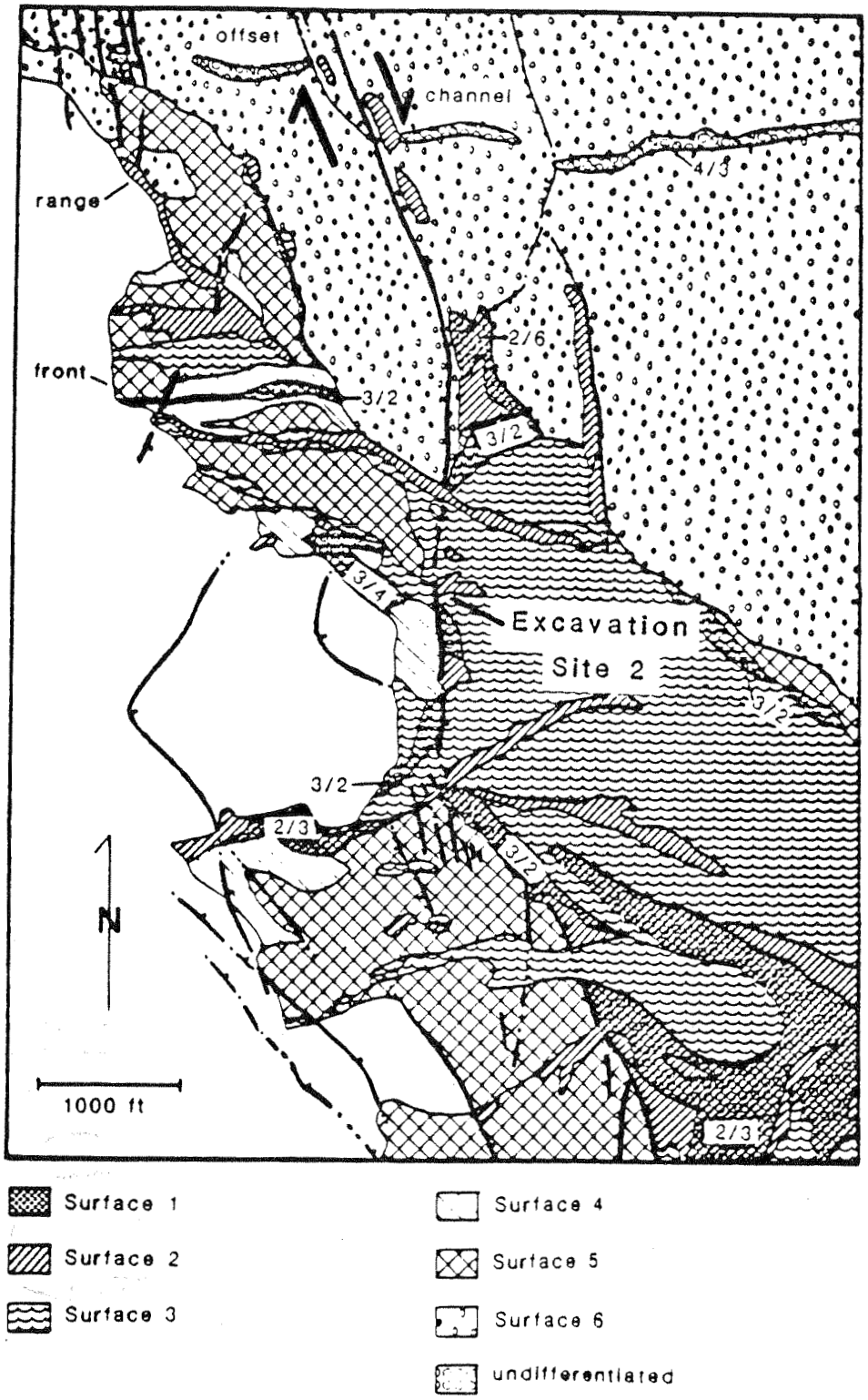

Figure 6. Distribution of surface map units on a portion of the Indian Creek alluvial fan in the vicinity of Excavation Site 2. Surface 7 not shown as it occurs to the beyond the map limit. Note offset channel near top of figure.

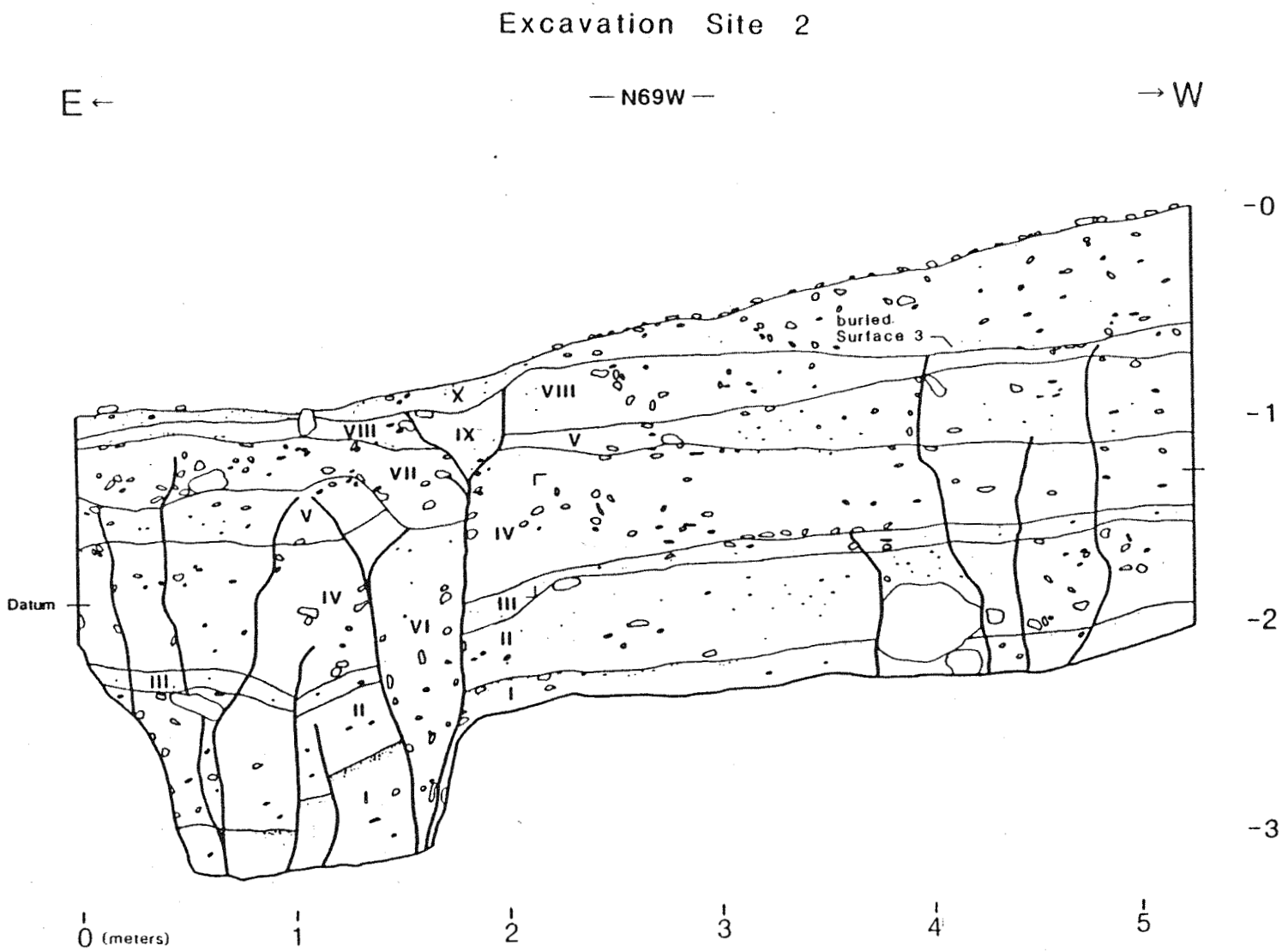

Figure 7. Graphical log of the south trench-wall at Excavation Site 2 on the Indian Creek alluvial fan.

SIMILARITIES BETWEEN THE PALEOSEISMIC SEQUENCES

There are several similarities between the sequences of paleoseismicity at the two excavation sites. Most notably, a sequence of three surface-faulting events is interpreted from stratigraphic/fault relations in both trenches. The first two events in the sequences resulted in similar relative amounts of vertical displacements, that are significantly larger than those associated with the most recent event. The youngest faulted surface at both sites is surface 3, which was offset during Event B. Furthermore, the erosion/deposition order, relative to individual events of the sequences, are similar. That is to say, at both excavation sites subsequent to the first event a period of erosion, which entirely degraded the Event A fault scarps, was followed by deposition of several stratigraphic units. Deposition was succeeded by Event B, during which these units were faulted. Following Event B, a period of fault scarp degradation, resulting in partially degrading the Event B fault scarps, preceded the most recent event.

These similarities suggest that the same three surface-faulting events are represented at both excavation sites. This is not unreasonable as the two sites are separated by less than 5 km along the main trace of the FLVFZ. In fact, based on historical rupture length data for events of similar displacements (Bonilla etal, 1984), rupture lengths from 40 to 60 km are estimated.

A possible test as to whether the two sequences of paleoseismicity are in fact the same sequence, their predicted chronologies are compared in Table 2. There is good agreement

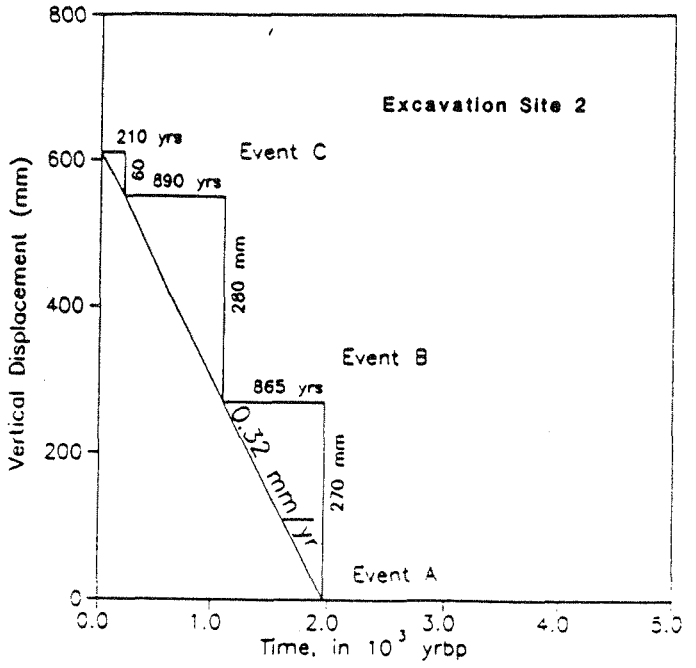

Figure 8. Time-predictable model developed for the timing and displacement constraints from Excavation Site 2. The timing of Event B is set at 1100 years b.p. (see explanation in text).

between the estimated time of the events and the corresponding interseismic intervals. Although the time of Event B in both time-predictable models (Figs. 5 & 8) was set at 1100 yr B.P., the time of the other two events varies relative to the estimated slip-rate and to coseismic-displacements. Both of which are unique for each of the sites. Therefore, the time of Events A & C are independent of the set time of Event B. The good agreement between the chronologies suggests that the same paleoseismic sequence is represented at both sites.

TABLE 2. Estimated timing and interseismic intervals for the paleoseismic sequences based on time-predictable models.

Paleo-seismic Event	Excavation Site 1 Event Time	Excavation Site 1 Inter-seismic Interval	Excavation Site 2 Event Time	Excavation Site 2 Inter-seismic Interval
A	1940 (yr B.P.)		1970 (yr B.P.)	
		840 (yr)		870 (yr)
B	*1100		*1100	
		930		890
C	175		210	

* Time of Event B set at 1100 yr B.P.

DISCUSSION

Events A and B resulted in similar amounts of displacement and may represent characteristic earthquakes for the northern FLVFZ. Event C resulted in only relatively minor coseismic-displacements, at least at the two excavation sites.

If the age range of 3400 to 4100 yr B.P. for the displaced tephra layer at Excavation Site 1 (Unit III; Fig. 5) is correct, then the estimated vertical slip-rate of 0.18 mm/yr, and hence the lateral slip-rate of 1.8 mm/yr, were not constant during the late-Holocene. Otherwise, the tephra would be displaced by a larger amount. This may suggest a temporal-cluster of paleoseismicity during the late-Holocene along the northern FLVFZ.

CONCLUSIONS

A sequence of paleoseismicity consisting of at least three discrete surface-faulting events occurred along the northern FLVFZ during the late-Holocene. The same three event sequence is represented at both excavation sites. Estimated vertical slip-rates range from 0.2 to 0.3 mm/yr and lateral slip-rates from 1.0 to 1.8 mm/yr are inferred for the northern FLVFZ. Geomorphic evidence along this portion of the fault zone support a dominantly right-slip style of faulting.

The predicted chronology of the three event sequence is: 1950 yr B.P. for Event A; 1100 yr B.P. for Event B; and 200 yr B.P. for Event C. Interseismic intervals from 850 to 900 years are also estimated from the time-predictable models. These tentative rates of activity suggest that during the late-Holocene the FLVFZ of the DVFS was among the most active faults in the Basin and Range. This study also suggests that in unique cases a time-predictable model may be used for temporal-correlation of paleoseismic sequences.

ACKNOWLEDGMENTS

I greatly appreciate the advice and knowledge of M. C. Reheis and F. F. Peterson furnished to me on soil development and geomorphology. This

project has benefited by chemical analyses and correlation of tephra layers by A. M. Sarna-Wojcicki. The project was funded by the Center for Neotectonic Studies, University of Nevada Reno. I thank Janet Sawyer and Paul Pase for assisting with surveying projects. Thanks also to G. S. Vick, J. L. Hoffard, S. J. Caskey, and C. M. dePolo for their thoughtful reviews of an eariler manuscript.

REFERENCES

Ball, S.H., 1907, A geological reconnaisance in southwestern Nevada and eastern California: U.S. Geol. Soc., Bull 308, 218 p.

Bonilla, M.G., Mark, R.K., and Lienkaemper, J.J., 1984, Statistical relations among earthquake magnitude, surface rupture length, and surface fault displacement, Seismological Soc. Am., v. 74, no. 6, p. 2379-2411.

Brady, R.H. III, and Troxel, B.W., 1981, Eastward termination of the Garlock fault in the Avawatz Mountains, San Bernardino County, California: Geol. Soc. Am., Abs. w/ Prog. v. 13, p. 46.

Carr, W.J., 1984, Regional structural setting of Yucca Mountain, southwestern Nevada, and Late Cenozoic rates of tectonic activity in part of the southwestern Great Basin, Nevada and California: Geol. Soc. Am., Open-file Report 84-854, 99 p.

Curry, H.D., 1938, Strike-slip faulting in Death Valley, California (abs.): Geol. Soc. Am., Bull., v. 49, p. 1874.

Elliott-Fisk, D.L., 1987, Glacial geomorphology of the White Mountains, CA-NV: Establishment of a glacial chronology: Physical Geography, v. 8, no 4.

Jenny, H., 1941, Factors of Soil Formation: McGraw-Hill, New York, 281 p.

McKee, E.H., 1968, Age and rate of movement of the northern part of the Death Valley-Furnace Creek fault zone, California: Geol. Soc. Am., Bull. v. 79, p. 509-512.

Peterson, F.F., 1981, Landforms of the Basin and Range Provience, Defined for soil survey: University of Nevada Reno, Tech. Bull. 28, 52 p.

Schwartz, D.P., and Coppersmith, K.J., 1986, Seismic Hazards: New trends in Analysis using geologic data: in Active tectonics, National Academy Press, Washington D.C., p. 215-230.

Shimazaki, K., and Nakata, T., 1980, Time-predictable recurrence model for large earthquakes: Geophy. Res. Lett., v. 7, p. 279-282.

Stewart, J.H., 1967, Possible large right-lateral displacement along fault and shear zones in the Death Valley-Las Vegas area, California and Nevada, Geol. Soc. Am., Bull., v. 78, p. 131-142.

Troxel B.W., Butler, P.R., 1986, Time relations between Quaternary faulting, Volcanism, and fan development, southern Death Valley, California: Field Guide, Pacific Cell, Friends of the Pleistocene, p. 31-36.

Wright, L.A., and Troxel, B.W., 1984, Geology of the northern half of the Confidence Hills 15-minute quadrangle, Death Valley region, eastern California: The area of the Amargosa chaos: California Division of Mines and Geology Map Sheet 34, 31 p.

Zoback, M.D., Zoback, M.L., Mount, V.S., Suppe, J., Eaton, J.P., Healy, J.H., Oppenheimer, D., Reasenberg, P., Jones, L., Raleigh, C.B., Wong, I.G., Scotti, O., Wentworth, C., 1987, New evidence on the state of stress of the San Andreas fault system: Science, v. 238, p. 1105-1111.

THE USE OF THE RELATIVE COMPARISON APPROACH AT YUCCA MOUNTAIN AND SIMILARITIES BETWEEN YUCCA MOUNTAIN AND THE 1932 CEDAR MOUNTAIN EARTHQUAKE AREA

Craig M. dePolo, John W. Bell, and Alan R. Ramelli

Nevada Bureau of Mines and Geology

One of the many approaches or techniques used in assessing the seismic hazard of a critical facility is the "relative comparison approach" (dePolo and Slemmons, in review). This approach involves the comparison of a potential source or source area with other sources or source areas which have either experienced historical earthquakes or have been studied in sufficient detail to definitively establish a seismotectonic history.

Seismotectonics of the Basin and Range province are very complicated and in general poorly understood. A relatively small number of active faults have been studied in detail, in comparison to the total number of potentially active "surface faults" and other sources. Further, several historical earthquakes occurring within the Basin and Range province have behaved in manners which are quite difficult to predict. This is typically not considered in a standard seismotectonic analysis (dePolo and others, in press). These earthquakes include events which have ruptured beyond their mapped fault or speculated segment lengths, events which have had widely distributed surface rupture patterns, and so called "floating" or "random" earthquakes. Other observations, such as spatial and/or temporal grouping or clustering of seismic events in the Basin and Range province (Wallace, 1987) are also not presently incorporated into seismotectonic analyses.

The relative comparison approach should be considered in the seismotectonic analysis of the proposed high-level nuclear waste facilities at Yucca Mountain. A number of historical earthquakes can be considered which have similarities with the Yucca Mountain site. One of the largest regional historical earthquakes which has many reasonable similarities is the 1932 Cedar Mountain earthquake (M_s=7.2).

When using a relative comparison approach it is important to document the similarities between the facility site and the comparable event or source. In the case of comparing the Yucca Mountain area with the 1932 earthquake area, the similarities are significant and substantiate the use of the 1932 event for seismotectonic analyses of the Yucca Mountain site.

Some of the principle similarities which are important in such analyses are similarities in tectonic setting, distributed surface fault patterns, and fault structures exposed in trenches. Similarities between the two areas in tectonic setting include:

* location within the Basin and Range province and the Walker Lane belt;
* northwest-oriented least principle stress directions;
* activity of both north-south and northeast-trending faults;
* proposals that detachment structures locally exist;
* conjugate structures locally exist;
* focal mechanisms are dominated by strike-slip displacement and include north-south nodal planes;
* adjacent or local caldera structures exist or have been proposed.

Distributed fault patterns and ruptures extending beyond mapped fault lengths are aspects of the 1932 earthquake which are not accounted for in standard seismotectonic analyses, but need to be considered in the seismotectonic input for the Yucca Mountain facilities. Evidence for distributed faulting at the Yucca Mountain site has been noted by Ramelli and others (1988) and includes basaltic ash infilling fault fractures along several parallel, closely spaced faults and similarities in fault scarp morphology and ages of displaced surfaces, possibly indicating a widely distributed paleoseimic event. Short faults which are not easily attributed to a seismogenic fault system or do not appear kinematically linked at the surface, may have the potential to fail in sequence or be expressions of deeper, larger systems, which have larger earthquake potentials.

Similarities between fault structures exposed in trenches the Yucca Mountain and Cedar Mountain areas are important for determining the existence of active strike-slip displacement in both regions and for documenting the need for strike-slip displacement to be evaluated in the Yucca Mountain area. Failure to account for lateral displacements may lead to underestimations of net displacements and slip-rates along faults in the Yucca Mountain area. Similarities noted in trenches in these two areas include vertical faults and flower structures.

REFERENCES CITED

dePolo, Craig M. and Slemmons, D. Burton, in review, Estimation of earthquake size for seismic hazards: Geological Society of America, Centennial Volume on Engineering Geology.

dePolo, Craig M., Clark, Douglas G., Slemmons, D. Burton, and Aymard, William H., in press, Historical Basin and Range province surface faulting and fault segmentation, in Conference on segmentation, Schwartz, David P. and Sibson, Richard H., eds.: U. S. Geological Survey, open-file report.

Ramelli, Alan R., Bell, John W., and dePolo, Craig M., 1988, Evidence for distributive faulting at Yucca Mountain, Nevada (abst.): Geological Society of America, Abstracts with Programs, v. 20.

Wallace, Robert E., 1987, Grouping and migration of surface faulting and variations in slip rates on faults in the Great Basin province: Seismological Society of America Bulletin, v. 77, p. 868-876.

Application of a refined method for determining principal stress orientations in southern Nevada

Virgil A. Frizzell
U. S. Geological Survey, Flagstaff, Arizona

Mary Lou Zoback
U. S. Geological Survey, Menlo Park, California

Local and regional principal stress orientations for both the present and recent past are essential to understanding the neotectonic history of an area. Several techniques have been successfully utilized for determining modern tectonic stress orientations, including analysis of geological data, focal mechanisms, and *in situ* measurements; Zoback and Zoback (1980) discussed the assumptions, inherent difficulties, and uncertainties of these various techniques.

Advances in quantitative analysis of data derived from grooves and slickensides on fault surfaces provide a powerful tool for determining both recent stress and paleostress orientations (Angelier, 1984). Underlying the technique are the assumptions that the slickensides indicate major fault motion in the direction of maximum resolved shear stress in response to a uniform regional tectonic stress (recognizing that local "block setting" may introduce some spurious data) and that the orientations determined on features which formed relatively close to the Earth's surface accurately reflect those at depth. This technique involves collection and analysis of fault-slip data. Data include the strike and dip of the fault surface, the orientations of the lineation defining the slip vector on that surface, and the sense and amount of offset. To determine both the orientations of regional principal stress and their relative magnitudes, lineation surfaces of various orientations must be measured within the fault zone. The plunge of the lineation must be determined for faults with dips less than 50°; either rake or plunge may be determined for more steeply dipping faults.

Determination of offset sense is essential for rigorous analysis, although data from faults with an unknown sense of offset can be used for a qualitative geometric analysis. In addition to using offset of planar features, such as

bedding, to determine sense of slip, Angelier and others (1985, p. 351-3) utilized four other criteria: orientation of small fractures, interpreted to be Riedel shears; asymmetry of grooves created by projections from the fault surface; rough facets with or without striae, and asymmetry of discoid cavities. Although care should be taken when determining sense of offset on all surfaces, the sense indicated by gently dipping beds that are offset by shallow-rake faults (less than 20°) requires special attention. If superposed sets of striae are present on a surface, the age of one set relative to the other should be determined.

The analysis uses a least-squares iterative inversion to determine the mean deviatoric principal stress tensor. As outlined by Angelier (1984) and applicable on both desktop and mainframe computers, the method determines the orientation of the principal stress axes and a ratio of relative stress magntudes by iteratively minimizing the mean angular deviation between the computed and observed slip vector for each measurement.

In a recent application of this technique to a structurally complex zone of strike-slip and normal faults in the Hampel Wash area of southern Nevada we (Frizzell and Zoback, 1987) have determined a normal faulting stress regime (maximum principal stress vertical), with a minimum horizontal stress orientation of N 60° W. The maximum horizontal stress was found to be intermediate in magnitude between the vertical and minimum horizontal stresses. The N 60° W minimum horizontal principal stress orientation obtained from the fault-slip inversion agrees with a geometric analysis of the data and is consistent with a modern least horizontal principal stress orientation of N 50° - 70° W inferred from earthquake focal mechanisms, wellbore breakouts, and hydraulic fracturing measurements in the vicinity of the Nevada Test Site (Stock and others, 1985). This solution fits all the data well except for a subset of strike-slip faults that strike N 30° - 45° E, subparallel to normal faults of the data set. Nearly pure dip-slip and pure strike-slip movement on similarly oriented faults, however, cannot be accommodated in a single stress regime. Superposed sets of striae observed on some faults suggest temporal rotations of the regional stress field or local rotations within the region of the fault zone.

This analysis of a modest data set indicates that the above assumptions are correct and that similar studies might be undertaken successfully in

areas where the results from other techniques are absent or sparse. For example, the technique should prove particularly useful in determining the orientations of principal stress directions within regional blocks constituting the Walker Lane belt (Stewart, in press).

References

Angelier, J., 1984, Tectonic analysis of fault slip data sets: Journ. of Geophys. Res., 89, 5835 - 5848.

Angelier, J., Colletta, B., and Anderson, R. E., 1985, Neogene paleostress changes in the Basin and Range: A case study at Hoover Dam, Nevada - Arizona: Geol. Soc. Am. Bull., 96, 347 - 361.

Frizzell, V. A., Jr., and Zoback, M. L., 1987, Stress orientation determined from fault slip data in Hampel Wash area, Nevada, and its relation to contemporary stress field: Tectonics, 6, 89 - 98.

Stewart, J. H., in press, Tectonics of the Walker Lane belt, western Great Basin - Mesozoic and Cenozoic deformation in a zone of shear: *in* Ernst, W. G., ed., Metamorphic and crustal evolution of the western United States: Rubey Volume VII, Prentice Hall, Englewood Cliffs, N. J.

Stock, J. M., Healy, J. H., Hickman, S. H., and Zoback, M. D., 1985, Hydraulic fracturing stress measurements at Yucca Mountain, Nevada, and relationships to the regional stress field: Journ. of Geophys. Res., 90, 8691 - 8706.

Zoback, M. L., and Zoback, M. D., 1980, State of stress in the conterminous United States: Journ. of Geophys. Res., 85, 6113 - 6156.

PALEOMAGNETIC RESEARCH IN THE BASIN AND RANGE PROVINCE, WESTERN UNITED STATES: HISTORICAL PERSPECTIVE, APPLICATIONS, AND LIMITATIONS

John Wm. Geissman
Department of Geology
University of New Mexico
Albuquerque, NM 87131

Mark R. Hudson
U.S. Geological Survey
Denver, CO 80225

James T. Faulds
James T. Callian
Steve S. Harlan
Qing Huang
University of New Mexico

Yianping Li
Department of Geophysics
Stanford University
Stanford, CA 94035

The wealth of paleomagnetic data from volcanic, plutonic, and sedimentary rocks from the western margin of North America has been used to clarify the often far-travelled and significantly rotated tectonic history of terranes comprising the borderland. In comparison, relatively little paleomagnetic work has been carried out in the Basin and Range province, lying inboard of and seemingly far less approachable and perhaps aesthetically less pleasing than the western North America borderland. Nonetheless, in the past decade considerable attention has been given by paleomagnetists, often in conjunction with structural geologists, to numerous problems in the Basin and Range province and immediately adjacent areas (e.g., Mojave Desert Block). Many of these endeavors have provided important results bearing, in particular, on the Cenozoic structural development of the province. This contribution is intended as a brief review of the historical development of paleomagnetic research in the Basin and Range province, a brief example of paleomagnetic research in the province from the UNM Paleomagnetism Laboratory, and a cautionary statement regarding the practical limitations of paleomagnetic research in a region which has potentially experienced several complicated periods of deformation and related events which may contribute to a complicated magnetization record.

General Goals and Historical Perspective

From a general standpoint, paleomagnetic studies in the Basin and Range province can be divided into endeavors involving pre-Cenozoic, "basement" layered sedimentary and volcanic rocks, and cross-cutting plutons; and Cenozoic, largely latest Eocene and younger, layered volcanic and sedimentary rocks, and plutons. Principal research goals fall into structural and diagenetic/tectonothermal categories. Structure-related studies are, in a relative sense, largely of local scale and include assessment of the amount and sense of vertical-axis rotation of crustal blocks, as well as dimensions of domains of uniform, rigid-body rotation; the amount and, perhaps, sense of horizontal-axis rotation (true tilting) of crustal blocks; and latitudinal translation of allochthonous terranes. The magnitude of Cenozoic extension at different latitudes across the Basin and Range province cannot be addressed through direct paleomagnetic studies of longitudinal translation, although paleomagnetic data from Mesozoic rocks of the Sierra Nevada clearly constrain variations in the amount of extension across the province (Magill et al., 1982; Bogen and Schweickert, 1985; Frei, 1986).

Evaluation of vertical axis rotation is most properly addressed using layered volcanic or sedimentary units, as reference to the paleohorizontal is usually, although not always, afforded. This problem will be further discussed below. If non-layered (e.g., plutons) or penetratively deformed rocks can be restored to the paleohorizontal at the time of magnetization acquisition, then such units can as well be used for studying vertical axis rotations. More commonly and often appropriately, data from these units may be used to infer amounts of crustal tilt. Finally, since early to mid-Paleozoic passive margin development, the Basin and Range province has been the site of several periods of deformation, magmatism, and regionally elevated thermal flux. Often superimposed upon or completely replacing primary magnetizations are those of secondary origin related to this complex history. Their recognition and evaluation in terms of age and origin may be useful in understanding particular tectonothermal processes, including the age and nature of mineral deposition.

Early paleomagnetic work in the province focussed on ash-flow tuffs and regional correlations (e.g., Grommé et al., 1972; Best et al., 1973). The first study to document vertical-axis rotation related to strike-slip motion was that of Gillett and Van Alstine (1982) along the Las Vegas Valley shear zone. Subsequently, this field of research has certainly expanded in importance (e.g., Las Vegas Valley shear zone: Nelson and Jones, 1986; Dixie Valley area: Hudson and Geissman, 1984, 1987; Hudson, 1988; Lake Mead Shear Zone: Ron et al., 1986, 1988; Geissman, 1986; Geissman et al., in prep., 1988; Nevada Test site: Rosenbaum and Scott, 1986; Walker Lane area: Geissman et al., 1984; Callian and Geissman, 1984; Bell et al., 1986; southwest Arizona: Calderone and Butler, 1984). Local scale tilting of the crust was studied by Geissman et al. (1982a, 1982b) in the Yerington area and confirmed field-based observations by Proffett (1977) that mid-Miocene and younger motion along east-dipping normal faults had resulted in significant (often over 90°) west-side down tilting of thick portions of the upper crust. Additional studies have been varied in scope and results (e.g., Mineral Mountains, Utah: Bruhn and Geissman, 1985; San Antonio Mountains, Shaver and McWilliams, 1987; Black and Eldorado Mountains, Faulds and Geissman, 1986; Ron et al., 1988; Faulds et al., in prep., 1988; Gilles Range: Keller et al., 1987; Dixie Valley area; Hudson, 1988; Kingston Range; Jones, 1983; Calzia et al., 1986.

Primary magnetizations in layered basement strata, which could be used to assess latitudinal motion of terranes, have been few in number. Pervasive remagnetization of Permian and Jurassic strata by plutonism has been reported by Russell et al. (1982) (Jackson Mountains) and Geissman et al. (1984) (Excelsior Mountains). Late Paleozoic remagnetization of Lower Paleozoic and latest Precambrian strata was recognized by Gillett and Van Alstine (1982) (Desert Range area) and has also been recorded in the Egan Range (Gillett and Geissman, unpublished data). Hudson and Geissman (1984) and Hudson (1988) have reported the absence of a statistically significant inclination anomaly in layered mafic rocks and equivalent extrusive rocks of the mid-Jurassic Humboldt Lopolith. A recent reinvestigation of the Jackson Mountains area (Maher and Kirschvink, 1987) has revealed that a primary magnetization is present in latest Triassic to Late Jurassic volcanic and sedimentary rocks and that considerable southward translation occurred prior to emplacement.

Example of Ongoing Research

Beginning with the detailed pioneering work by R.E. Anderson (e.g., 1971, 1973), the Lake Mead area has attracted considerable interest from numerous geoscientists. Paleomagnetic studies have been prompted by the possibility of recovering significant vertical axis rotations related to crustal shear. Documented rotations must be taken into account in the evaluation of pre-existing structures and causitive stress-fields. Angelier et al.'s (1985) evaluation of fault-slip data from the mid-Miocene Tuff of Hoover Dam at and near Hoover Dam suggested that the ca. 10 Myr clockwise rotation of least principal stress direction, evidenced in other portions of the Basin and Range province, was recorded at Hoover Dam and that faulting spanned the reorientation of least principal stress directions. They cautioned, however, about the the possibility of considerable relative rotation of a portion of their study area in response to motion along the Lake Mead shear zone. Paleomagnetic studies in the Hoover Dam area have concentrated on the Tuff of Hoover Dam but older and younger volcanic rocks (Patsy Mine and Mt. Davis

sequences) as well as sills, dikes, and plutons (Boulder City, Wilson Ridge) have been sampled (Figure 1). The Tuff of Hoover Dam usually responds extremely well in progressive demagnetization. Alternating field and thermal methods both isolate a magnetization of shallow inclination and westward to northwestward declination which is well-grouped at the site level. In in situ coordinates, sites from west and northwest of Hoover Dam and the Colorado River consistently exhibit westward declinations, which those southeast and east of Hoover Dam yield northwestward declinations (Figure 2). The mean inclinations determined from the two populations of directions are statistically indistinguishable. To restore magnetizations to the paleohorizontal, simple tilt corrections about present strike axes of eutaxitic structures have been used. The magnitudes of tilt used in these corrections are in good agreement with dips of underlying or overlying volcanogenic sedimentary units. With local structural correction, site means steepen slightly in inclinations, but again the mean inclinations for the two populations are statistically indistinguishable and the declination discrepancy, approximately 35°, remains and is statistically significant (+/- 8°, at the 95% confidence level). Even with structural correction, the magnetization characteristic of the Tuff of Hoover Dam is anomalously shallow in inclination and was in all likelihood acquired during a geomagnetic field excursion or true field reversal. The unit is a recorder of a short-lived, anomalous field direction and therefore the absolute amount of vertical axis rotation in the area cannot be inferred. In a relative sense, the region west and northwest of Hoover Dam has rotated approximately 35° in a counterclockwise fashion with respect to the area to the south and east. Our preliminary data (Figure 3) suggest that the rotation does not appear to be gradual over a broad deforming zone, leaving one with the difficult problem of evaluating how a significant declination anomaly (i.e. rotation) can abruptly occur over such a short distance. The consistency in inclination data in both in situ and corrected coordinates, nonetheless, leads us to suggest that counterclockwise rotation in the region occurred after regional east-side down tilting.

Practical Concerns and Limitations

Paleomagnetic research in the Basin and Range Province has a healthy future, if workers recognize both the limitations of the research techniques and the importance of close collaboration with geoscientist colleagues more familiar with structural and other complexities of the rocks in question. First, assessment of absolute axis rotation, tilting, and latitudinal displacement requires adequate averaging of the geomagnetic field by the units in question. For sequences of lava flows, for example, demonstration of considerable time between individual eruptions, a dual polarity record, and reasonable angular standard deviation of virtual geomagnetic pole (VGP) data (e.g., Merrill and McElhinny, 1983) derived from individual flows, dikes or sills, are all considerations which must not be overlooked. Even thick (>200 m) ash flow tuffs act as geologically instantaneous recorders of the geomagnetic field (e.g., Geissman et al., 1982a; Wells et al., 1987). Relative rotations or crustal tilts (e.g., Geissman 1986; Wells et al., 1987) can be investigated using a single igneous unit or sedimentary bed, providing a homogeneous magnetization is present.

The local scale tilt-correction of in situ (geographic) paleomagnetic data is not straightforward, especially when stratal tilt is ascribed to

extensional processes. As discussed by MacDonald (1980), the present strike axis of tilted units may reflect a combination of both tilting and vertical axis rotation. Whether simple correction of data about the present tilt axis is appropriate can be assessed in at least some cases by referencing the fact that the angular relationship between the inclination of magnetization and the paleohorizontal is fixed unless disturbed by internal, penetrative deformation. Restoration of paleomagnetic data from tilted fault blocks to the paleohorizontal should result in a constant inclination, yet possibly dispersed declination, explained by vertical axis rotation.

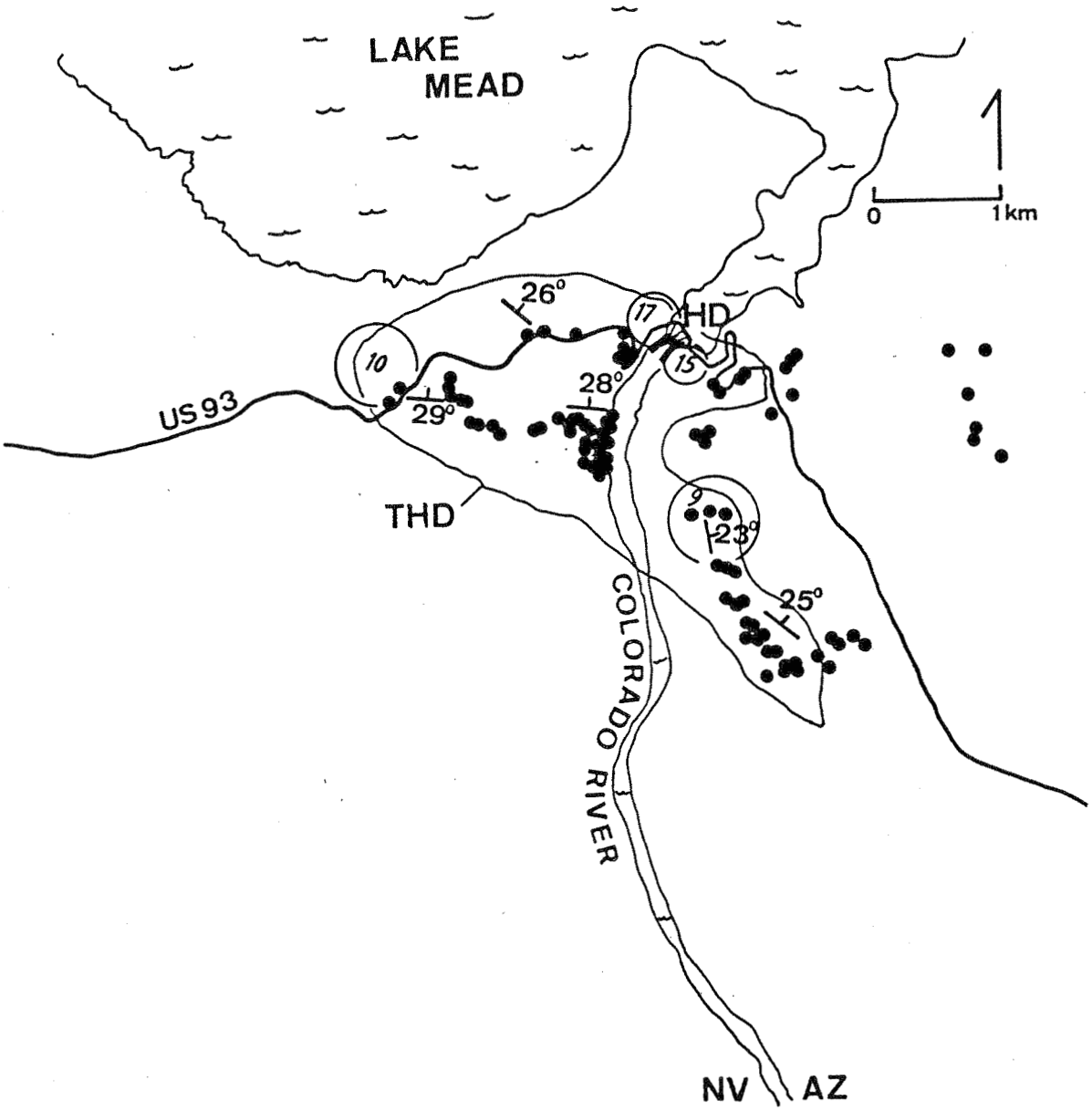

Figure 1. Location map of the Hoover Dam area. Paleomagnetic sampling sites are given as dots; in congested areas, the large circle and associated number refers to the number of sites within that area. Attitudes of eutaxitic structures in the Tuff of Hoover Dam are also shown.

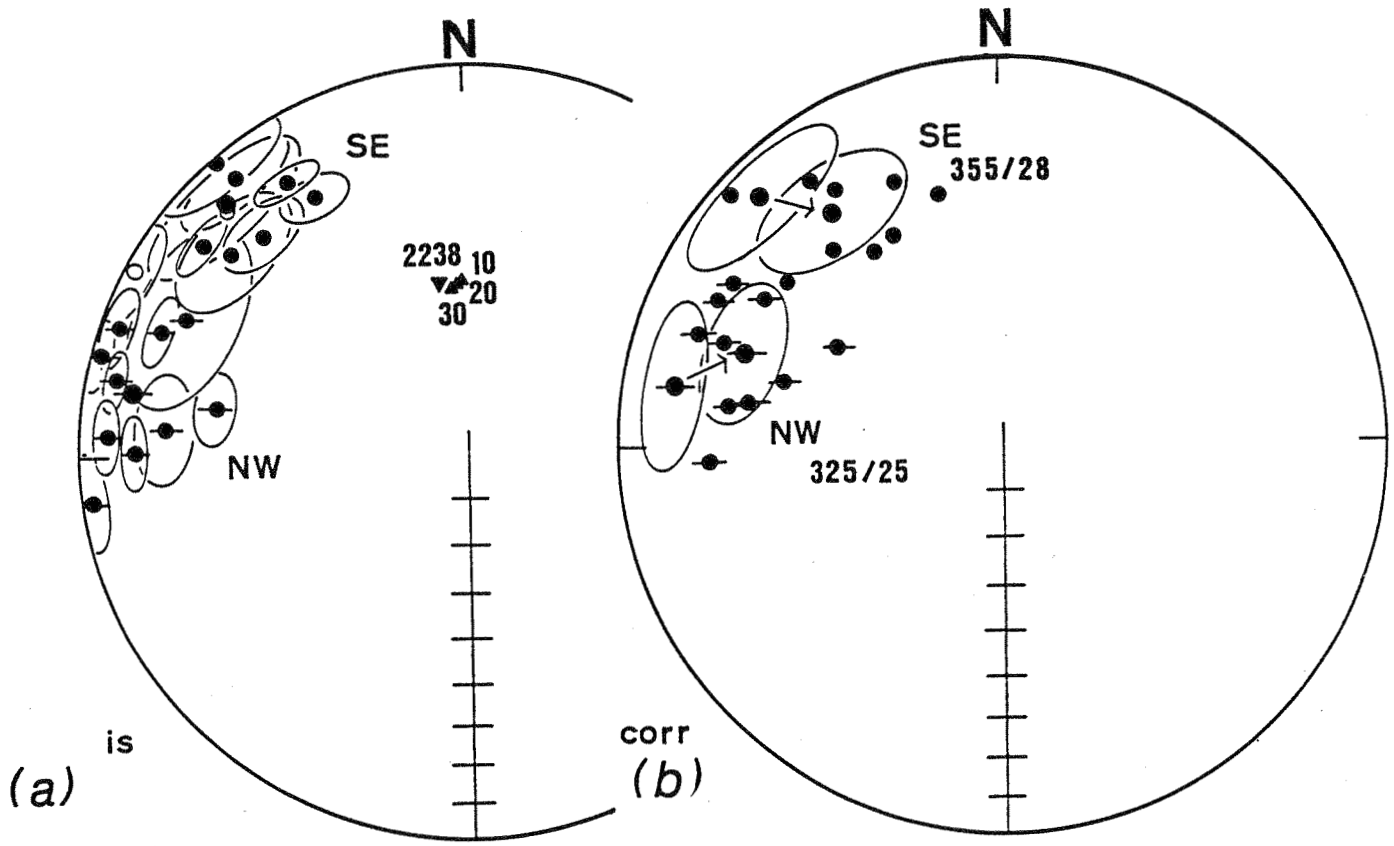

Figure 2. Equal area projections of paleomagnetic data from the Tuff of Hoover Dam. Small circles refer to individual site means, with projected cones of 95% confidence (in a). Large circles refer to locality means, with projected cones of 95% confidence (in b). Open (closed) symbols refer to upper (lower) hemisphere projections. (a) in situ coordinates. (b) structurally corrected (paleohorizontal) coordinates. Site means with horizontal tics refer to those northwest and west of Hoover Dam.

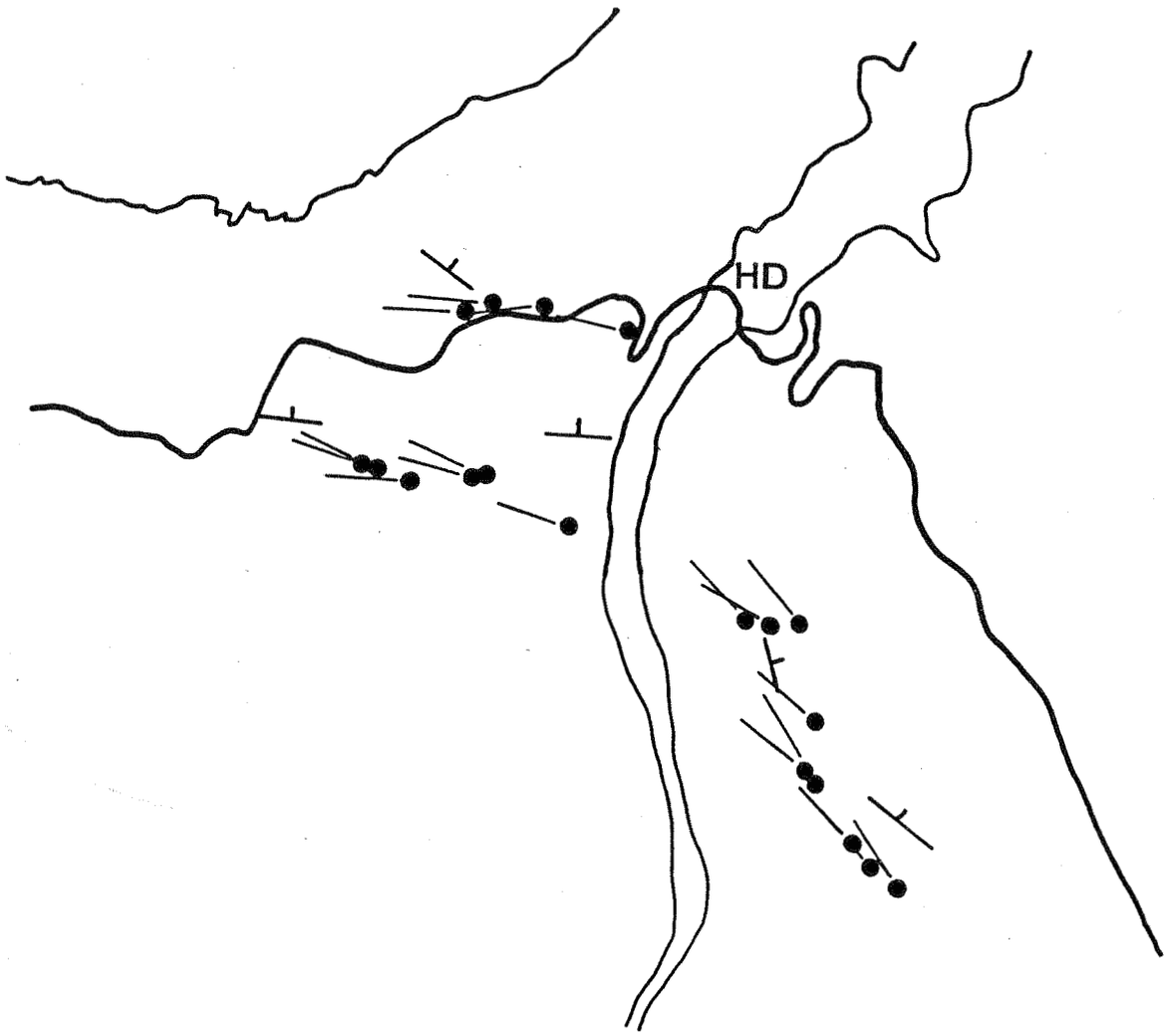

Figure 3. Geographic map showing in situ declination data from 19 sites in the Tuff of Hoover Dam. Site mean declinations are plotted as lines from individual site locations.

REFERENCES

Anderson, R.E., 1971, Thin-skinned distension in Tertiary rocks of southeast Nevada, Geol. Soc. Amer. Bull., v. 82, p. 43-58.

Anderson, R.E., 1973, Large magnitude late Tertiary strike-slip faulting north of Lake Mead, Nevada, U.S. Geol. Surv. Prof. Paper 794, 18 p.

Angelier, J., B. Colletta, and R.E. Anderson, 1985, Neogene paleostress rotation and permutation in the Basin and Rage--A case study at Hoover Dam, Nevada-Arizona, Geol. Soc. Amer. Bull., v. 96, p. 347-361.

Bell, M., J.W. Geissman, J.T. Callian, and J.S. Oldow, 1986, Paleomagnetism of the mid-Cretaceous Silver Dyke Pluton and Pluton of Teels Marsh, west-central Nevada: Further implications for tectonism in the Walker Lane area [Abstract], EOS, Trans. American Geophys. Union, v. 67, p. 922.

Best, M.G., R.T. Shuey, C.F. Caskey, and S.K. Grant, 1973, Stratigraphic relations of members of the Needles Range Formation at type localities in southwestern Utah, Geol. Soc. Am. Bull., v. 84, p. 3269-3278.

Bogen, N.L., and R.A. Schweickert, 1985, Magnitude of crustal extension across the northern Basin and Range province: Constraints from paleomagnetism, Earth and Planetary Science Letters, v. 75, p. 93-100.

Bruhn, R.L., and J.W. Geissman, 1985, Reconnaissance paleomagnetic study of the Mineral Mountains, eastern Great Basin, Utah, and tectonic implications [Abstract], EOS, Trans. Amer. Geophys. Union, v. 66, p. 876.

Calderone, G., and R.F. Butler, 1984, Paleomagnetism of Miocene rocks from southwestern Arizona: Tectonic implications, Geology, v. 12, p. 627-630.

Callian, J.T., and J.W. Geissman, 1984, Further paleomagnetic data from basement intrusives and metasedimentary rocks, Walker Lane area, west-central Nevada: a case of local structural irregularities [Abstract], EOS, Trans. Amer. Geophys. Union, v. 65, p.

Calzia, J.P., K.L. Verosub, and R.C. Jachens, 1986, Tilting and faulting of the Late Miocene Kingston Peak Granite, southern Death Valley, California [Abstract], EOS, Trans. American Geophys. Union, v. 67, p. 1189.

Faulds, J.E., and J.W. Geissman, 1986, Paleomagnetic evidence of tilted basement, central part of the Black Mountains, northwestern Arizona [Abstract], EOS, Trans. American Geophys. Union, v. 67, p. 1226.

Faulds, J.E., J.W. Geissman, and C.K. Mawer, 1988, Geometry and kinematics of a major middle Miocene accommodation zone in the highly extended terrane of the northern Colorado River trough, northwestern Arizona and southern Nevada, Geol. Soc. America Spec. Paper, in prep.

Frei, L.S., 1986, Additional paleomagnetic results from the Sierra Nevada: further constraints on Basin and Range extension and northward displacement in the western United States, Geol. Soc. Amer. Bull., v. 97, p. 840-849.

Geissman, J.W., 1986, Paleomagnetism and Late Cenozoic strike-slip tectonism in the Hoover Dam area, southeast extension of the Lake Mead Fault Zone, Nevada and Arizona [Abstract], EOS, Trans Amer. Geophys. Union, v. 67, p. 922.

Geissman, J.W., H. Ron, and A. Nur, 1988, Paleomagnetic evaluation of crustal rotation caused by strike-slip faulting at and near the latitude of Las Vegas, Nevada, southern Basin and Range Province, Geol. Soc. America Special Paper, in preparation.

Geissman, J.W., J.T. Callian, J.S. Oldow, and S.E. Humpries, 1984, Paleomagnetic assessment of oroflexural deformation in west-central Nevada and significance for emplacement of alloohthonous assemblages, Tectonics, v. 3, p. 179-200.

Geissman, J.W., R. Van der Voo, and K.L. Howard, Jr., 1982a, A paleomagntiec study of the structural deformation in the Yerington District, Nevada I. Tertiary units and their tectonism, Amer. Jour. Sci., v. 282, p. 1042-1079.

Geissman, J.W., R. Van der Voo, and K.L. Howard, Jr., 1982b, A paleomagnetic study of the structural deformation in the Yerington District, Nevada 2. Mesozoic "basement" units and their total and pre-Oligocene tectonism, Amer. Jour. Sci., v. 282, p. 1080-1109.

Gillett, S.L., and D.R. Van Alstine, 1982, Remagnetization and tectonic rotation of upper Precambrian and lower Paleozoic strata from the Desert Range, southern Nevada, Jour. Geophys. Res., v. 87, p. 10929-10953.

Gromme, C.S., E.H. McKee, and M.C. Blake, 1972, Paleomagnetic correlations and potassium-argon dating of middle Tertiary ash-flow sheets in the eastern Great Basin, Geol. Soc. America. Bull., v. 83, p. 1619-1638.

Hagstrum, J.T., and P.B. Gans, 1988, Paleomagnetism of the Kalamazoo Tuff: Its application to the structural analysis of Middle Tertiary extension in east-central Nevada, Jour. Geophys. Res., in review.

Hudson, M.R., and J.W. Geissman, 1987, Paleomagnetic and structural evidence for middle Tertiary counterclockwise block rotation in the Dixie Valley region, west-central Nevada, Geology, v. 15, p. 638-642.

Hudson, M.R., 1988, Paleomagnetic and structural evaluation of Mesozoic and Cenozoic deformation, northern Dixie Valley area, west-central Nevada, unpublished Ph.D. Dissertation, Colorado School of Mines, Golden, 250 p.

Jones, C., 1983, Paleomagnetism of the Kingston Range, San Bernadino Co., CA: A tectonic interpretation [abstract], EOS, Trans. American Geophys. Union, v. 64, p. 686.

Keller, R.P., J.S. OLdow, R.F. Hardyman, and J.W. Geissman, Transtensional development of low-angle detachment faults: Walker Lane, western Great Basin [Abstract], EOS, Trans. American Geophys. Union, v. 68, p. 1475.

MacDonald, W.D., 1980, Net tectonic rotation, apparent tectonic rotation, and the structural tilt correction in paleomagnetic studies, Jour. Geophys. Res., v. 85, p. 3659-3669.

Magill, J.R., A. Cox, and R. Duncan, 1981, Tillamook volcanic series: Further evidence of tectonic rotation of the Oregon Coast Range, Jour. Geophys. Res., v. 86, p. 2953-2970.

Maher, K.A., and J.L. Kirschvink, 1987, Paleomagnetism and tectonics of the Jackson Mountains, NW Nevada [Abstract], EOS, Trans. American Geophys. Union, v. 68, p. 1253.

Merrill, R.T., and M.W. McElhinny, 1983, The Earth's Magnetic Field, Academic Press, New York, 401 pp.

Nelson, M.R., and C.H. Jones, 1987, Paleomagnetism and crustal rotations along a shear zone, Las Vegas Range, southern Nevada, Tectonics, v. 6, p. 13-33.

Proffett, J.M., Jr., 1977, Cenozoic geology of the Yerington District, Nevada, and implications for the nature and origin of Basin and Range faulting, Geol. Soc. Amer. Bull., v. 88, p. 247-266.

Ron, H., A. Aydin, and A. Nur, 1986, Strike-slip faulting and block rotation in the Lake Mead Fault System, Geology, v. 14, p. 1020-1023.

Ron, H., J.W. Geissman, A. Nur, and J.E. Faulds, 1988, Kinematics of Neogene and contemporary deformation along the Lake Mead Fault System, southern Nevada, Geol. Soc. America Abstr. with Progs., v. 20, p. 225.

Russell, B.J., M.E. Beck, Jr., R.F. Burmester, and R.C. Speed, Cretaceous magnetizations in northeastern Nevada and tectonic implications, Geology, v. 10, p. 423-428.

Shaver, S.A., and M.O. McWilliams, 1987, Cenozoic extension and tilting recorded in Upper Cretaceous and Tertiary rocks at the Hall molybdenum deposit, northern San Antonio Mountains, Nevada, Gull. Geol. Soc. Amer., v. 99, p. 341-353.

Wells, R.E., and J.W. Hillhouse, 1987, Tectonic rotations in the Peach Springs Tuff, Colorado River extensional corridor, California and Arizona, Geol. Soc. America Abstracts with Progs., v. 19, p. 886.

EARTHQUAKE CLUSTERING NEAR MINA NEVADA, JULY AND AUGUST 1987

Kenneth D. Smith, William R. Walter, Raul R. Castro,

Keith F. Priestley, Abdol R. Anooshepoor

Seismological Laboratory, Mackay School of Mines

University of Nevada Reno

ABSTRACT

Earthquake clustering is a characteristic of the regional seismicity pattern in the west central Great Basin. Clustering in the Mina, Nevada region during the summer of 1987 indicates activity on secondary faults associated with a major range bounding structure, the Soda Springs Valley fault, within the Walker Lane structural trend. This activity is clearly of the same character as that that preceded the 1986 M_L 6.4 Chalfant, California earthquake and which has been seen in several clustering episodes in the region. Tendencies in the clustering centers include; activity confined to a small volume at mid crustal depths, no clearly defined mainshock with several events in the upper M_L 3 range, and as distinct from standard mainshock-aftershock sequences no well defined decay of the rate of activity with time.

Source mechanisms determined with spectral methods from near source digital recording, within a mine tunnel 12 km distance, indicate low stress drops and nearly a constant source radius for several of the larger events. These results are in agreement with source studies of Basin and Range earthquakes by Douglas and Ryall (1972) for the same magnitude range. There is evidence that the site effect is controling the spectral shape and calls into question these source parameter determinations. A study is currently underway to determine the site characteristics at this particular recording site.

Regional estimates of Q for travel paths to USGS Southern Great Basin Network at NTS, result in a frequency dependent Q of,

$$Q(f) = 16.60\,f + 172.26$$

in the frequency range 5 to 25 Hz

INTRODUCTION

An M_L 4 and several M_L 3.5+ earthquakes occurred within a shallow localized cluster of activity during July and August 1987 near the small town of Mina, Nevada. The larger earthquakes were strongly felt by local residents. This area is of particular interest in terms of earthquake potential because it is within the proposed White Mountains 'seismic gap' (Hill *et al*, 1985). The 'seismic gap' is defined to the

south by the northern extent of the 1872 M_L 8 Owens Valley earthquake, just south of the town of Bishop (Figure 1), and to the north by southern extent of the 1932 M_L 7.1 Cedar Mountains event (star in Figure 1). The earthquake cluster occurred in the northern part of the 'gap' where it crosses the Walker Lane, a structurally complex northwest trending zone of significant right-lateral offsets (130 to 190 km of lateral displacement during the late Cenozoic, Stewart 1978; Stewart *et al*, 1968; Nielsen, 1965; Shawe, 1965). The activity was just to the west (≈ 7km) of the Pilot Mountains Range front fault which does show holocene off-sets and was initially thought to be the causative structure. Earthquake clustering has been recognized as a characteristic of seismicity of the the Mina, Nevada area since good quality hypocentral locations became available in the 1970's. Ryall and Priestley (1974), in a study of the Excelsior Mountains region east of Mina, noted the high levels of seismicity in this region with a cooresponding lack of moderate to large events and suggested that the bulk of the stress release was being accommodated by smaller events. The Mesozoic tectonics of the Pilot Mountains-Mina, Nevada region has been discussed in detail by Oldow (1981, 1983).

Shallow clustering of small earthquakes has preceded several of the $M_L \approx 6$ events of the Bishop-Mammoth Lakes, California earthquake sequence (1978-present), 100 km to the southwest of Mina along the eastern front of the Sierra Nevada (Ryall and Ryall, 1981; Smith and Priestley, 1988; Priestley *et al*, 1988). In particular, the two most recent earthquakes in this region, the 1984 M_L 5.8 Round Valley and 1986 M_L 6.4 Chalfant, California earthquakes, occurred in close association with significant range front faults, and were preceded by some degree of earthquake clustering. The seismotectonics of the Bishop, California area is somewhat similar to the Mina region in that we see dominantly strike slip faulting and the seismicity rarely conforms to major range bounding faults. Also, periods of localized clustering are a characteristic of the seismicity of this entire region (Figure 1).

We shall define clustering in a qualitative sense. In the region, clustering, as opposed to aftershock sequences, tends to include a significant number events at the M_L 3-4 level with no particular event being dominant (no clearly identified main shock), and there is not the characteristic exponential decay with time of earthquake occurrance and size that is usually observed in classic mainshock-aftershock sequences. Also, these phenomena usually occur at shallow depth, are confined to a small volume of the crust and represent a significant amount of energy release for the restricted volume.

In this study we analyze the 1987 Mina activity, attempt to isolate the causative faults and discuss recent regional seismicity patterns with respect to localized clustering and active faulting.

DATA

The University of Nevada Seismological Laboratory (UNSL), in cooperation with the U.S. Geological Survey (USGS), monitors earthquake activity along the Sierra Nevada-Great Basin boundary of Nevada and California and with USGS funding extends coverage to the west central Great Basin of Nevada. Data from the UNSL short period seismic network are telemetered to the Reno Lab where it is digitized and recorded. Seismograms are analyzed by Lab personnel and earthquakes of $M_L \approx 1.5$ and greater are routinely located. The trace data is archived and earthquake locations are published in a yearly catalog.

Between July 28 and August 31, 1987, 140 events were located by UNSL in the Mina area. Of these, 13 were M_L 3 or greater, 1 was an M_L 4 (Table 1), and 45 were in the M_L 2.5-3.0 range (duration magnitudes in all cases). Beause the activity occurred to the east of the network, earthquake location quality based on network data alone was poor (gaps in locations greater than 180°). Three component digital seismographs were deployed from July 29 through August 4, to supplement the permanent network. These stations provided coverage to the east, near source S-wave arrival times, near source P-wave first motions to constrain focal mechanisms and digital waveform data for source parameter studies. Timing control was maintained in the field for the portable instruments, clock drifts were measured and P and S wave phase arrivals were time corrected prior to merging with network phase data. One instrument was placed 100 meters within a mine tunnel, 12 km epicentral distance, to obtain digital waveform data not contaminated by surface effects.

A master event was chosen (1119 UTC July 31; M_L 2.7; depth 6.0 km) which included several P and S arrival times from the portable instruments assuring a good location. All events for the July to August time period were then relocated using P wave residual times from this event as stations corrections. A simple layered velocity model was used (Table 2) in the University of Washington SPONG hypocentral location program in the relocation of all events. The reliability of such a technique depends on the accuracy of the location of the master event which in turn is dependent on the velocity model. The relocation process significantly decreased the scatter in the preliminary locations, both in the lateral and depth distribution, and moved the epicentral distribution approximately 2 km to the east. Phases from the portable stations were not used in the relocation process other than to determine the locaton of the master event. We found that using a consistant station set was more reliable. In this sense we have placed more confidence in the master event location and the relative locations and avoided hypocentral shifts that result from deviations from the velocity model for near in phase arrivals.

HYPOCENTRAL DISTRIBUTION, FOCAL MECHANISMS AND RELATION TO MAPPED FAULTS

July and August 1987 Mina earthquake activity was confined to a small shallow volume of the crust. Map views and cross sections of the relocated hypocentral distribution are shown in Figures 2 and 3. The mean depth of the hypocentral distribution is approximately 7 km. The vertical extent of activity is slightly greater than the lateral extent and this may be somewhat due to the trade off between origin time and focal depth that can occur in the location process when there is poor station coverage. Focal mechanisms for those events with enough first motion data to constrain fault planes show little to no variation and indicate nearly pure strike slip motion (Figure 4); right-lateral on a NNE striking near vertical fault or left-lateral on a WNW striking near vertical plane. This is precisely the location where left lateral trending faults of the Excelsior Mountains region meet the right-lateral offsets of the Walker Lane, so a combination of both left-lateral and right-lateral strike slip motion cannot be ruled out. Recent earthquake sequences in the Bishop, California area include both right-lateral and left-lateral strike slip motion in near conjugate planes of faulting (Smith and Priestley, 1988; Priestley *et al*, 1988). The slight northeasterly trend in the epicentral distribution (Figure 2) would favor right-lateral strike slip on the NNE striking fault plane, although this is based on only several earthquake locations.

For the Soda Springs Valley range front fault, 7 km to the east of the earthquake activity along the base of the Pilot Mountains, to be the causative fault would require it to dip less than 45 degrees (Figure 3). Considering that its sense of motion is predominantly strike slip (Nielsen, 1968) would suggest that it probably dips more steeply. Also, focal mechanisms for the larger events (Figure 4) are not consistent with right-lateral strike slip on a northwest striking fault plane.

The projection of the northeast striking right-lateral slip plane, seen in all focal mechanisms, is consistent with a series of northeast trending faults approximately 2 km east and southeast of the town of Sodaville (Figure 5). These structures are oblique to the range front. The slight northeasterly trend in the epicentral distribution (Figure 2) also supports the interpretation that these are the operative faults. The auxiliary plane from the focal mechanisms, or what is the east-west striking left-lateral slip plane, in all cases projects to the surface north of the town of Sodaville and north of the activity. It would therefore be difficult to place these earthquakes on faults seen in aerial photographs that occur south of the epicentral area (Figure 5). Another factor to be considered is that this seismicity may be associated with ground water activity in the Sodaville springs, the most dominant feature in the aerial photograph (Figure 5).

A check of seismicity of the past several years (Figures 6) indicates that small tight clusters of activity are not unusual in the Mina region. Several of these clustering points are active for short periods of

times and others remain active for years. This is the first time this particular point has been active since good quality locations became available in the 1970's.

CLUSTERING AND MODERATE EARTHQUAKES IN THE REGION

The two most recent moderate size earthquakes in the region, the 1984 M_L 5.7 Round Valley and 1986 M_L 6.4 Chalfant, California events, occurred on faults with a similar geometry with respect to local range fronts as those apparently responsible for the 1987 Mina activity (Figure 7). Aftershock distributions consistent with focal mechanisms define conjugate sets of fault planes for both the Round Valley and Chalfant events that are oblique to their respective range fronts. The main shocks occurred on the NE striking plane at Round Valley and on the the NW striking plane at Chalfant. The NE striking plane in the Chalfant area is that associated with an M_L 5.7 foreshock.

The Chalfant earthquake was preceded for three weeks by a localized shallow cluster of activity very similar in character to that seen at Mina (Figure 8) and was one of the motivations for deploying portable instruments in the Mina area. Location qualities for Chafant precursory activity are excellent, and show a tight cluster at 7 km (mean depth of Mina activity). The Chalfant cluster was within 4 km hypocentral distance of the nucleation point of the mainshock and was at the hypocenter of the M_L 5.7 event that occurred 24 hours before the main shock (Smith and Priestley, 1988). Similarly, a cluster of activity, again in the epicentral region, preceded the Round Valley event (Figure 9), but this was approximately 1 year prior to the earthquake (Smith and Priestley, 1988). At the time of Round Valley precursory activity the UNSL-USGS network did not extend to the east, location qualities are poor and these events have not been relocated.

SOURCE PARAMETERS

Spectral methods have been used to estimate source parameters from the digital recordings at the portable stations (Table 3). These stations consisted of 1 Hz three-component velocity sensors paired with Sprengnether DR100's. The data was sampled at 100 Hz and a 50 Hz anti-aliasing filter was applied prior to recording. One instrument, located approximately 100 meters within a mine adit, in competent rock, shows an excellent signal to noise ratio in the frequency range, 1 to 40 Hz (Figure 10). P-wave and S-wave spectra have been calculated from vertical and horizontal components, respectively, for the ten largest events (M_L 2.6 - 3.4) recorded at the mine site. One to two second velocity time series were windowed with a ten percent cosine taper at each end. The windowed time series were then transformed with an FFT routine, corrected for instrument response and resulting velocity spectra were converted to displacement.

The log-log displacement spectra were interactively fit for the the long period level, corner frequency and high frequency fall-off. Frequencies beyond 1.0 Hz (the instrument free period) were considered, corner frequencies were picked by hand and a least-squares fit was applied to the high frequency fall-off from the corner to approximately 40 Hz. No attenuation correction has been applied.

The seismic moment is determined from the long period level of the P or S spectra, Ω_o according to Keilis-Borok (1960),

$$M_o = \frac{4\pi\rho\alpha^3 R\Omega_o^P}{kR_{\Theta\Phi}} = \frac{4\pi\rho\beta^3 R\Omega_o^S}{kR_{\Theta\Phi}} \tag{1}$$

where ρ is the density, α and β are the P and S wave velocities, R is the hypocentral distance, k is the free surface correction (taken as unity for the tunnel site) and $R_{\Theta\Phi}$ is the average radiation pattern. The values in Table 3 were calculated using ρ = 2.8 gm/cm^3, α = 6.0 km/s and β = 3.5 km/s. The radiated seismic energy, E_s, was determined from the integration of the P and S wave velocity squared spectra in the frequency band 1 to 40 Hz according to Wu (1968),

$$E_s(p,s) = I\rho(\alpha,\beta)R^2 \int_{-\infty}^{\infty} |f\Omega(f)|^2 df. \tag{2}$$

where *I* is a constant equal to $4\pi / 15$ for P-waves and $24\pi / 15$ for S-waves, and $f\Omega(f)$ is the velocity spectrum. In this case the P-wave energy is 5% of the S-wave energy. The total radiated seismic energy was calculated for each component using equation 2 for that particular phase, plus the energy in the other body wave phase according to *I*.

Stress parameters were estimated in three ways. First, the apparent stress can be determined directly from the radiated energy and the seismic moment,

$$\sigma_{app} = \frac{\mu E_s}{M_o} \tag{3}$$

where μ is the rigidity. Secondly, stress drops were estimated from the hand picked corner frequencies according to Brune (1970,1971),

$$\Delta\sigma = \frac{7M_o}{16r^3} \tag{4}$$

where r is the source radius of the Brune circular model and is related to the corner frequency, f_c by,

$$r = \frac{2.34\alpha}{2\pi f_c^{(P)}} = \frac{2.34\beta}{2\pi f_c^{(S)}} \tag{5}$$

Since the Brune model was developed for S-waves, we have made the additional assumption that the

corner frequency shift for P-waves relative to S-waves is α / β as determined in several studies (e.g. Hanks 1981). Thirdly, the Snoke (1987) method of determining the Brune stress drop was applied to the spectra. Due to the fact that the stress drop is proportional to f_c^3, small uncertainties in hand picked corner frequencies will have a significant effect upon the stress drop determination. Using the Brune (1970, 1971) model, Snoke (1987) derived a relationship between J the integrated squared velocity spectrum,

$$J = 2 \int_0^\infty | \omega \Omega(f) |^2 df \tag{6}$$

and the corner frequency,

$$f_c = \left[\frac{J}{2 \pi^3 \Omega_o^2} \right]^{1/3} . \tag{7}$$

This new corner frequency is then used with (3) and (4) to determine the Brune stress drop. The Snoke method has the advantages of an objectively determined observable J that is linearly proportional to stress drop. Both the Snoke method and the apparent stress apply integration of the velocity squared spectrum to determine the stress. It can be shown that if the contibution of the P-wave energy is negligable, the Snoke method gives a Brune stress drop that is about 4.3 times the apparent stress.

The apparent stress and the Snoke method stress drops, Table 3, cover a smaller range than the hand fit Brune stress drops. Brune stress drops determined with the Snoke method fall between about 0.1 and 3 bars. The apparent stress levels are consistantly about a factor of 4 lower than the Snoke stress drops (this is because the P-wave energy is not quite negligable). Low stress drops of similar magnitude have also been found for small, $M_o < 10^{20}$, events in the Basin and Range (e.g. Douglas and Ryall, 1972) and at hard rock sites at Anza (Fletcher *et al.*, 1987). Furthermore, corner frequencies and inferred source radii show little correlation with the more than a factor of ten range in seismic moment. Fletcher *et al.*, (1987) found that the corner frequencies and inferred source radius remained essentially constant for these low moment events at Anza. Another factor to be considered here at Mina is that several of the corner frequencies imply source dimensions on the order of the width of the hypocentral distribution (≈ 2 km).

Many spectra show a steeper falloff than the f^{-2} predicted by the Brune (1970) model. This steep falloff could be explained by attenuation (low Q). Hanks (1980) defined f_{max} as the frequency at which the high frequency acceleration spectrum decreases from a constant level due to path attenuation or some site condition, or where the theoretical f^{-2} falloff beyond the corner frequency in the displacement spectra steepens significantly. Acceleration spectra of the smallest events recorded were calculated in order to realize high corner frequencies. We found little evidence for an f_{max} below 20 Hz but some suggestion of a 22 Hz f_{max}. The highest corner frequencies in Table 3 are about 15 Hz, near this 22 Hz f_{max}, so it may be

the case that the low stress drops and the approximately constant inferred source radii are due path or site effects associated with f_{max}. The short hypocentral distances (about 11 to 15 km for the mine tunnel site) and steep fall-offs require a frequency independent Q of less than 200 for many of these events if the high frequency fall-offs at the source are actually f^{-2}. This Q function is in distinct disagreement with preliminary values for the regional Q function determination discussed below.

REGIONAL ESTIMATES OF Q

Regional Q values have been estimated for travel paths to the USGS Southern Great Basin (SGB) network. Spectral ratios have been determined for several event pairs common to the portable array and the SGB network for shear waves recorded on horizontal components of motion. To calculate Q from the spectral ratio, we assume that the S-wave displacement spectra A(f) can be approximated by,

$$A(f) = S(f)\,\frac{e^{\frac{-\pi f r}{\beta Q}}}{r^n}, \tag{8}$$

where S(f) is the source excitation, r is the hypocentral distance and β is the shear wave velocity (3.5 km/sec). r^n accounts for the geometrical spreading where n=1 (direct S-wave at near source distances) for near source stations (r < 15 km) and n=1/2 (L_g at regional distances) for SGB stations (r > 100 km). Since the source excitation, S(f), is the same for both recordings, equation (8) can be solved for Q.

Figure 11 shows estimates of Q calculated from the spectral ratio of the portable station OLI (r=5.2 km) and station GMNH (r=137.4 km) of the SNB array (both free field stations). This result is preliminary and only includes one event. The spectra was smoothed and interpolated at 0.2 Hz intervals. A least-squares fit was applied to the data in Figure 11 to yield $Q(f) = 16.60\,f + 172.26$ in the frequency range 5 to 25 Hz with a correlation coefficient of 0.98 for the linear fit. Although Figure 11 is only a representative sample, $Q(f)$ consistantly shows a strong frequency dependence. This is apparently the case whether using the mine recordings or the free field data. Although the portable instruments sample different parts of the focal sphere, the strong frequency dependence is consistanlty observed.

SUMMARY AND CONCLUSIONS

Earthquake clustering in the Mina, Nevada region during the summer of 1987 has been interpreted to be occurring on a series of NNE striking secondary faults evident on aeriel photographs south and east of the town of Sodaville. These faults are oblique to the main range bounding fault, the Soda Springs Valley fault which borders the Pilot Mountains and does shows significant holocene right-lateral displacement. The relocated hypocenters plot above a 45° down dip projection of the range front fault, and a similar focal

mechanism for all events also rules out the range front fault as the causative structure. Focal mechanisms indicate nearly pure right-lateral strike slip motion on near vertical faults.

Faults with similar geometry with respect to local range fronts were involved in the two most recent moderate earthquakes in the Bishop - Mammoth Lakes area, the 1984 M_L 5.8 and 1986 M_L 6.4 Chalfant events. These two events were also preceded by precursory clustering very similar in character to that seen at Mina. This is particularly true in the case of the Chalfant event, whereas Round Valley precursory clustering is less well defined.

Secondary structures, oblique to large scale holocene structural trends, which have been responsible for much of the recent seismicity in the region are accounting for strike slip deformation in close association with range front normal fault systems. If this is indicative of the process of stress accumulation within the major fault zones and not regional stress release, we may only be seeing the secondary effects of stress build up which may make it even more difficult to recognize the potential nucleation zones of future Basin and Range earthquakes.

Source parameters determined from the spectra of several of the larger events recorded on a portable digital array indicate very low stress drops and apparent stresses. These results are consistant with studies at the Anza, California digital array, where low stress drops correlate with low seismic moments (below 10^{20} dyne-cm) and by Douglas and Ryall (1970) for a microearthquake study in the Basin and Range. Attentuation effects are surely playing some role. Attempts to correct the steep high frequency fall-offs in the near source spectral shapes suggest a strong frequency dependent Q. Calculations of regional attentuation for paths to the USGS Southern Great Basin network do show a strong freqeuncy dependent Q function in the 5 to 20 Hz band.

Since the present study we have gathered data from a dense multi-station digitally recorded portable array at the tunnel site to help answer some of the source versus site questions. This array included three stations equally spaced within the 100 meter tunnel and one located directly above the center of the tunnel ({approx} 30 meters) on the free surface (all hard rock sites). Preliminary results show significant site effects and may result in complete reinterpretation of the spectra corner frequencies. Site effects may be the most important factor in controlling the spectra shape in the low magnitude range of concern in this study and if this is the case it is not surprising that our results are similar to the 1972 Douglas and Ryall study for Basin and Range earthquakes.

Acknowlegements

This research was funded by U.S. Geological Survey research grant 14-0007-G1326. Wally Nicks, Austin Wilson and Greg Klemesrud were responsible for maintaining the UNR network during the study period and Diane dePolo was responsible for processing the network phase data. Craig dePolo supplied the fault maps used in the figures. This study has been dependent on their efforts.

References

Brune, J.N. (1970). Tectonic stress and spectra of seismic shear waves form earthquakes, *J. Geophys. Res.* 75, 4997-5009.

Brune, J.N. (1971). Correction, *J. Geophys. Res.* 76, 5002.

Douglas, B. M. and A. Ryall, (1972). Spectral Characteristics and stress drop for microearthquakes near Fairview Peak, Nevada, *J. Geophys. Res. 77*, 351-359.

Fletcher, J., L. Harr, T. Hanks, L. Baker, F. Vernon, J. Berger and J.N. Brune (1987). The digital array at Anza, California: processing and initial interpretation of source parameters, *J. Geophys. Res. 92*, 369-382.

Hill, D.P., R.E. Wallace, and R.S. Cockerham (1985). Review of evidence on the potential for major earthquakes and volcanism in the Long Valley-Mono Craters-White Mountains regions of eastern California, *Earthquake Predict. Res. 3*, 571.

Keilis-Borok, V. (1960). Investigation of the mechanism of earthquakes, *Sov. Res. Geophys. 4*, 201 pp.

Nielsen, R.L. (1965). Right-lateral strike-slip faulting in the Walker Lane, west central Nevada, *Geol. Soc. Am. Bull. 76*, 1301-1308.

Oldow, J.S. (1983). Tectonic implications of a late Mesozoic fold and thrust belt in northwestern Nevada, *Geology 11*, 542-546.

Oldow, J.S. (1981). Kinematics of late Mesozoic thrusting, Pilot Mountains, west central Nevada, U. S. A., *J. Struc. Geol. 3*, 39-49.

Priestley, K.F., K.D. Smith, and R.S. Cockerham (1988). The 1984 Round Valley California earthquake sequence, submitted to *Geophys. J. R. Astr. Soc.*

Ryall, A.S. and K.F. Priestley (1975). Seismicity, secular strain and maximum magnitude in the Excelsior Mountains area, western Nevada and eastern California, *Bull. Geol. Soc. Am. 86*, 1585-1592.

Ryall, A.S. and F. Ryall (1981). Spatial-temporal variations in seismicity preceding the May 1980, Mammoth Lakes, California earthquakes, *Bull. Seism. Soc. Am. 71*, 747-760.

Shawe, D.R. (1965). Strikes-slip control of Basin-Range structure indicated by historical faults in western Nevada, *Geol. Soc. Am. 76*, 1361-1378.

Smith, K.D. and K.F. Priestley (1988). The foreshock sequence of the 1986 M_L 6.4 Chalfant, California earthquake, *Bull. Seism. Soc. Am. 78.*

Snoke, J.A. (1987). Stable determination of (Brune) stress drops, *Bull. Seism. Soc. Am. 77*, 530-538.

Stewart, J.H. (1978). Basin and range structure in western North America, in Smith, R.B. and G.P. Eaton, eds., Cenozoic tectonic and regional geophysics of the western Cordillera: *Geological Society of America Memoir 152*, 1-31.

Stewart, J.H., J.P. Albers and F.G. Poole (1968). Summary of regional evidence for right-lateral displacement in the western Great Basin, *Geol. Soc. Am. 79*, 1407-1413.

Table 1

Larger Events of 1987 Mina Activity

Origin Time	Latitude	Longitude	Depth (km)	M_L	Event #†
870728 0905 8.44	38-19.75	118- 6.67	5.48	3.7	-
870728 1855 11.91	38-19.63	118- 6.73	5.33	3.8	-
870729 0352 32.61	38-19.84	118- 6.85	6.33	3.8	-
870729 0357 33.40	38-20.02	118- 6.81	7.67	3.5	-
870730 1014 23.10	38-19.87	118- 6.59	5.46	2.8	1
870730 1213 59.62	38-19.96	118- 6.31	6.12	3.3	2
870801 1119 26.19	38-19.73	118- 7.32	8.49	2.9	3
870801 1921 30.07	38-19.56	118- 6.94	6.24	2.7	4
870802 0156 16.26	38-20.26	118- 6.91	8.29	2.7	5
870802 0556 31.77	38-20.25	118- 6.45	7.14	2.6	6
870802 0633 03.52	38-20.03	118- 6.95	8.38	2.8	7
870802 0634 53.98	38-20.00	118- 6.68	7.78	2.8	8
870803 0948 04.79	38-20.03	118- 7.22	10.13	4.0	-
870803 1008 56.19	38-19.68	118- 7.06	6.95	3.1	9
870804 0557 13.14	38-19.50	118- 6.88	8.62	3.4	10
870804 0825 37.94	38-19.66	118- 6.54	7.02	2.7	11
870805 1137 27.46	38-19.71	118- 6.12	7.20	2.8	12
870807 1147 49.15	38-19.59	118- 6.55	7.79	3.5	-
870807 1938 03.12	38-19.89	118- 6.20	6.91	3.0	-

† Event number refered to in Table 3

Table 2

Depth	P-wave velocity
0.0	0.0
2.0	5.85
22.0	6.70
28.0	7.85

Table 3

Event†	Log M_o (cgs)	Log E_s (ergs)	σ_{app} (bars)	Hand Picked Spectra			Snoke Method	
				f_c (Hz)	$\Delta\sigma$ (bars)	rad. (m)	f_c (Hz)	$\Delta\sigma$ (bars)
1 V-P-wave	19.45	13.01	.13	12.56	2.13	179.80	7.79	.51
1 R-S-wave	19.01	12.81	.22	9.25	1.60	140.86	7.62	.89
1 T-S-wave	18.81	12.64	.23	10.06	1.29	129.53	9.08	.95
2 V-P-wave	20.37	13.84	.10	2.62	.16	860.14	3.57	.41
2 R-S-wave	19.94	13.52	.13	2.51	.27	518.80	3.12	.53
2 T-S-wave	19.56	13.09	.12	3.08	.21	423.15	4.06	.48
3 V-P-wave	19.09	12.68	.13	14.85	1.53	152.03	10.54	.55
3 R-S-wave	18.78	12.59	.22	9.94	1.17	131.07	9.11	.90
3 T-S-wave	18.53	12.37	.24	11.70	1.08	111.36	11.29	.97
4 V-P-wave	18.97	11.74	.02	4.80	.04	470.77	6.10	.08
4 R-S-wave	18.71	11.98	.06	6.16	.24	211.53	6.29	.25
4 T-S-wave	18.45	11.58	.05	5.14	.08	253.47	6.97	.19
5 V-P-wave	18.85	12.13	.06	13.09	.61	172.52	9.89	.26
5 R-S-wave	18.89	12.91	.35	11.58	2.41	112.57	9.75	1.44
5 T-S-wave	18.89	12.66	.20	8.82	1.05	147.82	8.12	.82
6 V-P-wave	19.24	12.45	.05	6.68	.20	338.08	6.95	.22
6 R-S-wave	18.96	11.92	.03	3.39	.07	384.39	4.11	.13
6 T-S-wave	18.97	11.53	.01	2.16	.02	602.53	3.02	.05
7 V-P-wave	19.25	13.01	.20	15.80	2.66	142.86	10.60	.80
7 R-S-wave	19.06	12.83	.20	8.36	1.32	156.00	7.12	.82
7 T-S-wave	18.75	12.49	.19	10.64	1.32	122.53	8.91	.78
8 V-P-wave	19.56	13.50	.30	14.27	3.97	158.22	9.66	1.23
8 R-S-wave	19.21	13.43	.56	9.78	3.01	133.32	8.91	2.28
8 T-S-wave	18.96	13.20	.60	12.22	3.31	106.65	11.02	2.43
9 V-P-wave	19.12	12.24	.05	5.49	.08	411.52	7.19	.19
9 R-S-wave	18.82	12.45	.15	8.87	.92	146.95	7.66	.59
9 T-S-wave	18.70	12.46	.20	8.46	.60	154.05	9.30	.80
10 V-P-wave	19.49	13.61	.46	14.35	3.44	157.36	11.68	1.86
10 R-S-wave	19.71	14.14	.93	9.05	7.42	144.06	7.23	3.79
10 T-S-wave	19.65	14.05	.86	8.19	4.84	159.18	7.33	3.48
11 V-P-wave	19.08	11.92	.02	4.64	.05	486.38	5.98	.10
11 R-S-wave	19.22	12.10	.03	2.73	.07	477.28	3.15	.10
11 T-S-wave	19.02	12.08	.04	4.53	.19	287.91	4.23	.16
12 V-P-wave	19.11	12.16	.04	5.27	.07	428.58	6.83	.16
12 R-S-wave	19.12	12.21	.04	3.14	.08	415.39	4.03	.17
12 T-S-wave	19.13	12.50	.08	5.06	.35	257.45	4.95	.33

† Includes event number from Table 1, V for vertical component R for radial, T for tranverse component of motion, and phase used to determine source parameters.

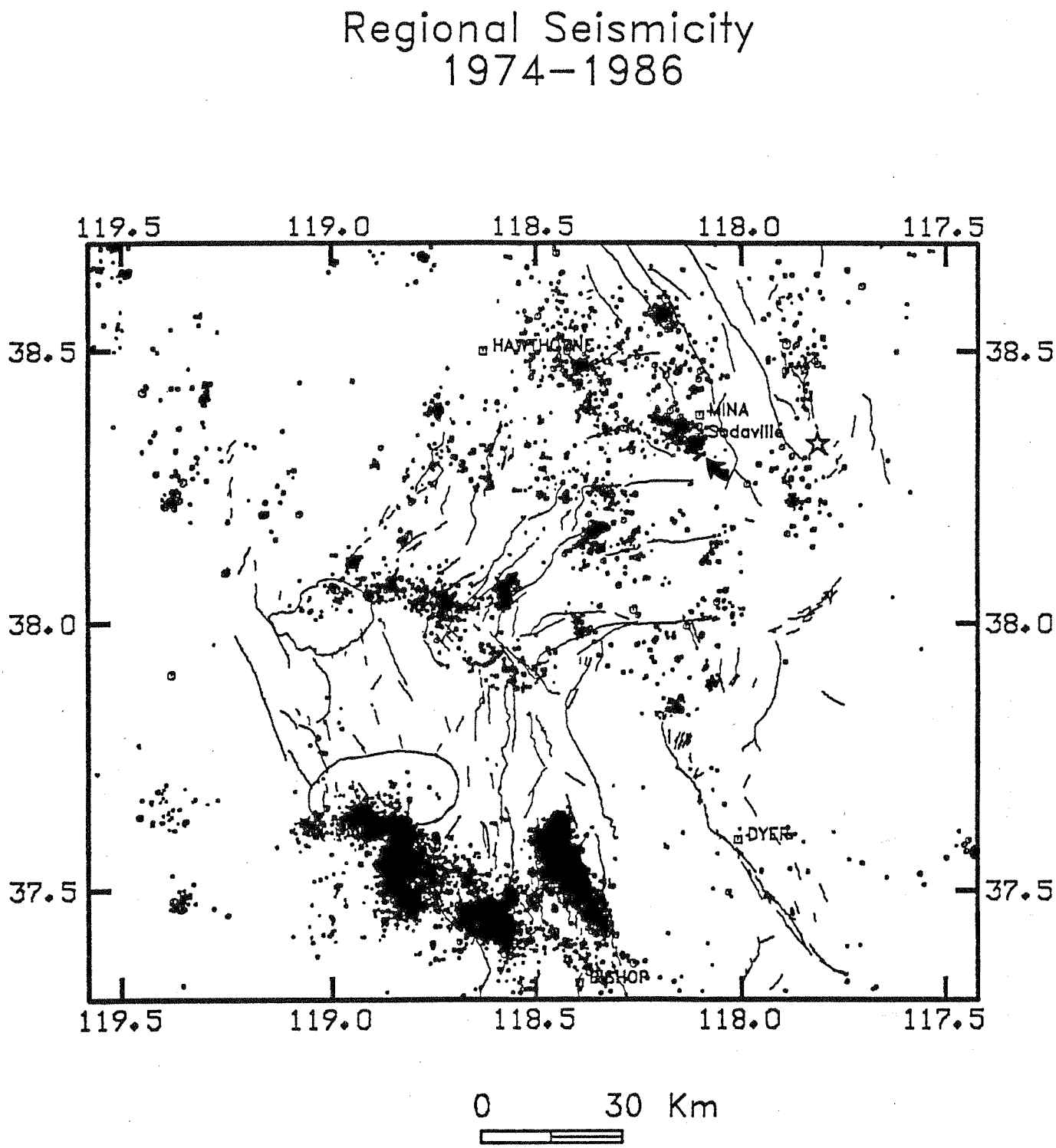

Figure 1. Regional activity and Holocene faults within the UNR-USGS network for 1974-1986. The three areas of significant earthquake activity in the lower portion of the figure are, from left to right, the 1980 Mammoth Lakes, 1984 Round Valley, and 1986 Chalfant, California, sequences. The arrow points to the cluster of activity of interest in this study. The star is at the southern extent of the surface ruptures associated with the 1932 Cedar Mountains earthquake and the northern extent of the Owens Valley rupture is just south of the town of Bishop, defining the White Mountains.

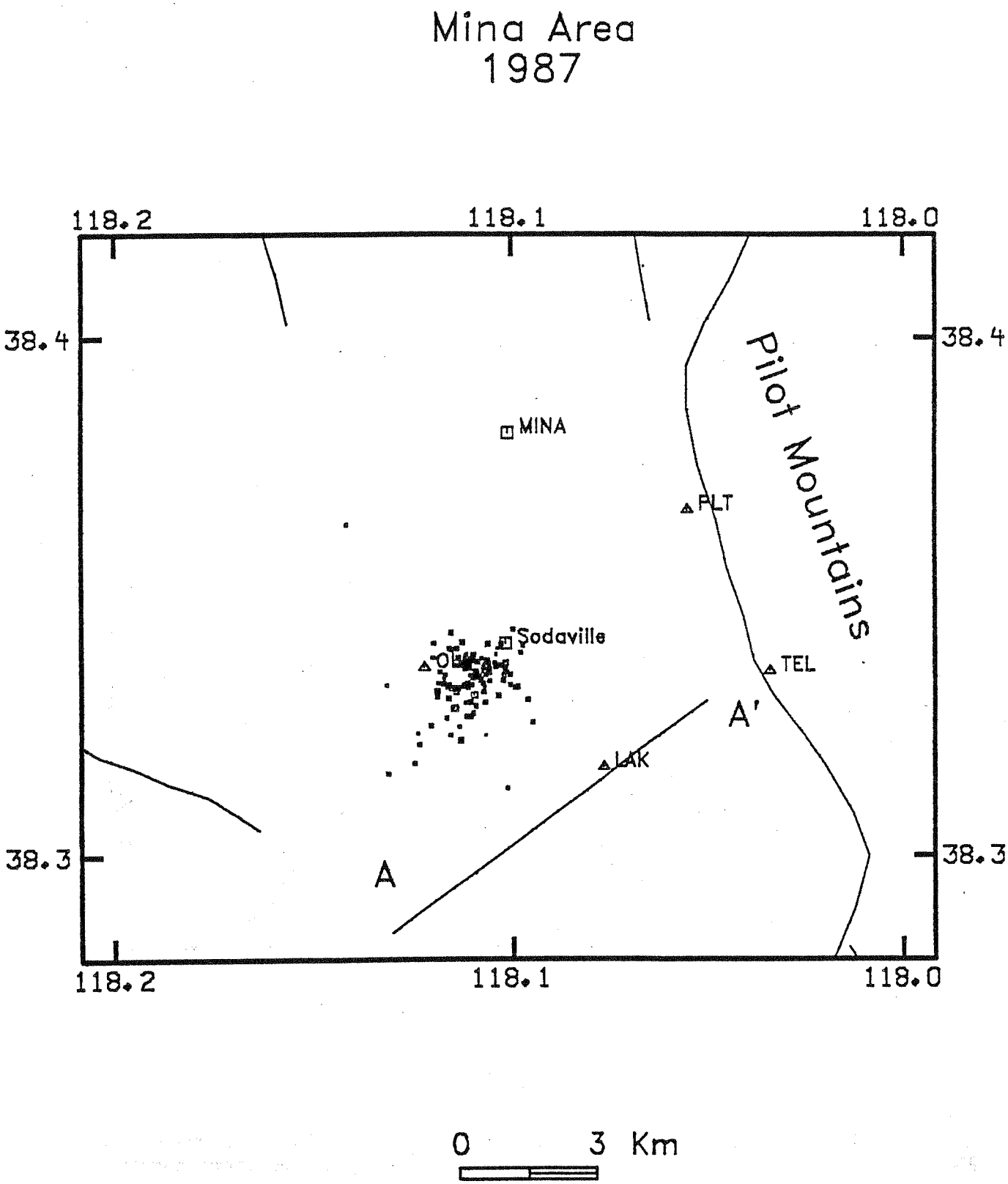

Figure 2. Epicentral distribution of July and August clustering in the Mina area. The Soda Springs Valley range front is represented by the solid line bordering the Pilot Mountains. The extent of the cross section for Figure 3 is labeled A-A'. The town of Sodaville would be less than 1 km north of the activity.

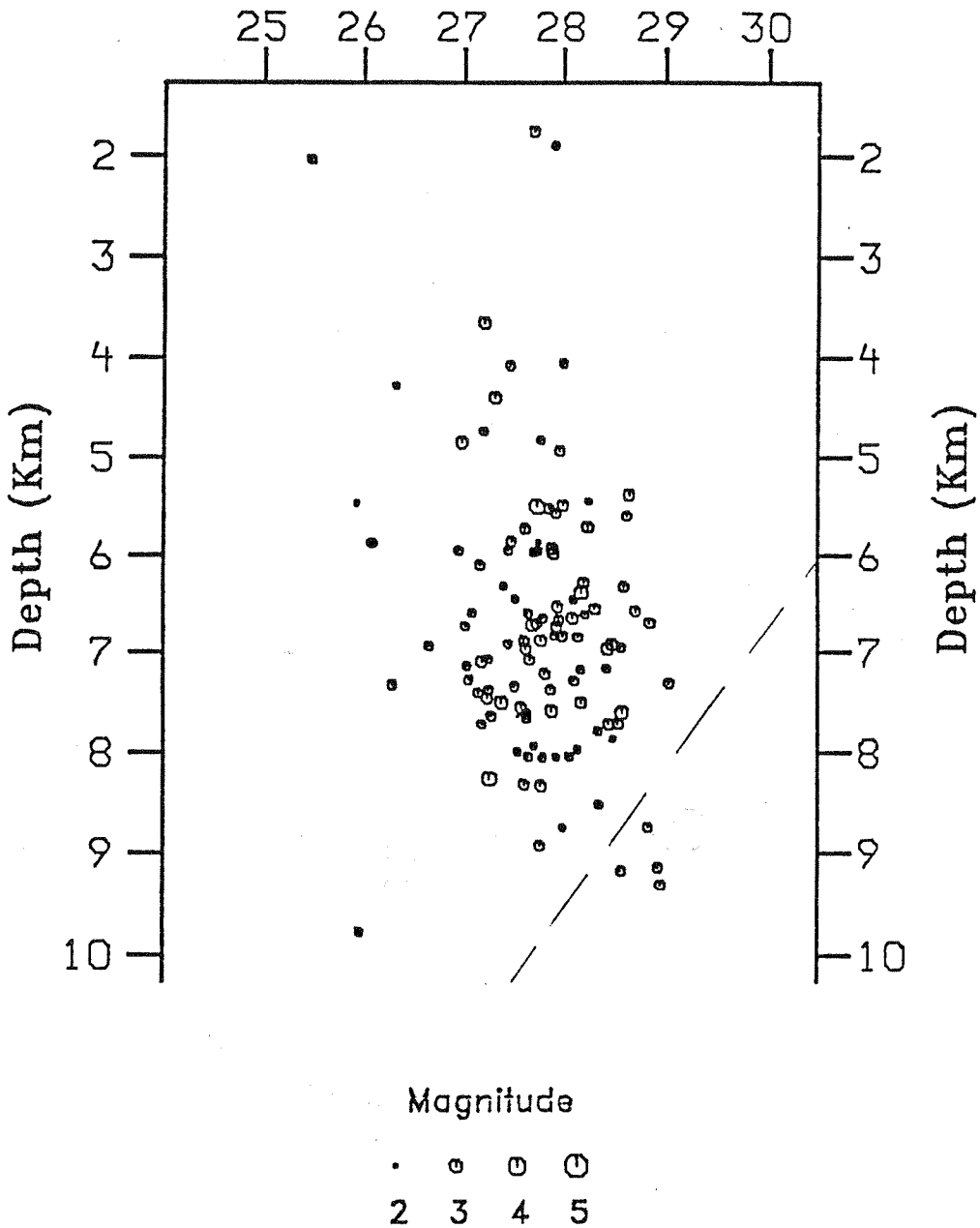

Figure 3. Cross section A-A' from Figure 2. The diagonal line is the 45° dip projection of the Pilot Mountains range front fault as discussed in the text.

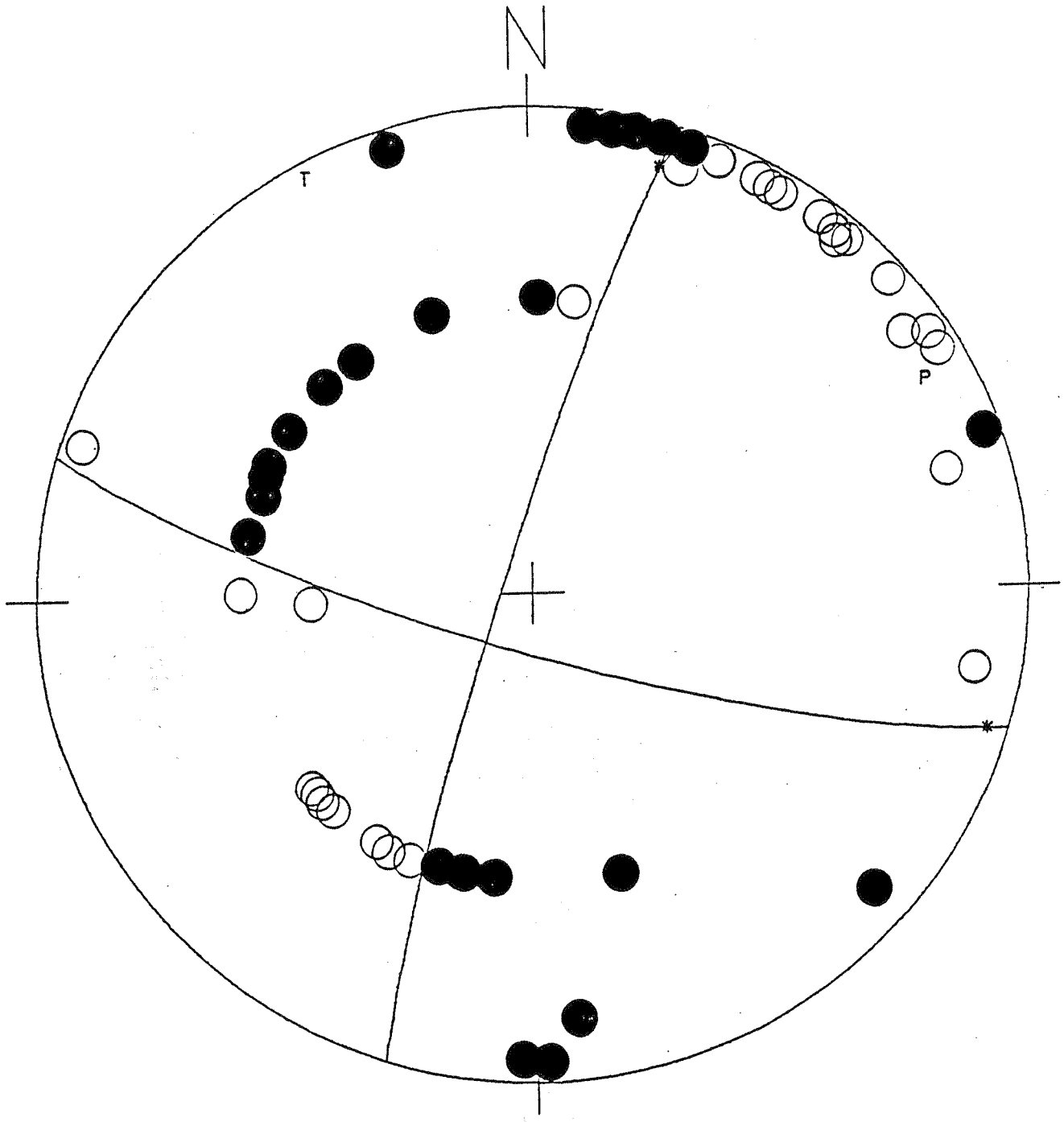

Figure 4. Lower hemisphere projection of the short period focal mechanism for the largest event; 0309 GMT August 8. This mechanism includes several first motions from the portable instruments. The preferred plane as discussed in the text and which conforms to a series of faults seen on the aerial photograph (Figure 5) is the NNE striking right-lateral near vertical plane. All mechanisms of M_L 3 events are nearly identical. The ENE striking left-lateral slip plane projects to the surface north of the activity and therefore would rule against considering faults seen south of the activity on aerial photos (Figure 5) as the causative structures.

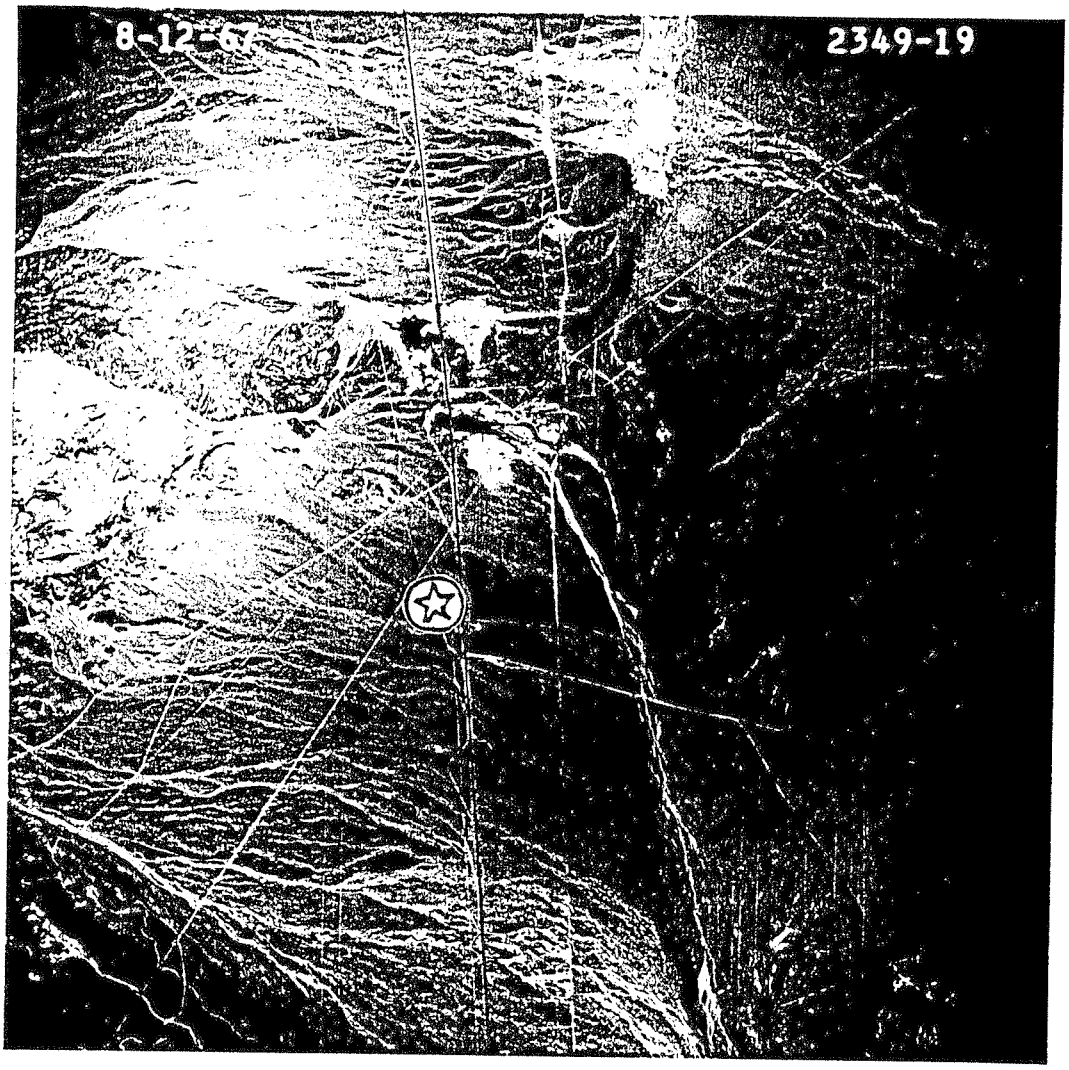

Figure 5. Aerial photograph covering the Sodaville area south of Mina. The star is the center of the epicentral distribution and the suggested causative faults are seen striking NE just east of the Sodaville springs (dominant feature in center of photo). The Pilot Mountains range front fault is to the east of the photo and these secondary faults interpreted to be responsible for the 1987 activity are oblique to the range front.

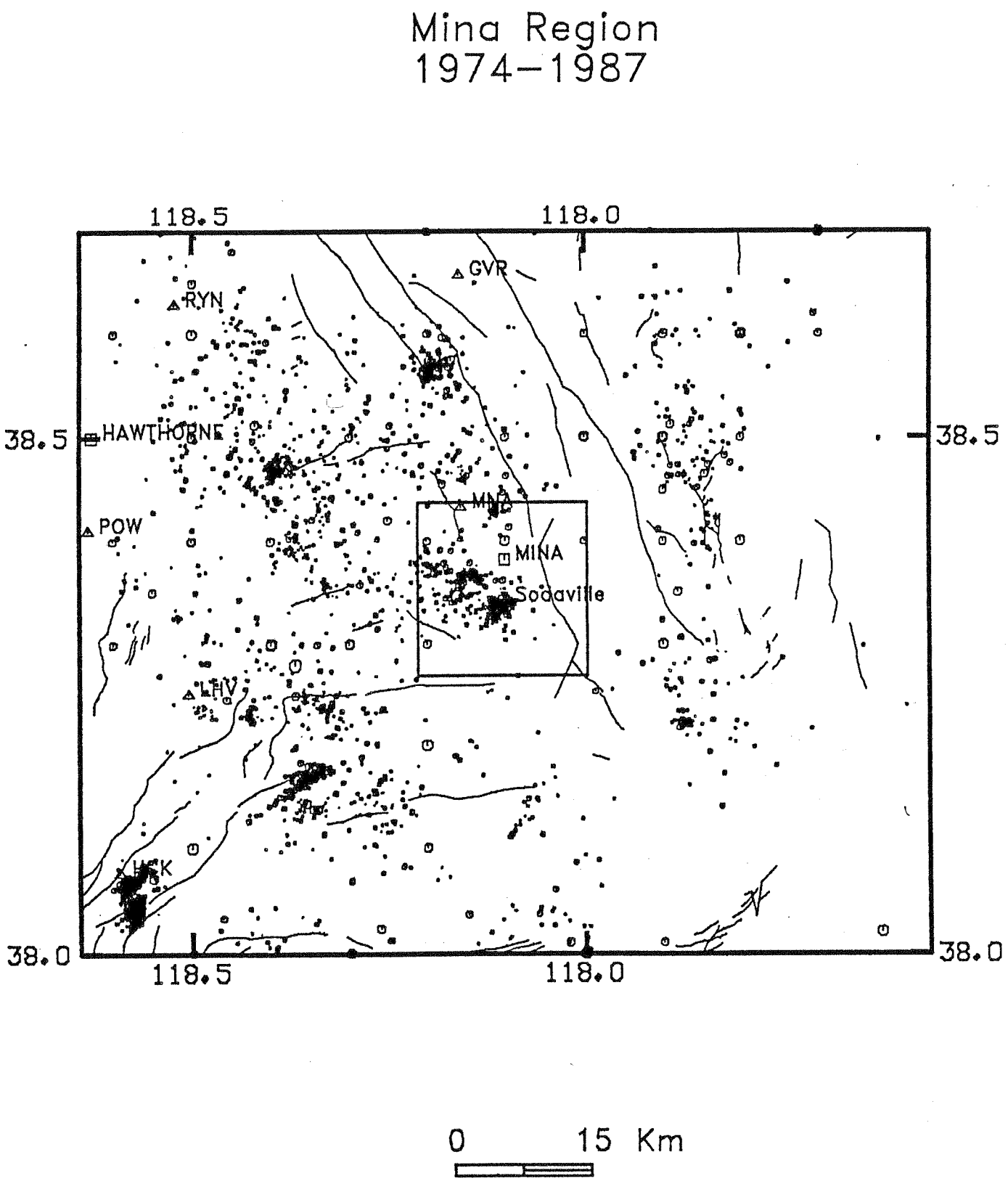

Figure 6. Mina area activity from the UNR catalog for 1974-1987. The box is the area covered in Figure 2.

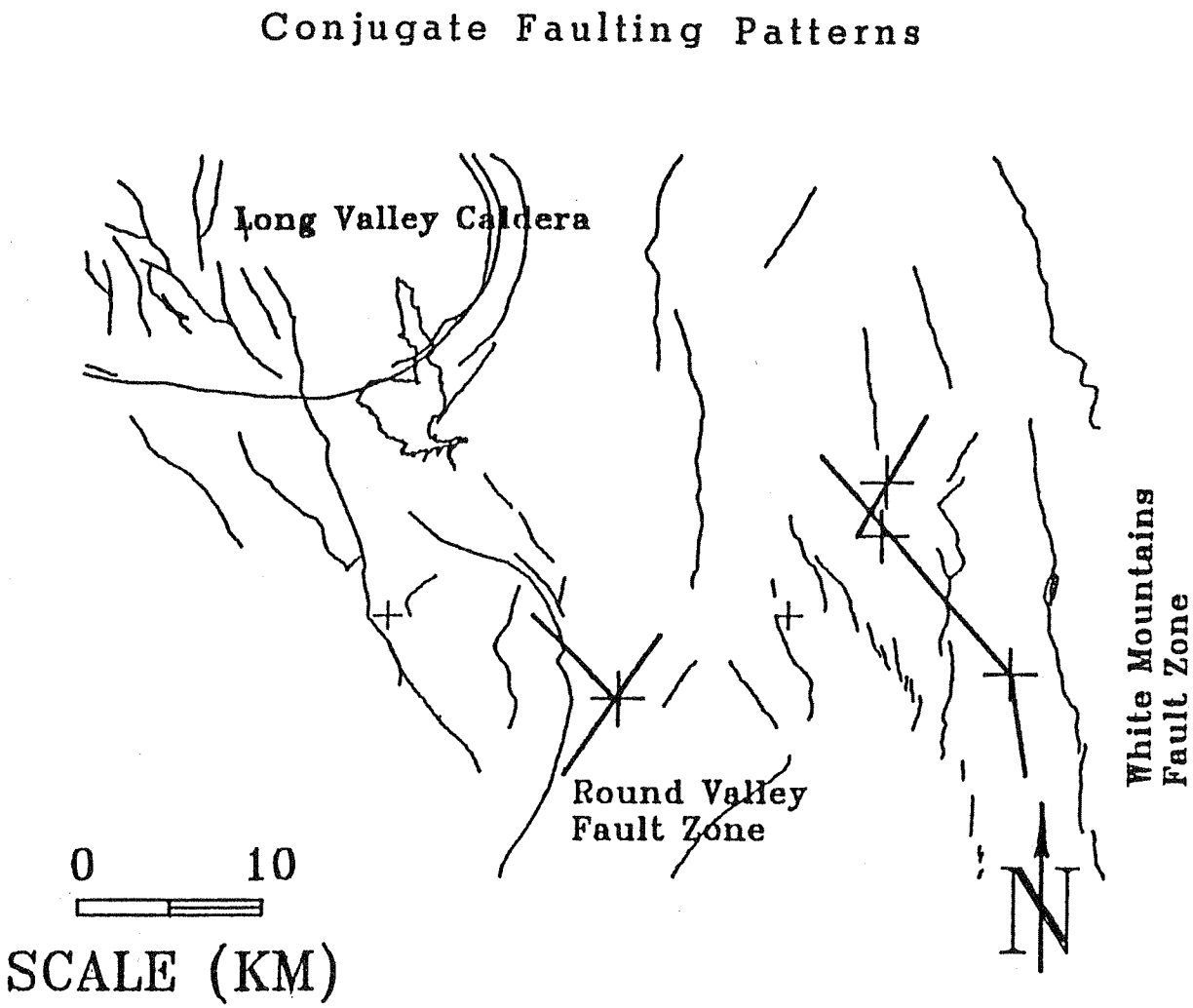

Figure 7. Fault planes active during the 1984 Round Valley and 1986 Chalfant sequences that also indicated nearly pure strike-slip motion and were oblique to their corresponding range-bounding fault, the Round Valley fault zone and the White Mountains fault zone, respectively.

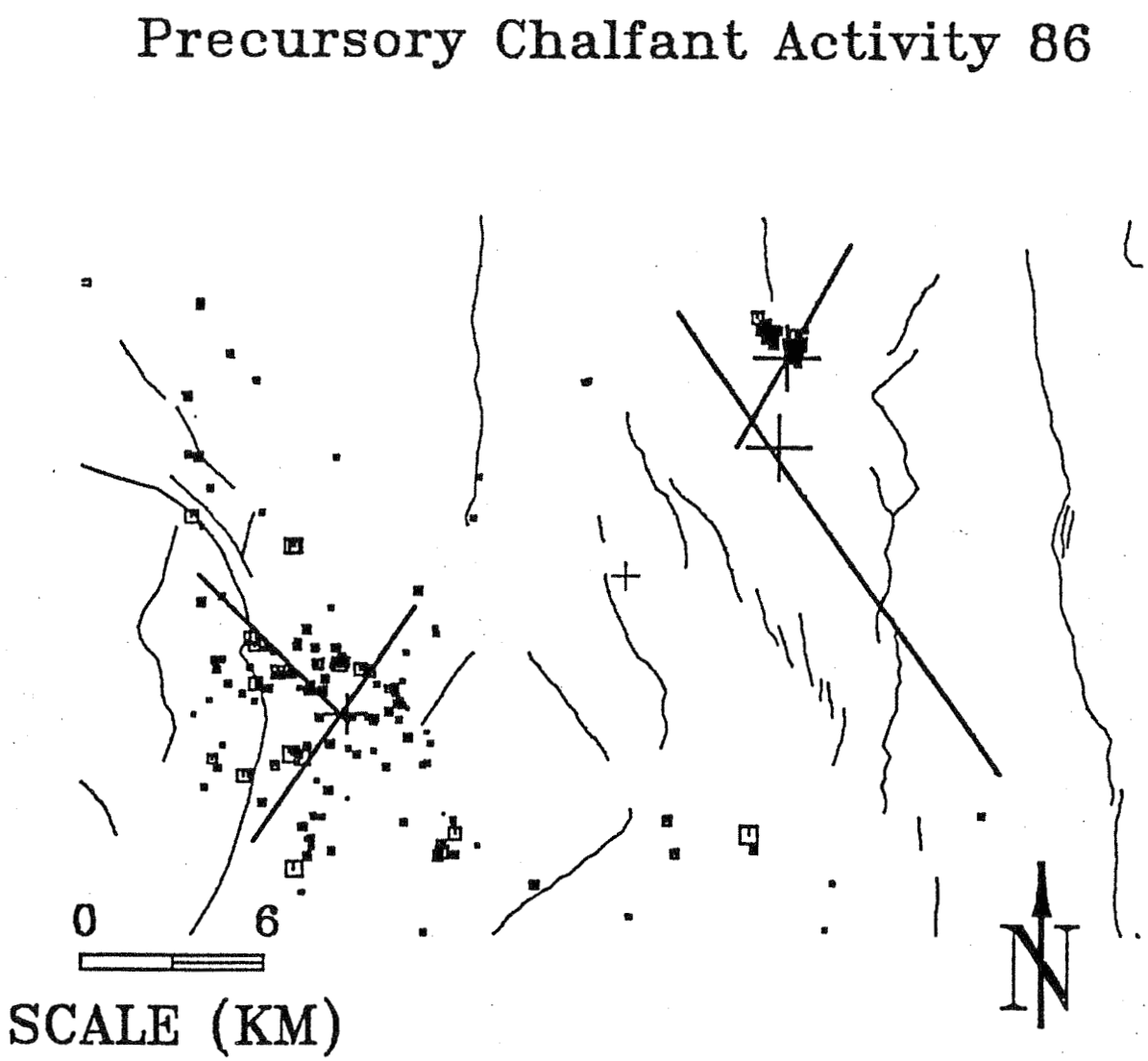

Figure 8. Precursory clustering in the Chalfant main shock source region. The large (+)'s are the epicenters of the M_L 5.9 foreshock, to the north, and the M_L 6.4 main shock to the south. The small (+) is the epicenter of the 1984 Round Valley main shock.

Precursory Round Valley Activity 83–84

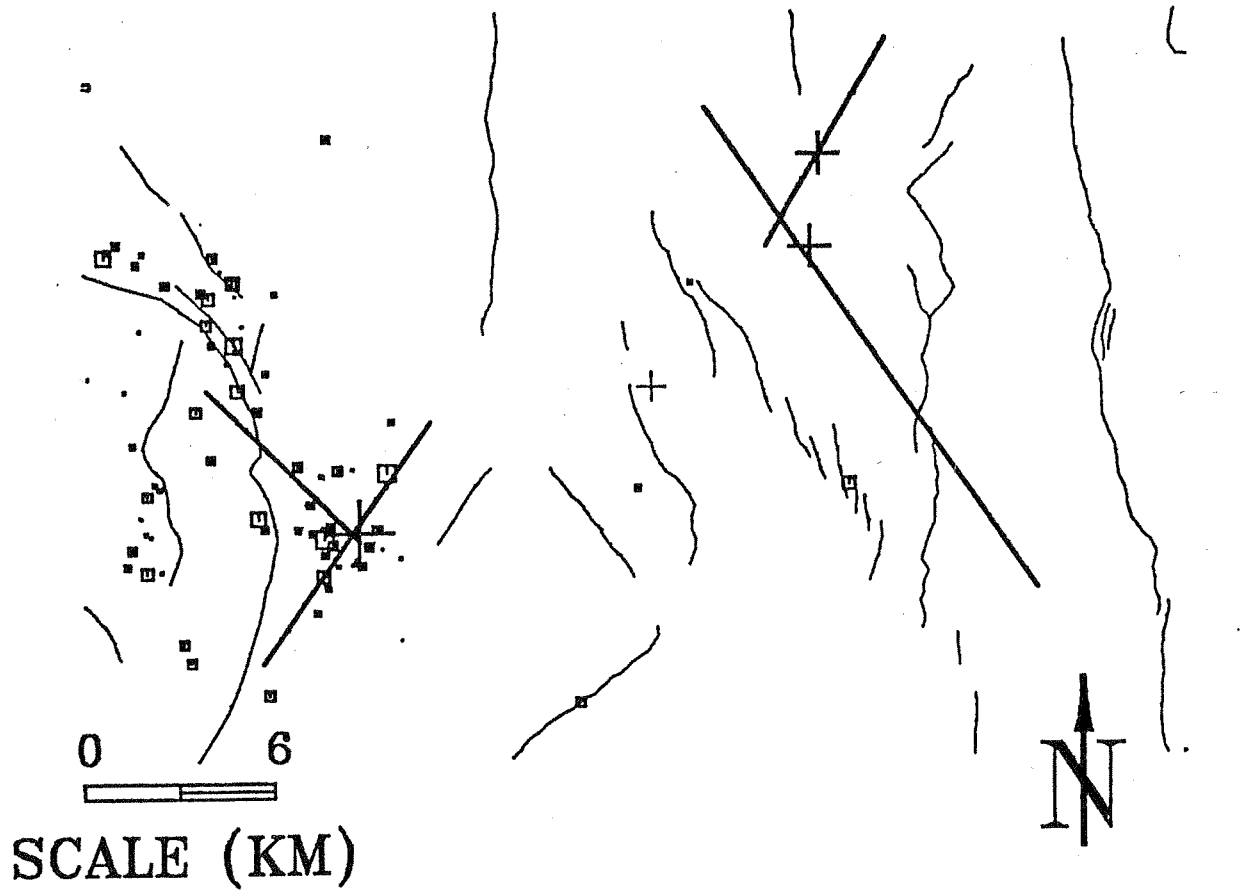

Figure 9. Precursory clustering in the Round Valley main shock source region. This clustering is less well defined than for the Chalfant event and mostly occurred 1 year before the earthquake.

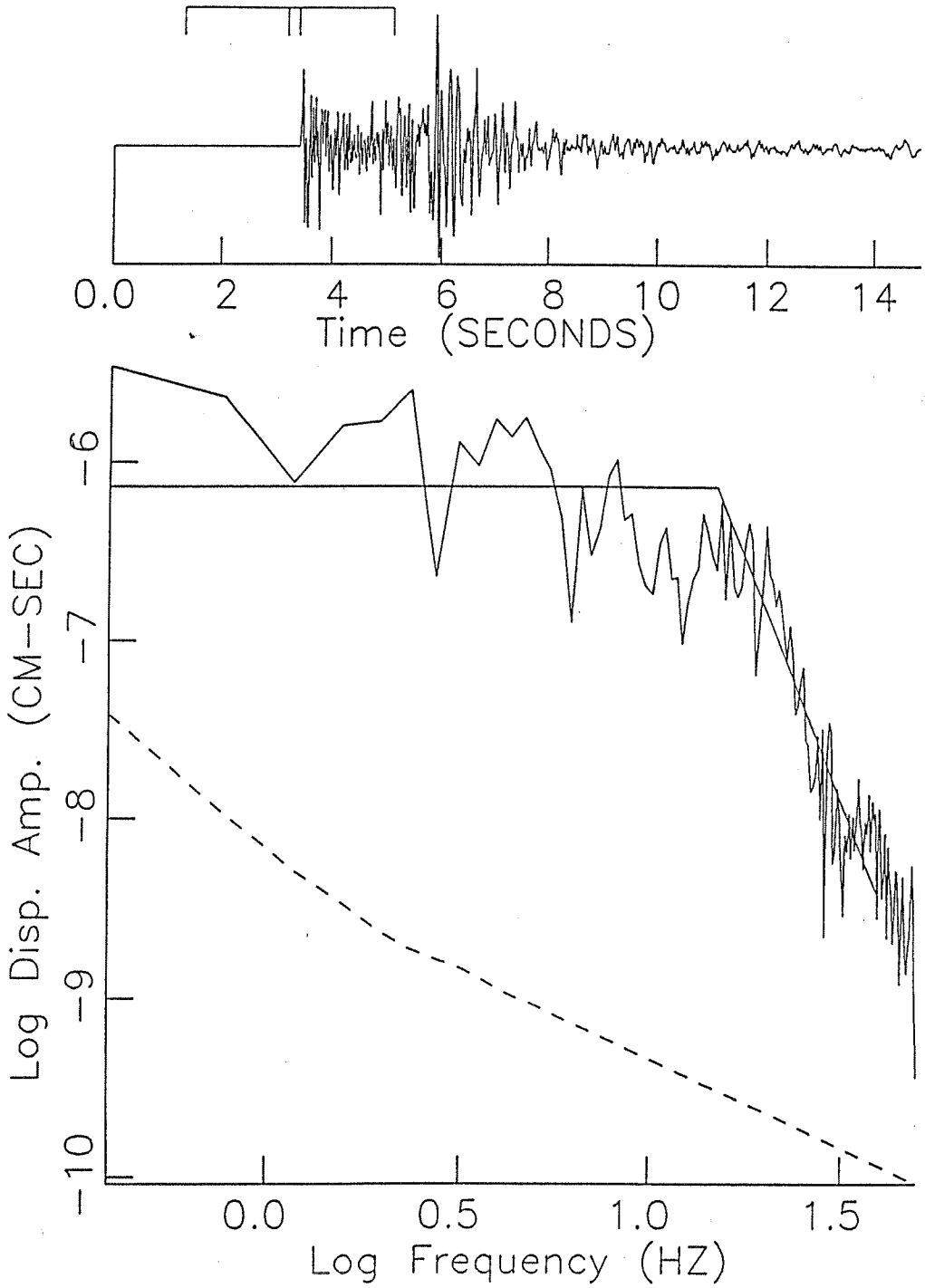

Figure 10. P-wave spectra of event #3 in Table 1 plotted as a solid line. Preceding noise window of equal length plotted as a dashed line. The good signal to noise ration from 1 to 40 Hz is typical of the events used in this study. The two line asymptotic hand fit is plotted over the P-wave spectra. Note the falloff at high frequencies is much steeper than f^{-2}.

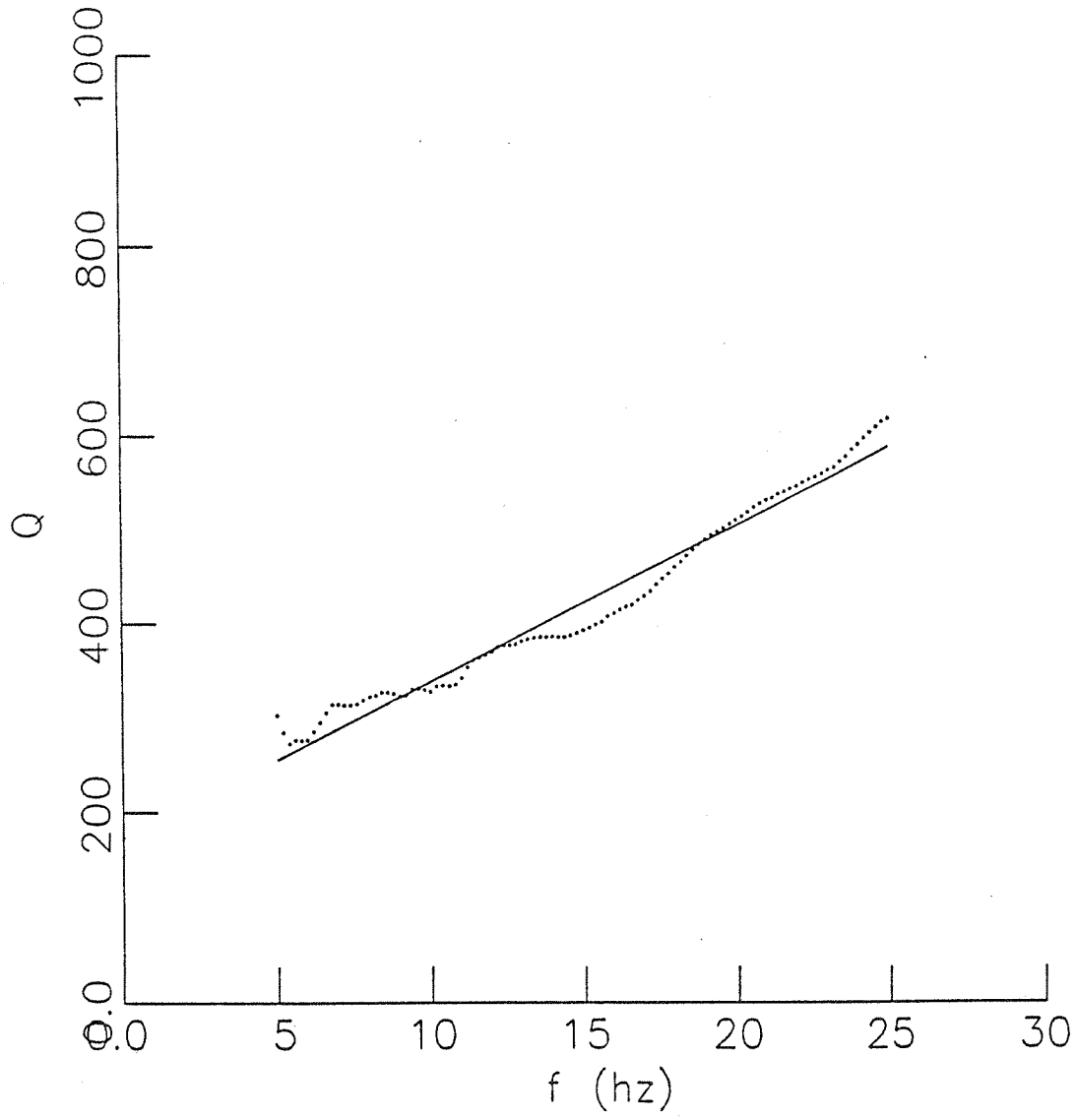

Figure 11. Q as a function of frequency for the Mina to Southern Great Basin travel path as determined from the spectral ratio of the horizontal component S-waves for one event common to the portable stations and the USGS Southern Great Basin network. These are preliminary results and are representative of the present data set.

SOURCE PARAMETERS OF THE 1987 EDGECUMBE NEW ZEALAND EARTHQUAKE

Keith F. Priestley

Seismological Laboratory, Mackay School of Mines

University of Nevada -- Reno, Reno, Nevada 89557

Russell Robinson

Geophysics Division, Department of Scientific and Industrial Research

Wellington, New Zealand

Abstract.

Moment tensor inversions of low frequency teleseismic surface wave and body-wave data for the March 2, 1987 Edgecumbe, New Zealand earthquake, give an average seismic moment of 7.0×10^{18} N m. Measurements of seismic moment at low frequencies are converted to spectral levels normalized to 10 km distance and combined with the acceleration spectrum from a strong-motion seismogram recorded at about 15 km epicentral distance to give a composite source spectrum for the main shock covering more than four decades in frequency. The source spectrum shows a constant low frequency level, a corner frequency of 0.22 Hz, and a high frequency slope of approximately ω^{-2}. The corner frequency implies a fault radius of 6 km giving an average fault displacement of 2 m and a stress drop of 5 MPa. Integration of the velocity-squared spectrum indicates an energy release of 1.1×10^{15} J.

Preliminary aftershock location extend over a 65 km long NE-SW trending zone, with the largest concentration in an area 12 to 15 km southwest of the main shock epicenter. Depths of the aftershocks range from 0.2 to 9.6 km with most of the events occurring between 4 and 6 km depth. Focal mechanisms primarily show normal faulting with varying degrees of strike slip motion. A suite of 255 three component, digital seismograph recordings of 57 aftershocks has been analysed to obtain estimates of seismic moment (M_o), source radius (r), and stress drop (ds). Seismic moments were calculated from the asymptotic long-period spectral levels range from 10^{11} N-m to 10^{13} N-m. The source radii inferred from the corner frequencies ranged from 200 to 300 m. Stress drops from the Brune formulation were low ranging from 0.01 to 1.0 MPa.

INTRODUCTION

The 1987 March 2 Edgecumbe earthquake (M_L 6.3, m_b 5.9, M_s 6.6) was a moderate, shallow, normal faulting event in a rifting environment. This event had a maximum intensity of IX on the Modified Mercalli scale and caused extensive damage in the surrounding region. The earthquake occurred in a rifting environment behind the convergent Pacific - Indian plate boundary. In this region, the Pacific plate is presently being subducted westward beneath the Indian plate at approximately 50 mm/year (Walcott 1978). Typically, earthquakes along the Benioff zone extend to 250 km depth (Reyners 1980); however, some events as deep as 600 km have been observed (Adams & Ware 1977). The earthquake occurred within the Central Volcanic Region (CVR) within the continental crust of the North Island, New Zealand. The CVR is characterized by large volumes ($\approx$12,000 km^3) of Quaternary rhyolitic volcanic rocks (Cole 1979), a mean heat flow of 700-800 mW/m^2 (Studt & Thompson 1969; Thompson 1977; Allis 1979), historical extension (Walcott 1978), thin crust ($\approx$ 15 km), and low P_n velocity (7.4 km/s) (Stern et al. 1986). Stern (1985) showed that the CVR is a direct continuation of a young oceanic back-arc basin into the continental structure of New Zealand.

The earthquake occurred at the southeastern margin of the CVR beneath the Rangitaiki Plains, a low lying alluvial basin consisting of volcanic and greywacke-derived sands and gravels with interbedded ignimbrites, silts, and peats, all of Pleistocene to Holocene Age (Anderson et al. 1987). The normal faulting surface rupture accompanying the main shock occurred along a number of strands over a $\approx$ 10 km broad and $\approx$ 15 km long region. The maximum vertical offset is 2 m; however Grapes et al. (1987) suggest that the more than 1 km of unconsolidated sediment underlying the plain may have taken up part of the faulting. Measurements made on fissures and cracks crossing the rupture indicate a total extension of up to 1.6 m. The overall trend of the surface faulting is 51°, and the strike of the most easterly striking section is 77° ± 6° (Grapes et al. 1987). For more details of the geological setting and nature of the surface faulting, see Beanland et al. (1989), Darby (1989) and Nairn and Beanland (1989).

Analysis of the Main Shock

TELESEISMIC SOURCE MECHANISM

Surface Wave Analysis:

Low frequency digital seismograms from the International Deployment of Accelerometers (IDA) and the Global Digital Seismic Networks (GDSN) were used in this analysis. The distribution of these stations relative to the epicenter is shown in Fig. 1. Analysis of low frequency (2 - 8 mHz) waves

constrains the low frequency portion of the source spectrum which is related to the overall dimension of the fault process. Six hour time series from vertical seismograms of the IDA and vertical and horizontal seismograms of the GDSN networks were used in a linear inversion procedure to recover the elements of the seismic moment tensor. These time series are shorter than have been previously used in such inversion procedures (e.g. Priestley & Masters 1986), but this was necessitated by the occurrence of a M_s 6.2 event in the Indian Ocean at 05:58 GMT. However, for moderate events such as the Edgecumbe earthquake, the instruments remain linear for the direct Love and Rayleigh wave arrivals, and these phases dominate the surface wave signal. The surface wave inversion procedure used is an extension of the procedure suggested by Buland & Gilbert (1976). Green's functions are computed for the 1066b (Gilbert & Dziewonski, 1975) spherical earth model. Then a linear relationship is constructed between the Green's functions and the observed wave forms, and this is solved for the six elements of the moment tensor. Synthetic wave forms are computed from the moment tensor elements and the misfit between the observed and synthetic wave form is used to compute adjustments to the source parameters and the moment tensor recalculated.

Results from the surface wave inversion are given in Table 1. The largest uncertainty in determining the seismic moment for shallow focus events results from the indeterminacy of the dip. A 10% error in the assumed dip will result in a 10% error in the determined moment. The fault finiteness and the finite rise time introduce a source process time τ causing a phase shift of the seismogram with respect to the seismogram from an equivalent point source. The phase of the event (Fig. 2) is well fit after accounting for the source process time; however, amplitude anomalies exist for several azimuths. Such effects can arise due to the finite source size or to aspherical Earth structure. For moderate earthquakes such as the Edgecumbe event, aspherical Earth structure is likely to be the dominant effect.

Body wave analysis:

Analysis of teleseismic body waves can constrain the estimated depth of the initial rupture, provide details of the source time history of the event, and provide an estimate of seismic moment at a higher frequency (0.03 - 1 Hz) than the surface wave analysis. Waveform inversion techniques for recovery of the seismic moment tensor have been discussed in a number of recent papers (e.g., Doornbos 1982, 1985; Ward 1980, 1983), and moment tensor solutions are routinely reported in the Preliminary Determination of Epicenters by the U.S. Geological Survey for earthquakes larger than about m_b 5.5. Time series for the teleseismic phases P, PP, PKP, S and SKS were extracted from the digital seismograms from the GDSN day tape. Greens functions used in the inversion procedure were calculated for these phases, and their near-source reflections (i.e., P plus pP and sP, S plus pS and sS, etc.)

for specific source depths using the WKBJ approximation (Chapman 1978) for earth model 1066B. Only bodywave arrivals at distances greater than 30° were used in the inversion procedure to avoid complications introduced by upper mantle structure.

Observed body wave arrival times may be as much as several seconds early or late with respect to the arrival times predicted by model 1066b. This arises from differences in the large scale velocity structure of the spherical earth model used and the aspherical Earth and local variations of earth structure in the vicinity of the source and receivers. The moment tensor fitting procedure is performed interactively, permitting the theoretical waveforms to be time-aligned with the observed waveform. If these constant time alignments of the synthetic seismograms are not made, the synthetic seismograms can be several seconds out of phase with the observed seismograms, the calculations between the synthetic and observed seismograms can be poor, and the resulting solution can be badly biased. Phases with high noise level or those displaying obvious interference were discarded. The quality of the solution was assessed by calculating the average variance reduction (VR) which is a quantitative measure of the misfit between the synthetic waveform calculated for the moment tensor solution and the observed waveform.

Results from the body-wave inversion are given in Table 1 and are compared with inversion and body-wave modeling results from other studies, and from surface and trenching observations.

MATAHINA STRONG MOTION RECORD

The Edgecumbe earthquake triggered five strong-motion accelerographs on and near the Matahina dam at about 15 km epicentral distance. Four of the instruments are sited on the dam, and the fifth is located a few meters in front of the dam (McVerry -- Pers. Comm. 1987). Figure 3 shows the acceleration records and the integrated velocity and displacement records from the instrument at the base of the dam. The surface trace of the fault passes within about 7 km of the instrument, thus considering the fault dimension, the instrument is in the near field. The peak horizontal ground acceleration is 0.33 g (Anderson et al. 1987), and the duration of the strong ground shaking is typical of earthquakes of this magnitude. The strong horizontal velocity pulse arriving roughly 6 to 8 seconds after the instrument triggered is correct in both polarity and shape with the expected pulse resulting from the passage of a propagating rupture front. The low frequency energy observed in the displacement record for times greater than 10 s has particle motion consistent with that expected from surface-wave energy trapped in the low velocity material comprising the Rangitaiki Plains.

It is difficult at this point to take into account the proximity of the dam. Brune et al. (1985) and Anooshehpoor (1988) have measured dam-foundation interaction on a foam rubber model and found the coupling of energy back into the ground from resonance of the dam structure for this model is less than 10%. Only data from the instrument near the base of the dam are considered in constructing the source spectrum since the waveforms for the instruments on the dam will be significantly distorted by the dam structure. Instruments at greater distance will suffer from pronounced attenuation effects.

Figure 4 are plots of the displacement spectra computed from the two horizontal accelerograms. The special windows could be chosen in various ways. The windows chosen in the upper part of figure 4 include the time series from just prior to the arrival of the S-wave pulse and includes all the high frequency energy in the accelerogram. These windows were chosen since the high frequency energy in the time-series may represent direct body wave energy radiated from the fault. However, comparisons were made between spectra computed for short windows which included only the direct s-wave arrival and long windows that included the whole record. These showed only minor differences in the spectra.

SOURCE SPECTRUM

Band limitation of existing seismic instrumentation makes estimation of the source spectrum for moderate and large earthquakes difficult. Acceleration data collected in the epicentral region are restricted by the poor low frequency response of typical strong-motion instrumentation. High frequency data do not normally exist from teleseismic recordings because of the high attenuation for teleseismic propagation paths and low level response of most teleseismic seismographs. To overcome this problem, I have constructed a composite source spectrum for the Edgecumbe earthquake.

Estimates of seismic moment from the surface wave and body-wave inversion, and from the surface-wave magnitude were converted to full-space spectral amplitudes at their observed frequencies for comparison with the spectral amplitude determined from the near-source acceleration data. Using a shear wave speed (β) of 3.6 km/s, a density (ρ) of 2800 kg/m^3 (Robinson 1989), and a radiation factor ($R_{\Theta\Phi}$) of 0.6 (Thatcher & Hanks 1973), the seismic moment M_o is related to the spectral amplitude normalized to 10 km by

$$\Omega(\text{fullspace})_{10\text{km}} = \frac{R_{\Theta\Phi} M_o}{4 \pi \rho \beta^3 (10\text{km})} = 3.65 \times 10^{-18} M_o$$

This gives values of Ω at lower frequencies for comparison with values of Ω obtained from the body-wave accelerograms.

The strong motion accelerograms could not be rotated into radial and transverse components because of the proximity of the accelerograph to the fault. Therefore, I have combined the horizontal data forming a vectorial sum (i.e. , $\sum = \sqrt{(N83E)^2+(N07W)^2}$). I normalized the resulting strong-motion accelerogram 10 km to a hypocentral distance, corrected it for the average radiation pattern, corrected the spectrum for the free surface amplification, and divided it by Ω^2 to convert it to a displacement spectrum. Since the Matahina strong motion accelerograph was located in the near field of the earthquake, the strong motion seismogram is dominated by energy radiating from nearby portions of the fault. I have used the procedure of Smith et al. (1988) as a first approximation to normalizing the accelerogram to 10 km hypocentral distance. The energy radiated per unit area of the fault is assumed to be constant. The observed spectral amplitude from the strong motion recording is multiplied by the ratio of twice the area of the fault (to account for the radiation from both sides of the fault) to the area of a patch of the fault of 7 km radius, the distance of the instrument from the nearest section of the fault. This value approximates the true amount of energy radiated from a point source double couple dislocation equivalent to the finite fault dimension appropriate for the Edgecumbe earthquake. The spectrum was then normalized to 10 km distance.

The acceleration spectrum was corrected for a range of attenuation values which seemed reasonable for greywacke. Since these produced negligible effects on the spectrum in the frequency band of interest, an arbitrary whole path Q of 300 was assumed. Contamination of the spectrum by local recording site effects (near surface structure) may also be important. Archuleta (1986) has analyzed data recorded at different depth levels in a borehole near Mammoth Lakes, California and found that the differences in spectra computed from data recorded at different depths could be predicted by taking into account the differences in the acoustic impedance of the rock at the different levels. He found that spectral ratios computed between surface and deep borehole recordings showed that the near surface amplification is uniform across the 2 - 50 Hz band. On the other hand, Anderson (1986) suggests that the spectral decay at high frequencies is an attenuation effect which may affect inferences of the corner frequency of events up to about $M_L \approx 6$.

To estimate the possible distortion of the spectrum from near surface structure, I have computed the response of the presumed recording site structure to a vertically incident SH wave. The structures considered (Fig. 5a) are from the velocity model determined by Robinson (1989). I assumed a Poisson's ratio of 0.25, and a density given by $p = 0.32\ Vp + 0.77$ to convert the compressional velocity model to a shear wave and density model. The response of the structure is compared in Fig. 5b. The reference (MODEL 1) model has the high velocity (3.4 km/s) layer extending to the surface, and MODEL 2 is

Robinson's velocity structure. The combined effect of the 1 km thick 1.4 km/s layer and the 5 km thick 2.9 km/s layer is to cause an average spectral amplification of a factor of about 2. Since it is impossible to account for lateral variations in the velocity model, there is little significance in the details of the spectral amplification shown in fig. 5b. Therefore the whole spectrum was corrected using this average amplification value of 2.

The composite displacement spectrum for the Edgecumbe earthquake (Fig. 6) shows a constant low frequency amplitude, a corner frequency at 0.22 Hz, and high frequency fall off of ω^{-2} above the corner frequency.

SOURCE PARAMETERS OF THE MAIN SHOCK

Source parameters for the Edgecumbe earthquake can be estimated by combining results obtained from the analysis of the main shock data with the rupture dimensions determined from patterns in the aftershock distribution. The estimate of the seismic moment from the teleseismic analysis is 7.0×10^{18} N-m. During the first days of the aftershock sequence, aftershocks occurred along a zone 20 km long. Surface faulting extended over a zone about 15 km long. This presumably represented the upper limit for the surface which slipped during the main shock. In several cases where dense seismograph networks were in place at the time of the main shock, allowing accurate aftershock locations immediately following a main event, it has been observed that the aftershock zone grew in size by 10 - 20 % in the first few hours (e.g., Smith & Priestley, 1988; Priestley et al. 1988). This is to be expected since aftershocks should be most frequent at the boundaries of the slip zone where the main shock has increased the stress.

The source spectrum can be interpreted in terms of spectral source parameters. The source radius r for the Edgecumbe event (Brune, 1970; 1971) is

$$r = \frac{2.34\,\beta}{2\pi f_c} \approx 5.8\text{km}$$

giving a fault area of 105 km^2. For comparison, early aftershocks (Robinson, 1989) extend over a 15-20 km zone extending to a depth of 10 km. This gives a fault area of approximately 175 km^2. Using these values as the bounds on the fault area, the average slip <u> is

$$1.4\,\text{m} < \langle u \rangle = \frac{M_o}{\mu A} < 2.2\,\text{m}$$

and the average stress drop $\langle \Delta\sigma \rangle$ (Kanamori & Anderson 1975)

$$3.5\,\text{MPa} < \langle\Delta\sigma\rangle = \frac{8}{3\pi}\mu\frac{\langle u\rangle}{W} < 5.7\,\text{MPa}$$

where W is the shortest dimension of the fault. Errors enter into these values through errors in M_o and A. M_o have been estimated both from low frequency surface wave data and teleseismic body wave data and these values are within 4% of each other.

To determine the radiated seismic energy I have integrated the composite velocity squared spectrum, scaled it for the S-wave radiation pattern according to Wu (1966), and included 5% of the S-wave energy as the P-wave contribution. The seismic energy is

$$E_s = \frac{24}{15}\pi\rho\beta R^2 \int_{-\infty}^{\infty} |\Omega(f)^2|\, df$$

where $\Omega(f)$ is the composite velocity spectrum. The calculated radiated seismic energy of the composite spectral shape from the main shock is 1.1×10^{15} J.

The shape of the spectrum beyond the corner frequency is important in the calculation of the total radiated energy; if the amplitude spectrum falls off as ω^{-2}, the velocity spectrum falls off as ω^{-1} and the velocity squared spectrum, which is proportional to energy, falls off as ω^{-2}, thus, there is relatively little contribution to the total energy for frequencies beyond the corner frequency. However, if the amplitude spectrum falls off as ω^{-1} beyond the corner frequency, the velocity spectrum and the velocity squared spectrum are constant, and the contribution to the total radiated energy is proportional to the band width of that portion of the spectrum (Smith et al. 1988). The additional high frequency energy causing the spectrum to drop off with a slope less than ω^{-2} past the corner frequency can arise due to fault roughness (Gusev 1983). Such effects have been observed for earthquakes over a wide magnitude range (Anderson et al. 1986; Brune et al. 1986; Smith et al. 1988). The lack of this roughness energy in the spectrum of the Edgecumbe earthquake indicates a relatively uniform rupture process. However, complexities in the source spectrum in the 1 to 3 Hz band may be the result of interference of the arrival of energy from the second source suggested by Anderson & Webb (1988) with the primary pulse.

ANALYSIS OF THE AFTERSHOCKS

LOCATIONS

Figure 7 shows locations for over 100 of the larger ($M_L > 3$) aftershocks using 11 portable and 3

permanent seismographs operating in the epicentral region between March 5 and 11. The epicenters of these events define a 65 km long, NE-SW trending, 10 km broad zone. There is a gap in the aftershock zone in the vicinity of the recent andesitic volcanic cone, Mt. Edgecumbe. The aftershock zone is much longer than both the zone of surface faulting and what would be expected based on the seismically observed moment of the mainshock. The length of the aftershock zone may be in part the result of subsidiary aftershock sequences associated with larger (M_L 5) events near the ends of the zone of faulting associated with the mainshock. Many offshore events form a secondary aftershock sequence associated with a M_L 4.2 event on March 3. Three of the six $M_L > 5$ aftershocks which occurred less than a day after the mainshock were located southwest of Mt. Edgecumbe and three occurred near the epicenter of the mainshock. Activity south of the Mt. Edgecumbe gap lies on an extension of the Tarawera rift formed in the large eruption of 1886 and may be part of a secondary aftershock sequence associated with these M_L 5 events. Healy et al. (1964) mapped several recent faults in this area however, no new surface faulting associated with the Edgecumbe earthquake was reported in this region. The distribution in seismicity may result from variations in rock properties or from a disruption in the pre-existing throughgoing fault system by the formation of the volcano. The extent of the aftershock distribution indicates that seismic strain release was much more widespread than would be estimated from the size of the mainshock.

Depths of aftershocks range from 0.2 to 9.6 km (Fig. 8) with most events occurring between 4 and 6 km. This shallow cutoff depth probably reflects the high temperature gradient. Aftershocks near the main surface fault appear to be in the footwall block and do not define the fault plane itself. The mainshock hypocenter is at the bottom, northeastern edge of the aftershock zone.

FOCAL MECHANISMS

Focal mechanisms for 27 aftershocks (Fig. 9) primarily show normal faulting with varying degrees of strike slip motion. If the northeast plane of the focal mechanism is chosen as the fault plane, this corresponds to right-lateral faulting. The tension (T) axes are mostly horizontal and strongly clustered in the 150 ± 20 degree azimuth range. The compressive (P) axes are clustered in a vertical direction or if not vertical, have a NE - SW azimuth. The most prominent direction of the P and T axes for the aftershocks are consistent with the mechanism of the main shock presented above and by Anderson and Webb (1989), with observed surface faulting (Beanland et al. 1989), with focal mechanisms observed in the Taupo region further to the southwest (Smith and Webb 1986), and with broad scale geodetic studies of the CVR (Sissous 1979). This stress regime reflects the tectonic setting of back-arc spreading and rift formation combined with a degree of right-lateral shearing due to the

oblique plate convergence boundary to the east.

SPECTRA

Fifty-seven representative aftershocks that were recorded on three or more digital seismographs during the period March 14 to 19 were chosen for spectral analysis. The hypocentral parameters of the aftershock for which spectra were determined are summarized in Table 2. All records used are less than 20 km epicentral distance and most are less than 10 km. The results of the spectral analysis are summarized in Table 3. The event number in column one of Table 3 correspond to the event number in column seven of Table 2. Seismic moments of the Edgecumbe aftershocks range from 10^{11} to 10^{13} N-m, and Brune stress drops range from 0.01 to 1.0 MPa.

Scaling of the Edgecombe aftershock source spectra is shown in Figure 10 where the logarithm of the low frequency spectral level or seismic movement is plotted as a function of the logarithm of the fault radius or S-wave corner frequency. Diagonal lines across the plot are contours of constant stress drops. Source radii for the Edgecombe aftershocks are almost constant over nearly three orders of magnitude in moment. This leads to a strong dependence of stress drop on moment. The largest events (10^{14} N-m) have a stress drop of $\approx$1 MPa whereas events of (10^{11} N-m) have a stress drop of 0.01 MPa or less. The dependence of stress drop on movement over this range has been noted in a number of studies (Tucker and Brune, 1977; Choute et al 1978; Fletcher 1980; Fletcher et al 1987). Such a cutoff in corner frequency could result from the effect of f^{max} (Hanks, 1982), a site related cutoff of the high frequency spectrum. However, spectra of the Edgecombe aftershocks typically show a second corner in the frequency range 16 to 23 Hz which more closely correspond to the f_{max} seen for spectra of California microearthquakes (Hanks,1982). This is significantly above the corner frequencies picked for the Edgecombe aftershock spectra so we do not feel that the near constant corner frequency with increasing moment in the range 10^{11} to 10^{14} N-m is a f_{max} effect.

Discussion and Conclusions

In this study, teleseismic surface wave and body wave data, and local acceleration data have been used to estimate the source spectrum and source parameters of the 1987 Edgecumbe, New Zealand earthquake. The teleseismic moment is 7×10^{18} Nm. The source mechanism from the body wave inversion is in good agreement with the fault plane solution from first motion data (Anderson & Webb 1988). The strike of the faulting inferred from surface wave data is closer to the overall trend of surface faulting (Grapes et al. 1987). The differences in the mechanism inferred from the surface wave and surface faulting data, and the teleseismic body wave and first motion data may arise from

complications introduced by the second source suggested by Anderson & Webb (1988). Seismic moments have been used to constrain the low frequency far field displacement spectrum, and near source acceleration data has been used to define the high frequency part of the displacement spectrum. This broad band spectrum covering more than four decades in frequency indicate a relatively simple source spectrum. Using bounds of the main shock slip area indicated by the corner frequency and the aftershock zone, the displacement occurring during the main shock is 1.8 ± 0.4m, compatible with surface measurements. The stress drop is 4.6 ± 1.1 MPa. From integration of the velocity squares source spectrum 1.1×10^{15} J of energy were radiated during the faulting process.

Stress drop for events of the Edgecombe sequence range from about 1 MPa for the largest aftershocks reported here, to about 0.01 MPa for the smallest events reported here. Similar observations have been made in a number of previous studies. Tucker and Brune (1977) noticed that there was a correlation between the estimated stress drop and the high frequency spectral falloff and suggested that this might be a result of the smaller stress drop events corresponding to partial stress drops while the larger events might correspond to total stress drop events. Brune et al (1986) found that the average slope of the high frequency falloff for events with stress drop greater than 10 MPa was 2.9 whereas the average slope for events with stress drop less than 0.2 MPa was 2.0, supporting the partial stress drop model of Brune (1970). The spectra of the Edgecumbe aftershocks do not show the same relationship between the rate of high frequency spectral falloff and stress drop. The high frequency falloff for most events is approximately 3.

Similarly, low stress drops have been found for other small $M_o < 10^{20}$ events in the Basin and Range (e.g. Douglas and Ryall, 1972; Smith et al, 1989b) and at hard rock sites such as Anza (Fletcher *et al.*, 1987). Furthermore, corner frequencies and inferred source radii show little correlation with the factor of five range in seismic moment. Fletcher *et al.*, (1987) found that the corner frequencies and inferred source radius remained essentially constant for these low moment events at Anza. Whether this is a source or a path effect was not determined. The spectra generally show a steeper falloff than the ω^{-2} predicted by the Brune (1970) model. This steep falloff could be interpreted as being due to attenuation (low Q). The short travel times and steep falloffs require a frequency independent Q of less than 200 for many of these events if the high frequency falloff at the source falloff is actually ω^{-2}.

Acknowledgments. This research was supported by a grant from the Nevada Nuclear Waste Site Investigation office. I thank Helen Anderson, John Anderson, James Brune, and Russell Robinson for helpful discussions; and thank Kenneth Smith for assistance with the computing. Dr. McVerry supplied copies of the Matahina strong motion data.

TABLE 1

	strike	dip	slip	M_o (N-m)	τ (sec)	VR	Records used
normal mode	239°	71°	59°	6.1×10^{18}	7.5	74%	20
body wave	211°	64°	73°	7.8×10^{18}	1.0	76%	17
body wave(1)	228°	58°	83°	6.4×10^{18}			
body wave(2)	225°	45°	80°				
geology(3)	235°	55°					

Mo = seismic moment
τ = source process time
VR = variance reduction

(1) Harvard solution
(2) Anderson & Webb (1989)
(3) Beanland et al (1989)

Table 2. Event Hypocentral Parameters

Date	Time	Latitude	Longitude	Depth (km)	M_L
March 14	0520 33.87	37.982	176.777	0.3	1
	0648 16.83	37.911	176.847	8.5	2
	0838 14.42	37.917	176.840	8.7	3
	0843 32.91	37.921	176.846	7.8	4
	1108 25.69	38.132	176.666	8.3	5
	1149 04.35	38.114	176.676	7.7	6
	1227 19.25	37.942	176.794	7.6	7
	2112 45.74	38.034	176.764	3.9	8
March 15	0001 42.87	38.008	176.773	0.5	9
	0029 05.59	37.912	176.840	8.9	10
	0031 50.85	38.042	176.757	6.1	11
	0047 32.64	38.134	176.666	5.2	12
	0109 46.07	37.918	176.861	5.0	13
	0931 09.02	37.975	176.778	3.0	14
	1117 45.19	38.040	176.751	5.4	15
	1340 30.36	38.037	176.750	8.3	16
	1350 52.86	38.114	176.649	7.7	17
	1442 36.82	38.012	176.804	5.3	18
	1519 09.68	38.034	176.733	4.6	19
	155 06.80	38.036	176.747	0.3	20
	161 51.73	37.982	176.739	5.9	21
March 16	0216 51.77	38.048	176.734	5.0	22
	0236 24.34	38.005	176.749	4.8	23
	0557 51.13	38.095	176.689	7.0	24
	0601 01.96	38.087	176.694	4.4	25
	0613 20.35	38.093	176.683	7.6	26
	0843 45.53	37.959	176.845	3.6	27
	0953 13.29	37.978	176.808	7.1	28
	1238 37.70	38.180	176.640	6.3	29
	1656 12.32	38.024	176.770	5.3	30
	1813 23.70	37.906	176.806	8.5	31
	1813 59.95	38.161	176.597	7.6	32
	1816 58.85	37.910	176.807	7.9	33
	1824 07.95	38.171	176.597	9.2	34
	1852 14.61	37.910	176.810	6.1	35
	1918 12.42	38.117	176.652	3.5	36
	2057 03.65	37.985	176.821	9.2	37
	2110 25.98	38.047	176.764	5.9	38
March 17	1115 23.99	37.927	176.861	5.4	39
March 18	0301 12.61	37.936	176.850	7.7	40
	0957 24.78	38.019	176.772	5.0	41
	1258 32.21	38.108	176.655	9.1	42
	1432 28.54	38.037	176.713	5.1	43
	1949 53.52	38.113	176.688	8.9	44
	2132 31.41	37.907	176.817	7.1	45
	2222 35.56	37.905	176.814	7.2	46
March 19	0452 16.80	37.905	176.817	6.6	47
	0546 39.67	37.984	176.817	9.3	48
	0608 32.64	38.046	176.742	8.1	49
	0634 27.32	38.117	176.680	8.4	50
	0819 34.59	37.913	176.797	5.1	51
	0839 31.50	37.918	176.797	5.3	52
	0907 06.50	38.046	176.741	7.8	53
	1130 28.99	38.042	176.755	6.0	54
	1456 36.92	38.001	176.765	5.9	55
	1656 35.11	38.040	176.767	8.5	56
	2206 49.22	38.125	176.669	7.6	57

† Event number refered to in Table 3

Table 3. Spectral and Source Parameters

					Spectral Fit			
No.	AMo	Afcp	Afcs	Ads	Ar	Afcp	Afcs	Ads
1	11.68	8.23	5.91	1.6	261	11.81	6.50	02.0
2	12.04	10.24	5.22	3.5	247	12.56	5.19	04.9
3	13.38	7.56	4.20	18.1	323	7.78	3.77	36.4
4	11.89	9.79	5.58	2.7	243	12.07	5.85	03.9
5	12.25	10.50	4.59	12.4	282	10.42	4.91	07.1
6	12.36	8.78	4.74	5.7	307	8.70	5.10	06.8
7	13.10	8.79	4.37	16.9	289	8.20	4.54	24.0
8	12.10	10.28	4.37	9.3	251	12.67	4.54	20.3
9	11.73	11.41	5.54	3.0	280	16.58	6.80	06.6
10	11.84	9.27	4.58	2.7	289	10.72	4.63	03.4
11	11.99	7.61	3.55	4.4	408	8.78	4.30	03.8
12	11.95	8.12	5.78	4.7	253	7.84	5.88	05.0
13	11.80	8.71	5.68	3.5	265	9.02	5.75	02.8
14	11.58	9.47	4.71	1.7	285	12.85	5.88	02.5
15	11.88	8.53	5.56	4.0	249	10.25	6.05	04.9
16	11.87	9.35	5.22	4.4	270	11.61	5.60	08.0
17	12.03	12.43	5.17	2.7	237	11.98	5.79	02.8
18	12.87	6.84	3.79	8.0	383	7.35	3.84	08.5
19	12.24	9.87	5.27	26.6	260	10.80	5.15	28.7
20	11.97	8.96	5.84	11.6	254	11.38	5.66	18.7
21	11.63	9.87	6.72	3.8	240	11.60	6.93	04.3
22	12.01	8.99	6.20	7.4	267	7.99	6.01	05.3
23	12.25	8.88	4.91	7.0	282	8.61	5.56	06.8
24	12.21	7.75	5.98	6.9	277	8.53	7.14	15.5
25	12.37	6.62	4.72	5.5	321	5.62	4.76	05.8
26	12.72	7.13	4.36	9.8	345	7.45	4.91	21.3
27	12.41	6.20	5.70	7.5	283	7.49	5.78	08.0
28	12.56	8.70	5.11	8.1	272	9.59	7.15	27.9
29	12.16	7.52	5.56	3.8	284	8.32	5.47	03.6
30	12.30	7.44	4.93	7.7	304	7.43	5.23	05.8
31	11.96	8.30	5.11	3.4	281	9.38	6.21	06.6
32	12.33	8.02	5.72	14.1	276	8.58	6.60	27.1
33	12.68	6.43	3.77	4.3	369	6.17	3.91	03.4
34	11.94	9.54	7.36	5.4	220	9.71	8.50	10.4
35	12.27	4.06	4.88	3.9	377	6.38	5.48	05.4
36	12.12	9.78	4.96	2.8	250	10.88	5.44	03.7
37	12.37	7.14	4.80	6.2	298	8.73	5.27	09.6
38	12.17	6.95	6.65	4.8	259	9.99	9.39	14.5
39	13.16	6.31	3.08	36.6	397	7.34	3.65	58.3
40	12.98	6.71	4.74	41.7	326	7.65	4.46	30.7
41	12.41	6.78	4.65	8.4	323	10.32	5.70	17.0
42	11.59	12.19	4.81	2.0	253	13.87	5.62	03.7
43	13.88	9.33		313.6	241	7.66		173.6
44	11.47	7.28	5.79	1.7	293	8.50	7.16	05.6
45	12.10	7.55	4.59	8.6	394	11.82	6.64	34.5
46	12.74	7.57	3.38	14.1	448	6.68	3.68	12.8
47	12.04	10.55	4.77	4.8	279	11.14	5.55	09.8
48	12.26	12.00	2.59	.66	315	10.91	2.58	.52
49	12.50	4.12	5.78	1.38	346	4.03	6.78	1.94
50	11.72	9.97	4.63	.17	303	10.59	5.11	.24
51	11.57	10.59	4.69	.22	298	11.72	6.90	.88
52	11.85	9.66	5.84	.24	284	12.35	6.55	.25
53	12.40	6.41	5.37	.95	320	7.39	5.59	.83
54	11.90	6.14	4.66	.32	327	7.12	5.05	.48
55	11.84	5.83	4.23	.23	377	4.84	4.42	.15
56	12.08	11.72	6.57	1.13	213	13.64	7.24	1.94
57	11.60	12.40	6.74	.54	257	12.29	7.12	.49

No. is the event number from Table 2, AMo is $\log_{10}$ of the average seismic moment in N-m, Afcp is the average p-wave corner frequency in Hz, Afcs is the average s-wave corner frequency in Hz, Ar is the average source radius, and Ads is the average stress drop.

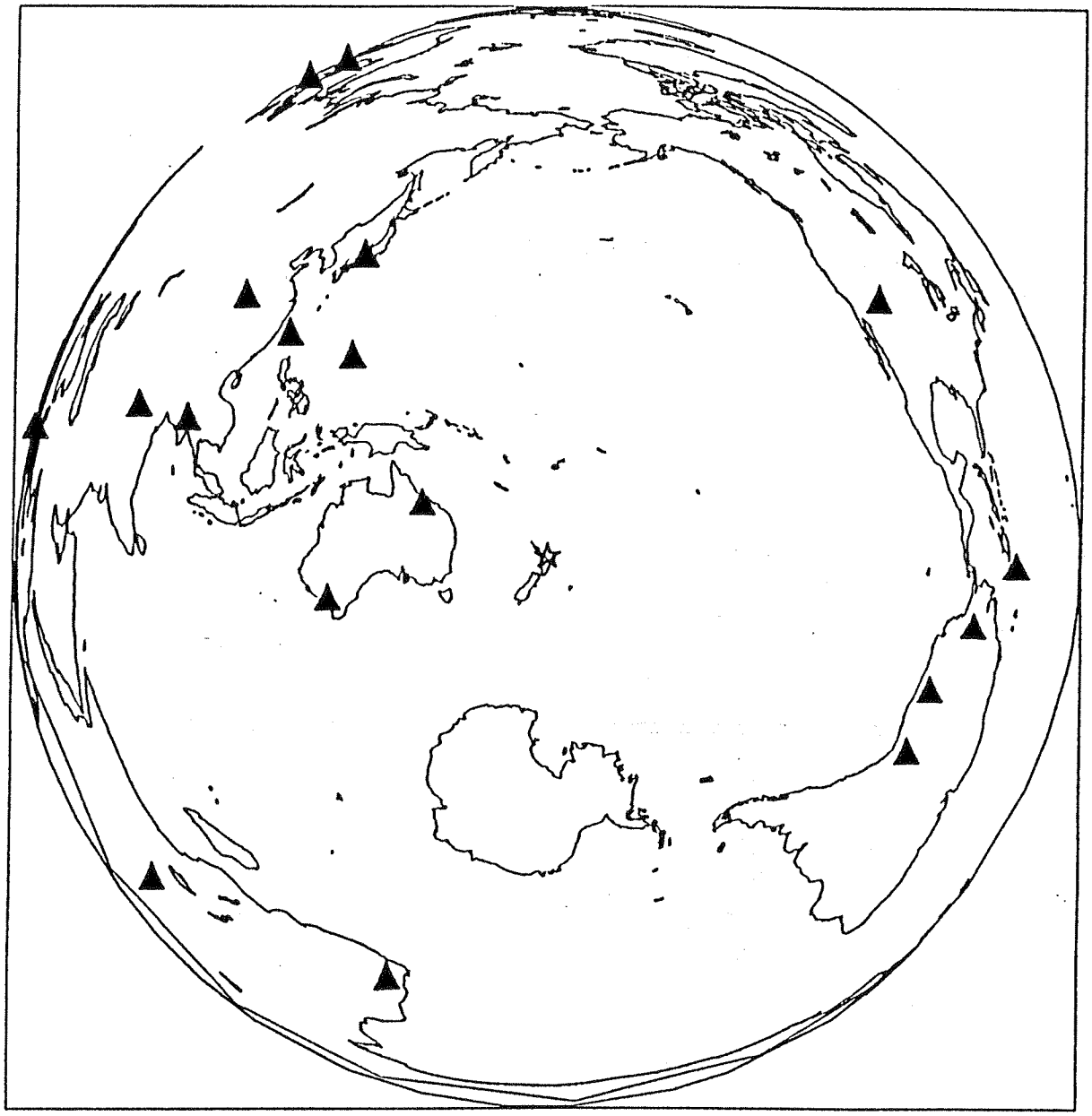

Figure 1. Location of digital teleseismic stations (▲) of the IDA and SRO relative to the location of the earthquake (☆).

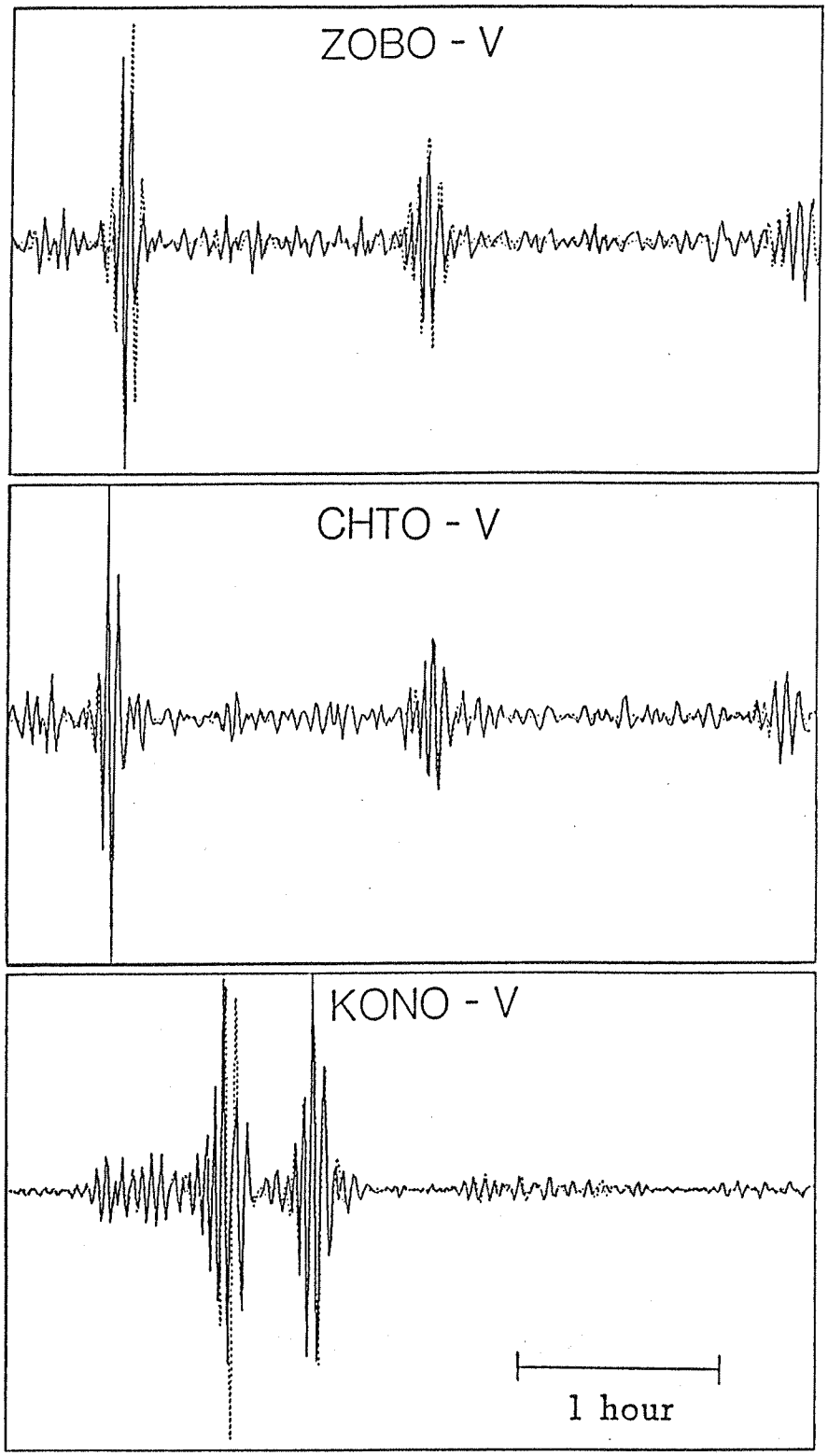

Figure 2. Comparison of the low frequency (2-8 mHz) observed waveforms (solid lines) from SRO seismic networks with synthetic waveforms (dashed lines) computed for the normal mode model of Table 1.

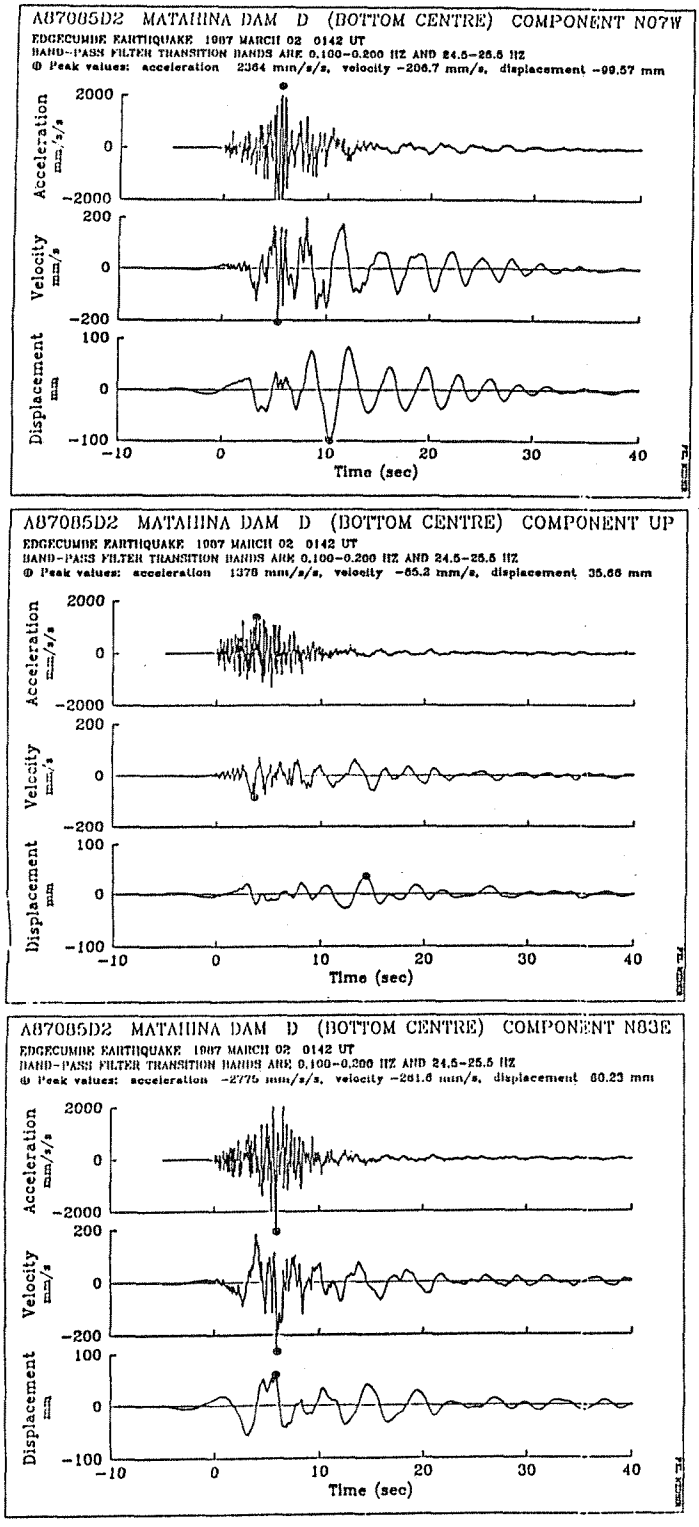

Figure 3. Acceleration, velocity and displacement records for the three components of strong-motion records collected near the base of the Matahina dam (NZPEL).

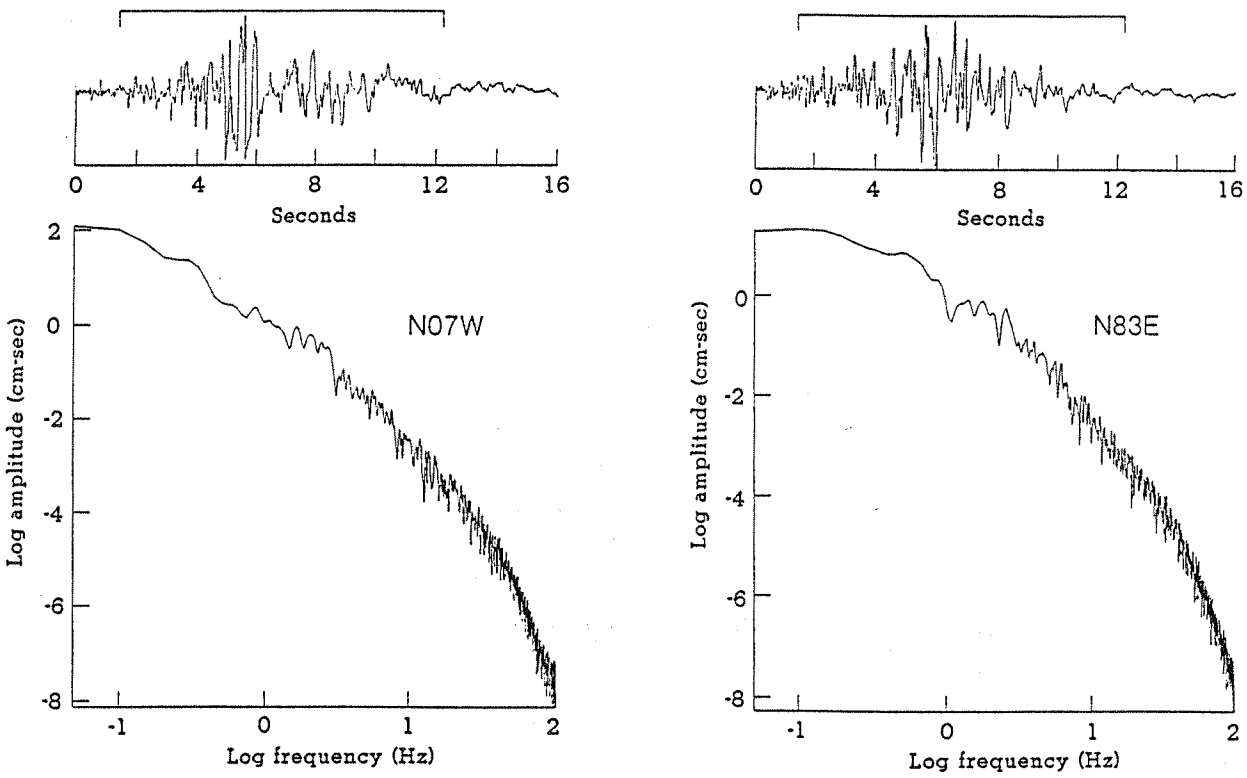

Figure 4. Fourier displacement amplitude spectra for the horizontal component accelerograms. The brackets above the seismograms denote the time window analyzed.

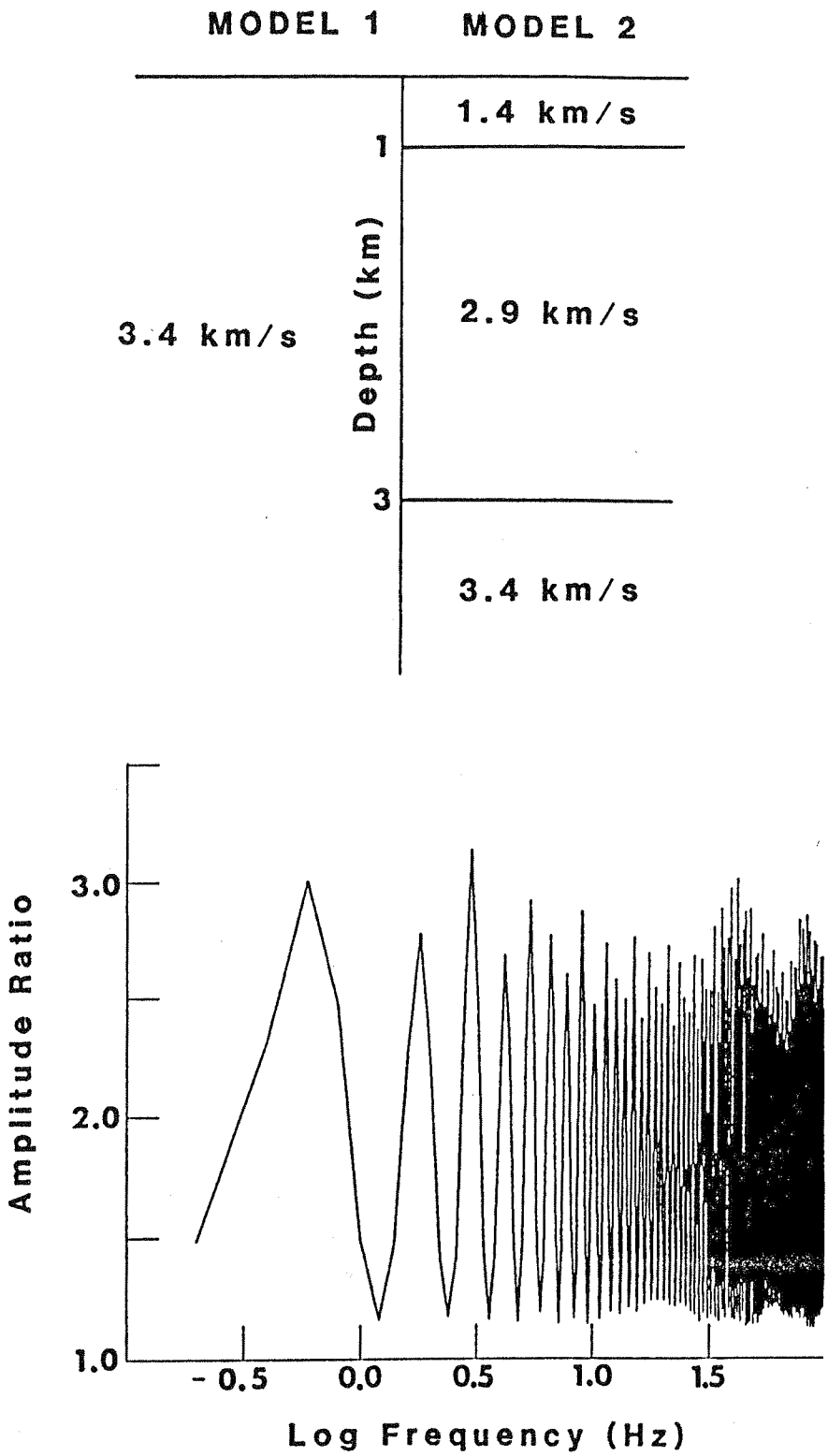

Figure 5. (a) Reference shear wave velocity structure (MODEL 1) and shear wave velocity structure (MODEL 2) adapted from Robinson (1989); (b) amplification of the Robinson velocity structure relative to the reference model.

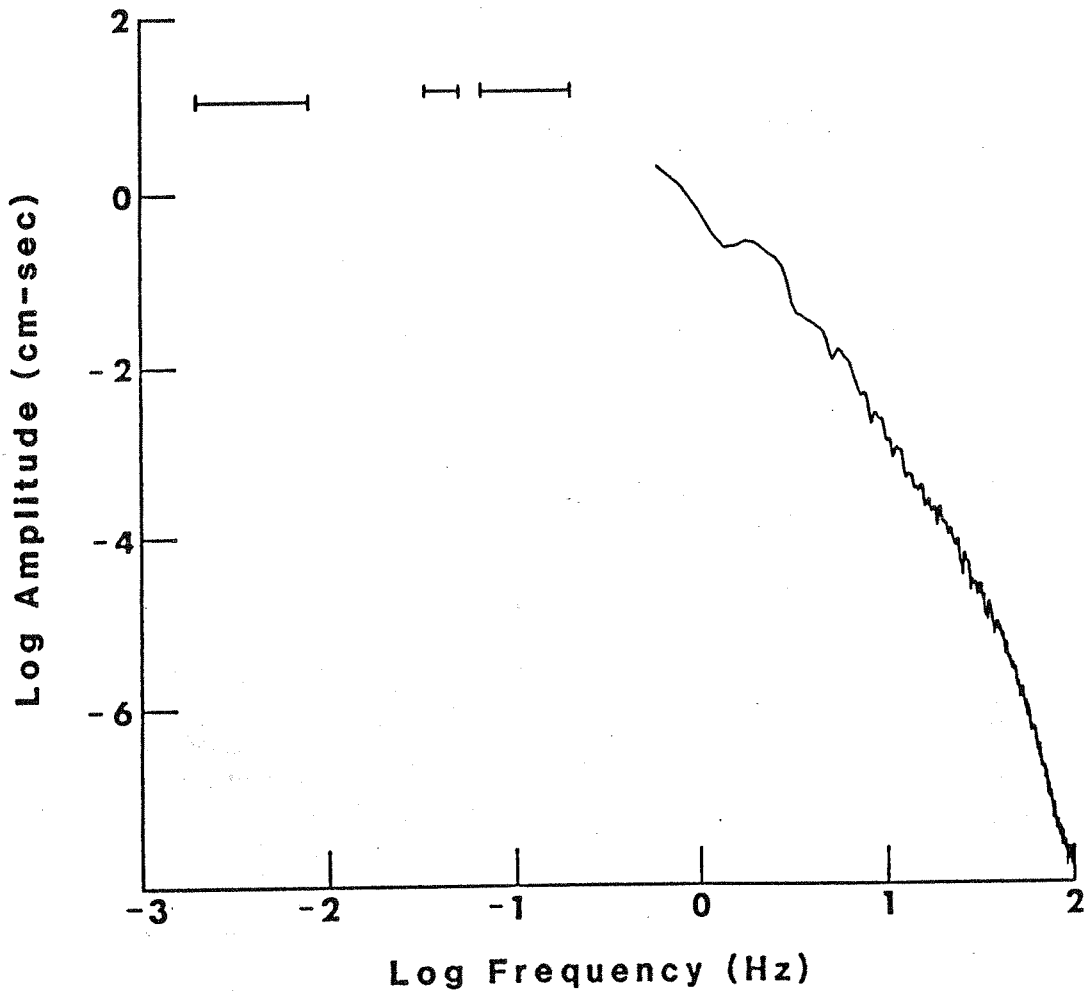

Figure 6. Composite displacement source spectrum and source parameters for the Edgecumbe main shock.

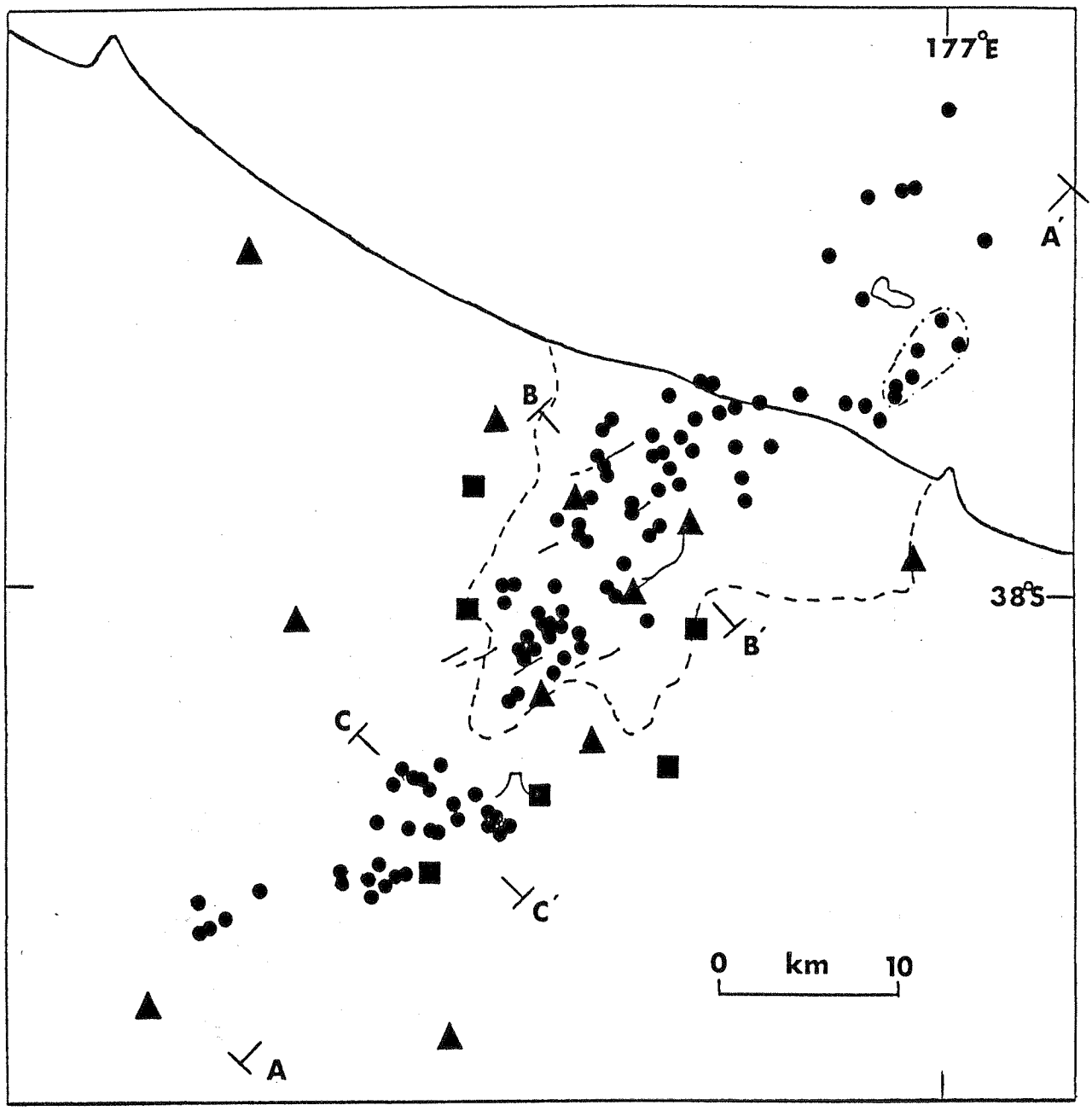

Figure 7. Location of the digital (■) and smoked paper (▲) seismographs superimposed on a general geologic map of the area. Location of the aftershocks analyzed in this report (●). The epicenter of the main shock is denoted by the large star and the extent of the aftershock zone is denoted by the hatchered region. The cross-sections shown in Figure 8 are indicated.

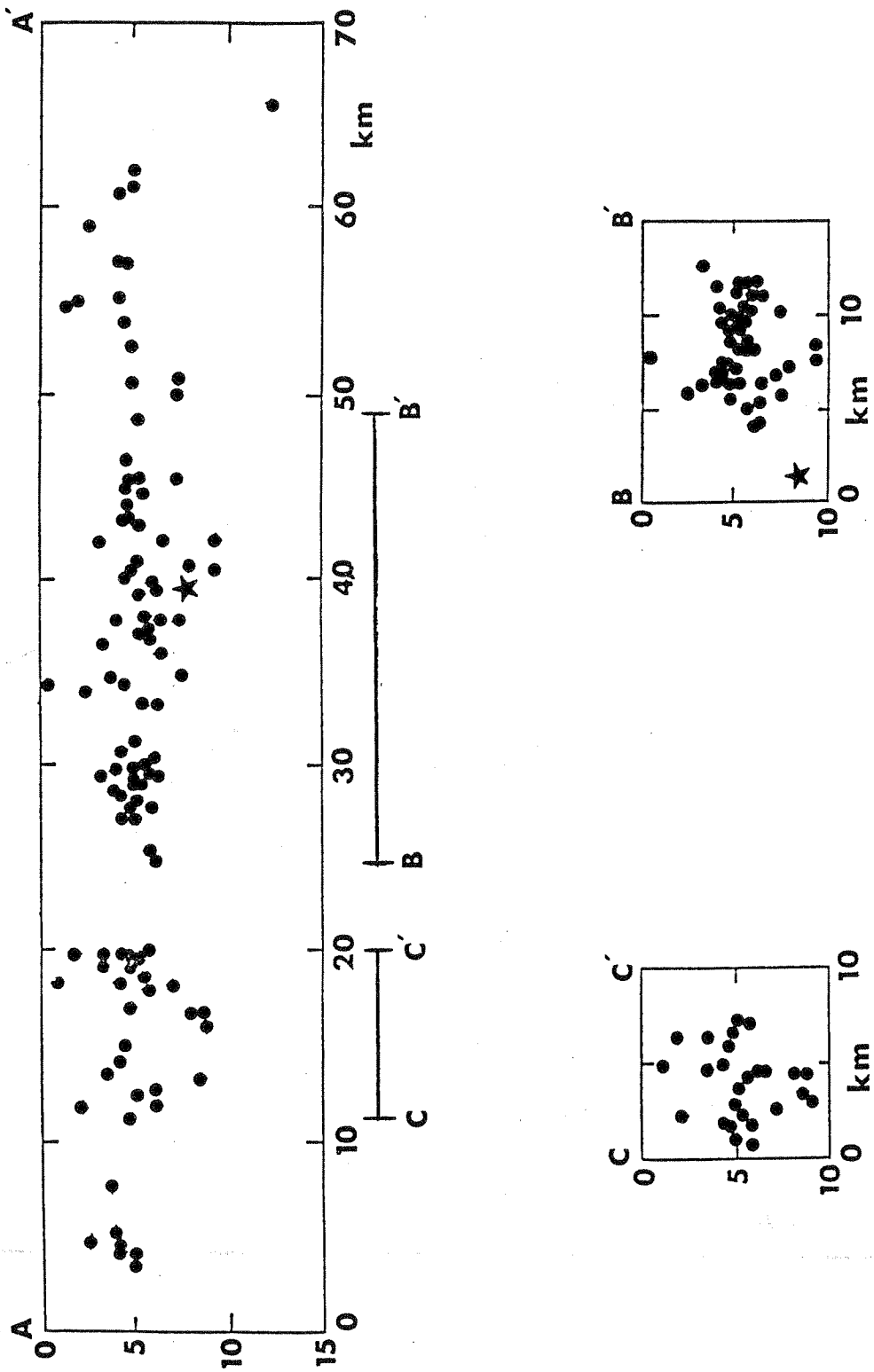

Figure 8. Projection of the aftershock hypocentres onto the cross-section indicated in Figure 7.

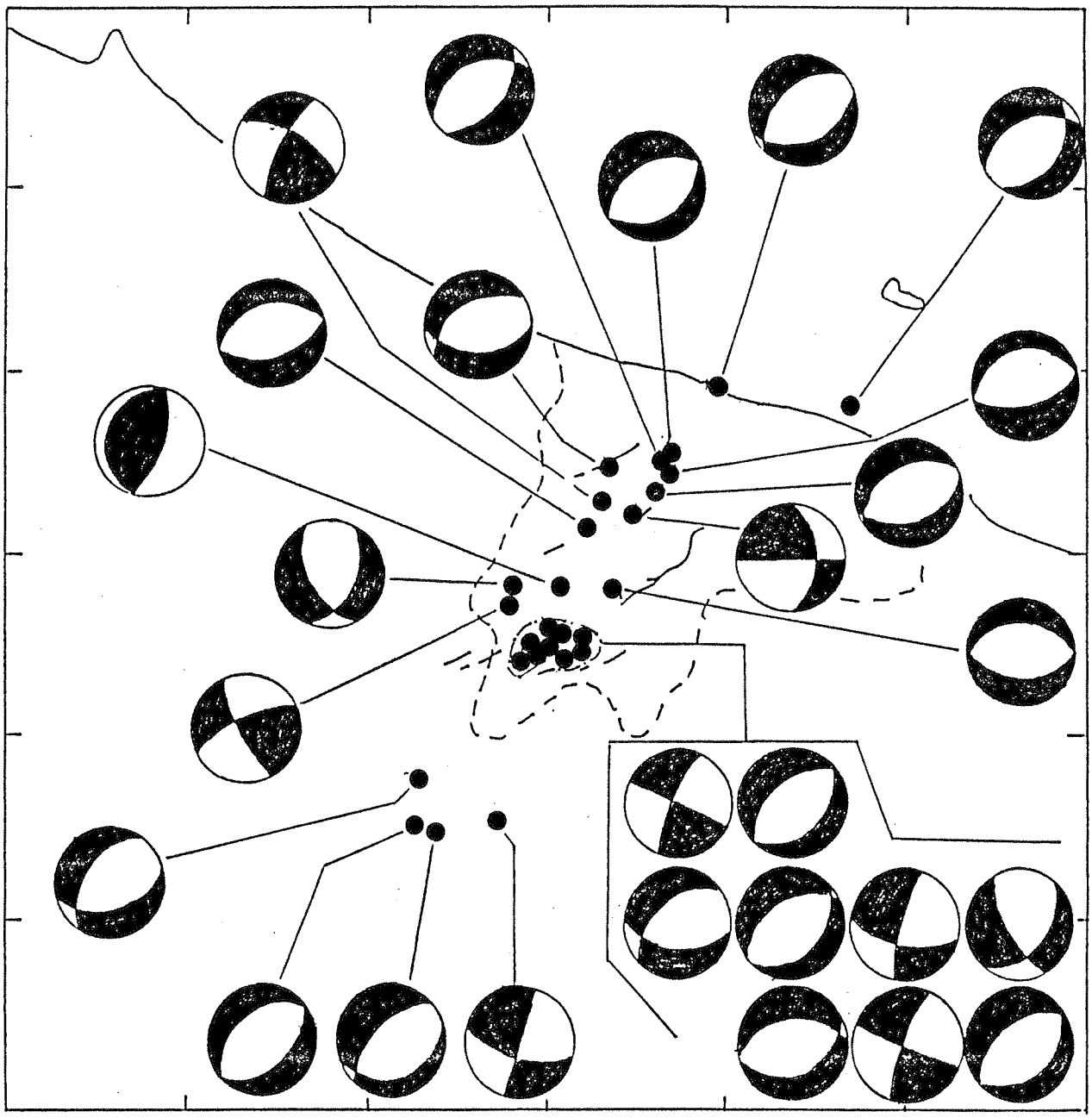

Figure 9. Summary of focal mechanisms (upper hemisphere) showing the position of each in the aftershock sequence. The nine mechanisms in the lower right corner are for events in the cluster enclosed by the dashed lines. The darkened regions are the regions of compressional first motion.

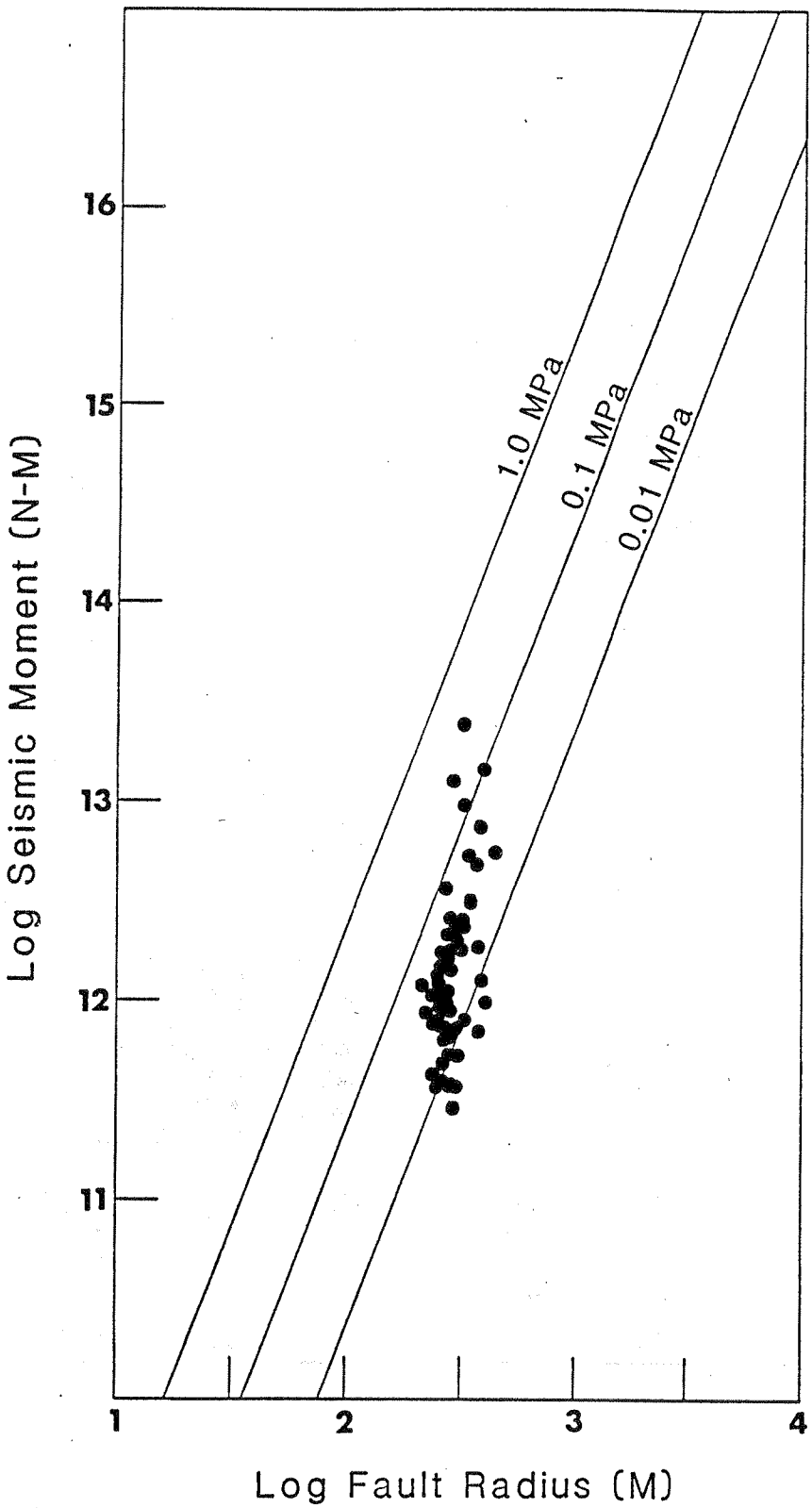

Figure 10. Plot of Log_{10} of the seismic moment vs Log_{10} of the fault radius.

REFERENCES

Adams, R.D.; Ware, D.E. 1977: Subcrustal earthquakes beneath New Zealand: locations determined with a laterally inhomogeneous velocity model. *New Zealand journal of geology and geophysics 20*: 59-83.

Allis, R.G. 1979: Heat flow, in: M.P. Hochstein and T.M. Hunt (Editors), *Scientific Excursion A5, Volcanic and Geothermal Areas of the North Island, New Zealand fR, Royal society of New Zealand, Wellington, 49.*

Anderson, J.G. 1986: Implication of attenuation for studies of the earthquake source, in *Earthquake source mechanics*, ed. S. Das, J. Boatwright, and C. Scholz, *American geophysical union monograph, 37*, 311-318.

Anderson, J.G.; Bodin, P.; Brune, J.N.; Prince, J.; Singh, S.K.; Quaas, R.; Onate, M. 1986: Strong ground motion from the Michoacan, Mexico, earthquake, *Science, 233*, 1043-1049.

Anderson, H.; and others 1987: The March 2, 1987, Earthquake near Edgecumbe, North Island, New Zealand, *EOS, 68*, 1162-1171.

Anderson, H.; Webb, T., 1989: The rupture process of the Edgecumbe earthquake, March 2, 1987, New Zealand, *New Zealand journal of geology and geophysics*, in press.

Anooshehpoor, A. 1988: Foam rubber model studies of problems in seismology and earthquake engineering, Ph.D. dissertation, University of California, San Diego, 133p.

Archuleta, R. 1986: Downhole recordings of seismic radiation, in *Earthquake source mechanics*, ed. S. Das, J. Boatwright, and C. Scholz, *American geophysical union monograph, 37*, 319-329.

Beanland, S.; Berryman, K.R.; Blick, G.H. 1989: Edgecumbe earthquake 2 March 1987: Geological investigation, *New Zealand journal of geology and geophysics*, in press.

Brune, J.N. 1970: Tectonic stress and the spectra of seismic shear waves from earthquakes, *Journal of geophysical research, 75*, 4997-5009.

Brune, J.N. 1971: Correction, *Journal of geophysical research , 76*, 5002.

Brune, J.N.; Anooshehpoor, R.; Lovberg, R.; Wang, L. 1985: Topographic seismic amplification and dam-foundation interaction on a foam rubber model of the topography near Pacoima dam, *Proceedings: strong-ground-motion simulation and earthquake engineering applications*, 26-1 - 26-8.

Brune, J.N.; Fletcher, J.; Vernon, F.L.; Harr, L.; Hanks, T.; Berger, J., 1986: Low stress-drop earthquakes in light of new data from the Anza, California telemetered digital array, *Earthquake Source Mechanics fR, Geophysical monogram 7, Maurice Ewing Vol., American Geophysical Union*, 269-274.

Buland, R.; Gilbert, F. 1976: Matched filtering for seismic moment tensor, *Geophysical research letters, 3*, 205-206.

Chapman, C.H 1978: A new method for computing synthetic seismograms, *Geophysical journal of the royal astronomical society, 54*, 481-51.

Chouet, B.; Aki, K.; Tsujiura, M. 1978: Regional variation of the scaling law of earthquake source spectrum, *Bull. Seis. Soc. Am., 68*, 49-80.

Cole, J.W. 1979: Structure, petrology and genesis of Cenozoic volcanism, Taupo Volcanic Zone, New Zealand - a review, *New Zealand journal of geology and geophysics, 22*, 631-657.

Darby, D.J. 1989: Dislocation modelling of the Edgecumbe earthquake, *New Zealand journal of geology and geophysics*, in press.

Doornbos, D.J. 1982: Seismic source spectra and moment tensors, *Physics of the earth and planetary interiors , 30*, 214-227.

Doornbos, D.J. 1985: Source solutions and station residuals from long-period waveform inversion of

deep events, *Journal of geophysical research* , *90*, 5466-5478.

Douglas, B. M.; Ryall, A 1972: Spectral Characteristics and stress drop for microearthquakes near Fairview Peak, Nevada, *J. Geophys. Res. 77*, 351-359.

Fletcher, J.B. 1980: Spectra from high-dynamic range digital recordings of Orville, California aftershocks and their source parameters, *Bull. Seis. Soc. Am.*, *70*, 735-756.

Fletcher, J.; Harr, L.; Hanks, T.; Baker, L.; Vernon, F.; Berger, J.; Brune, J.N. 1987: The digital array at Anza, California: processing and initial interpretation of source parameters, *J. Geophys. Res. 92*, 369-382.

Gilbert, F.; Dziewonski, A.M. 1975: An application of normal mode theory to the retrieval of structural parameters and source mechanisms from seismic spectra, *Philosophical translations of the royal society of London, Series A* , *278*, 187-269.

Grapes, R.H.; Sissons, B.A.; Wellman, H.W. 1987: Widening of the Taupo volcanic zone, New Zealand, and the Edgecumbe earthquake of March 1987, *Geology*, *15*, 1123-1125.

Gusev, A.A. 1983: Descriptive statistical model of earthquake source radiation and its application to an estimation of short-period strong motion, *Geophysical journal of the royal astronomical society* , *74*, 787-808.

Hanks, T.C. 1982: f_{max}, *Bull. Seis. Soc. Am.*, *72*, 1867-1879.

Kanamori, H.; Anderson, D.L. 1975: Theoretical basis of some empirical relations in seismology. *Bulletin of the seismological society of America*, *65*, 1073-1095.

Nairn, I.A; Beanland, S. 1989: Geological setting of the March 1987 Edgecumbe earthquake, New Zealand, *New Zealand journal of geology and geophysics*, in press.

Priestley, K.F.; Masters, T.G. 1986: Source mechanism of the September 19, 1985 Michoacan earthquake and its implications, *Geophysical research letters*, *13*, 601-604.

Priestley, K.F.; Smith, K.D.; Cockerham, R.S. 1988: The Round Valley, California earthquake sequence, *Geophysical journal of the royal astronomical society* , *95*, 215-235.

Reyners, M.E. 1980: A microearthquake study of the plate boundary, North Island, New Zealand, *Geophysical journal of the royal astronomical society* , *63*, 1-22.

Robinson, R. 1989: Aftershocks of the Edgecumbe earthquake: seismological and structural studies using portable seismographs in the epicentral region, *New Zealand journal of geology and geophysics*, in press.

Sissons, B.A. 1979: The horizontal kinematics of the North Island of New Zealand, Ph.D. Disertation, Victoria University, Wellington, New Zealand.

Smith, E.G.C.; Webb, T.H. 1986: The seismicity and related deformation of the Central Volcanic Region, North Island, New Zealand, in I.E.M. Smith (ed), *Late Cenozoic Volcanism in New Zealand*, Royal Society of New Zealand Bulletin 23, 112-133.

Smith, K.D.; Priestley, K.F., 1988: The Foreshock Sequence of the 1986 Chalfant, California Earthquake, *Bulletin of the seismological society of America*, *78*, 172-187.

Smith, K.D.; Brune, J.N.; Priestley, K.F.,: Seismic Energy, Spectrum, and the Savage and Wood Inequality for Complex Earthquakes, *Procedings of the Hundredth Anniversary of the Berkeley Seismograph Station*, in press.

Smith, K.D.; Walter, W.R.; Castro, R.R.; Priestley, K.F.; Anooshepoor, A.N.: Earthquake clustering near Mina, Nevada, July and August, 1987, this volume.

Stern, T.A. 1985: A back-arc basin formed within continental lithosphere: The Central Volcanic region of New Zealand, *Tectonophysics*, 112, 385-409.

Stern, T.A.; Davey, F.J.; Smith, E.G.C. 1986: Crustal structure studies in New Zealand, in *Reflection*

Seismology: A global perspective, ed. M. Barazangi and L. Brown, *American geophysical union, geodynamic series* , *13*, 121-132.

Studt, F.E.; Thompson, G.E.K. 1969: Geothermal heat flow in the North Island of New Zealand, *New Zealand journal of geology and geophysics* , *12*, 673-683.

Thatcher, W.; Hanks, T.C. 1973: Source parameters of southern California earthquakes, *Journal of geophysical research* , *78*, 8547-8576.

Thompson, G.E.K. 1977: Temperature gradients within and adjacent to the North Island volcanic belt, *New Zealand journal of geology and geophysics* , *20*, 85-97.

Tucker, B.E.; Brune, J.N 1977:

Walcott, R.I. 1978: Tectonic and late Cenozoic evolution of New Zealand, *Geophysical journal of the royal astronomical Society* , *52*, 137-164.

Ward, S.N. 1980: A technique for the recovery of the seismic moment tensor applied to the Oaxaca, Mexico, earthquake of November 1978, *Bulletin of the seismological society of America*, *70*, 717-734.

Ward, S.N. 1983: Body wave inversion: Moment tensors and depths of oceanic intraplate bending earthquakes, *Journal of geophysical research*, *88*, 9315-9330.

Wu, F.T. 1966: Lower limit of the total energy of earthquakes and partitioning of energy among seismic waves, Ph.D. Thesis, California Institute of Technology, Pasadena.

RATES AND PATTERNS OF PIEDMONT EVOLUTION IN THE SOUTHWEST BASIN AND RANGE

John C. Dohrenwend, U.S. Geological Survey, MS 901, Menlo Park, CA 94025

Average long-term erosion rates have been estimated for a number of piedmont areas across the southwestern Basin and Range. These estimates, based on measurements of the average vertical distance between remnant piedmont surfaces of known age and adjacent modern surfaces, document region-wide similarities in the patterns and rates of late Tertiary and Quaternary piedmont evolution. As predicted by the concept of the threshold of critical stream power, a general pattern of upland erosion, upper piedmont quasi-euqilibrium, and lower piedmont and basin deposition prevails in most closed basin systems. Two significant exceptions to this general pattern are (1) piedmonts along the fronts of highly active fault-bounded ranges that have undergone more or less continuous alluvial deposition, and (2) areas isolated from the sediment influx of upland drainage systems that are drained solely by streams arising on the piedmont surface and have experienced one or more relatively short-lived pulses of rapid dissection. Average long-term rates of erosion typically range between 1 and 4 cm/10^3 yr in upland areas and systematically decrease in a basinward direction. Therefore, many middle piedmont areas in a variety of tectonic settings have changed little, remaining for long periods of time in approximate geomorphic adjustment with little net erosion or deposition. For example, relations with K-Ar dated lava flows document conditions of approximate geomorphic equilibrium for periods of: (1) at least 5.9 m.y. along both flanks of the Reveille Range and at least 1.1 m.y. along both flanks of the Pancake Range in central Nevada; (2) at least 0.5 to as much as 6 m.y. on the flanks of pediment domes in the area of the Cima volcanic field in the eastern Mojave Desert; and (3) at least 1 m.y. along the east flank of the Sierra Nevada in Owens Valley. Moreover, the widespread preservation in both middle and distal piedmont areas of relict and shallowly buried piedmont remnants of late and middle Pleistocene age also indicates that most of the region's alluvial piedmonts are underlain by deposits of considerable antiquity that have been only superficially affected by Quaternary geomorphic processes. These relatively slow rates of late Tertiary and Quaternary change imply an initially rapid erosional-depositional response of newly formed range-basin systems folowed by an asymptotic slowing in range erosion and basin deposition as these systems approach a long term condition of slow, nearly constant decay.

LATE QUATERNARY PALEOCLIMATE STUDIES--
GEOLOGIC PROBLEMS AND QUESTIONS

Emily M. Taylor, U.S. Geological Survey, MS 913,
Box 25046, Denver, Colorado, 80225

To assure the prolonged integrity of any nuclear-waste repository site, the long-term environmental stability of that site needs to be considered. This stability will be strongly affected by future climatic change. On the assumption that future climates will most likely resemble those of the recent geologic past, the U.S. Geological Survey has begun several studies aimed at characterizing the past climatic variability near the potential nuclear-waste repository site at Yucca Mountain, Nevada.

One explanation advanced for climatic change is variation in net global solar-energy input, a consequence of the procession of Earth's orbit and the obliquity and eccentricity of its axial position. Major climatic changes occur at intervals of 10,000 to 100,000 yr. The Holocene Epoch is the most recent in a long series of relatively brief (7,000-20,000 yr) interglacials that punctuate much longer (90,000-150,000 yr) periods of glaciations. A permanent nuclear-waste repository must be able to withstand the effects of a major climatic change. A climatic change that results in greater effective moisture may cause percolating water and (or) ground water to move within the zone of the waste material during the time that the material is still hazardous. Therefore, the focus of the geologic investigations is to help understand the hydrologic responses to cooler and wetter climates.

The geologic approaches to evaluating the paleoclimate of an area in Southern Nevada can be summarized under six main topics: (1) characterization of the modern climate, (2) paleolake, marsh, and playa studies, (3) terrestrial paleo-ecology, (4) paleoenvironmental history, (5) paleoclimate-paleoenvironmental synthesis, and (6) numerical climatic modeling. Each of these approaches contributes to the overall characterization of the paleoclimate in the region.

The modern climate is being characterized by a network of weather stations throughout the southern Great Basin. The types of data being collected include air-temperature, precipitation, soil temperature, and solar radiation measurements, though not all properties are measured at all sites. These data establish a baseline for climatic modeling.

The paleolake, marsh, and playa studies consist primarily of drilling and trenching projects aimed at better understanding the sedimentological record of internal basins

that do not drain to the sea. Dated sediments and the associated paleontological specimens can be related to the climate under which they were deposited. The sites under study are Walker Lake, Pyramid Lake, Ruby Marsh, and Kawich, Frenchman, and Desert Dry Lake Playas. The initial results suggest that the records are of variable quality because different basins respond differently to similar climates. The basins are influenced not only by climate, but also by tectonism and stream captures, among other factors.

The terrestrial paleoecological record includes datable macro- and microfaunal assemblages and pollen found in packrat middens. These data record the vegetation pattern at the time of deposition, which can be related to paleoclimate by analogy to existing environments. Packrat midden sample sites have been selected for their nearness to existing Quaternary paleoclimatic studies, for their availability, and to complete the faunal record for a given area. Because packrats collect their midden building material within 10 meters, these records are site specific. Very localized climatic influences affect vegetation patterns which directly affect the pollen and packrat midden assemblages.

The paleoenvironmental history approach to paleoclimate depends primarily on studies of soils, geomorphology, and climatic analog sites. Properties of Quaternary surfaces representing a variety of ages, paleoclimates, and parent materials have been studied. The sites under study are the alluvial deposits in the Yucca Mountain, Kyle Canyon, Cima Volcanic field, and Silver Lake areas. The physical and chemical properties of the soils developed on dated geomorphic surfaces were compared. For example, the presence of soluble salts or $CaCO_3$ at depths much greater than those at which such concentration occur in soils formed under the modern climate, suggest the influence of a former wetter climate. These properties can be compared to computer-generated models based on climates different than the present. The analog sites are areas that seem to be climatically similar to southern Nevada during the last glacial maximum, based on packrat midden data and hydrologic properties. These sites offer data similar to those produced by the soil and geomorphic studies.

Finally, the paleoclimatic and paleoenvironmental data can be combined and synthesized in order to compare trends. This synthesis should help to resolve questions concerning specific regional climatic trends at the Holocene-Pleistocene boundary. Paleoclimatic conclusions derived from the geologic and paleoenvironmental studies will be compared with those derived from numerical climatic modeling.